Université de Montréal

The role of Mechanistic Target Of Rapamycin (mTOR) pathway and synaptic protein $GABA_A$-R in cortical GABAergic cell connectivity

by
Mayukh Choudhury

Départment de Sciences Biomédicales
Faculté de Médecine

Thesis presented to the Faculté de médecine
for obtaining the doctoral degree in Sciences biomédicales

September 2015

Résumé

Quelque 30 % de la population neuronale du cortex mammalien est composée d'une population très hétérogène d'interneurones GABAergiques. Ces interneurones diffèrent quant à leur morphologie, leur expression génique, leurs propriétés électrophysiologiques et leurs cibles subcellulaires, formant une riche diversité. Après leur naissance dans les éminences ganglioniques, ces cellules migrent vers les différentes couches corticales. Les interneurones GABAergiques corticaux exprimant la parvalbumin (PV), lesquels constituent le sous-type majeur des interneurones GABAergiques, ciblent spécifiquement le soma et les dendrites proximales des neurones principaux et des neurones PV+. Ces interneurones sont nommés cellules à panier (Basket Cells –BCs) en raison de la complexité morphologique de leur axone. La maturation de la connectivité distincte des BCs PV+, caractérisée par une augmentation de la complexité de l'axone et de la densité synaptique, se déroule graduellement chez la souris juvénile. Des travaux précédents ont commencé à élucider les mécanismes contrôlant ce processus de maturation, identifiant des facteurs génétiques, l'activité neuronale ainsi que l'expérience sensorielle. Cette augmentation marquante de la complexité axonale et de la synaptogénèse durant cette phase de maturation suggère la nécessité d'une synthèse de protéines élevée. La voie de signalisation de la cible mécanistique de la rapamycine (Mechanistic Target Of Rapamycin -mTOR) a été impliquée dans le contrôle de plusieurs aspects neurodéveloppementaux en régulant la synthèse de protéines. Des mutations des régulateurs Tsc1 et Tsc2 du complexe mTOR1 causent la sclérose tubéreuse (TSC) chez l'humain. La majorité des patients TSC développent des problèmes neurologiques incluant des crises épileptiques, des retards mentaux et l'autisme. D'études récentes ont investigué le rôle de la dérégulation de la voie de signalisation de mTOR dans les neurones corticaux excitateurs. Toutefois, son rôle dans le développement des interneurones GABAergiques corticaux et la contribution spécifique de ces interneurones

GABAergiques altérés dans les manifestations de la maladie demeurent largement inconnus. Ici, nous avons investigué si et comment l'ablation du gène *Tsc1* perturbe le développement de la connectivité GABAergique, autant *in vitro* que *in vivo*.

Pour investiguer le rôle de l'activation de mTORC1 dans le développement d'une BC unique, nous avons délété le gène *Tsc1* en transfectant CRE-GFP dirigé par un promoteur spécifique aux BCs dans des cultures organotypiques provenant de souris $Tsc1^{lox}$. Le *knockdown in vitro* de *Tsc1* a causé une augmentation précoce de la densité des boutons et des embranchements terminaux formés par les BCs mutantes, augmentation renversée par le traitement à la rapamycine. Ces données suggèrent que l'hyperactivation de la voie de signalisation de mTOR affecte le rythme de la maturation des synapses des BCs. Pour investiguer le rôle de mTORC1 dans les interneurones GABAergiques *in vivo*, nous avons croisé les souris $Tsc1^{lox}$ avec les souris *Nkx2.1*-Cre et *PV*-Cre. À P18, les souris Tg(*Nkx2.1-Cre*);$Tsc1^{flox/flox}$ ont montré une hyperactivation de mTORC1 et une hypertrophie somatique des BCs de même qu'une augmentation de l'expression de PV dans la région périsomatique des neurones pyramidaux. Au contraire, à P45 nous avons découvert une réduction de la densité des punctas périsomatiques PV-gephyrin (un marqueur post-synaptique GABAergique). L'étude de la morphologie des BCs en cultures organotypiques provenant du *knock-out* conditionnel *Nkx2.1*-Cre a confirmé l'augmentation initiale du rythme de maturation, lequel s'effondre ensuite aux étapes développementales tardives. De plus, les souris Tg(*Nkx2.1Cre*);$Tsc1^{flox/flox}$ montrent des déficits dans la mémoire de travail et le comportement social et ce d'une façon dose-dépendante. En somme, ces résultats suggèrent que l'activation contrôlée de mTOR régule le déroulement de la maturation et la maintenance des synapses des BCs.

Des dysfonctions de la neurotransmission GABAergique ont été impliquées dans des maladies telles que l'épilepsie et chez certains patients, elles sont associées avec des mutations du récepteur $GABA_A$. De quelle façon ces mutations affectent le processus de maturation des BCs demeuret toutefois inconnu. Pour adresser cette question, nous avons utilisé la stratégie Cre-lox pour déléter le gène *GABRA1*, codant pour la sous-unité alpha-1 du récepteur $GABA_A$ dans une unique BC en culture organotypique. La perte de *GABRA1* réduit l'étendue du champ d'innervation des BCs, suggérant que des variations dans les entrées inhibitrices en raison de l'absence de la sous-unité $GABA_AR$ α1 peuvent affecter le développement des BCs. La surexpression des sous-unités $GABA_AR$ α1 contenant des mutations identifiées chez des patients épileptiques ont montré des effets similaires en termes d'étendue du champ d'innervation des BCs. Pour approfondir, nous avons investigué les effets de ces mutations identifiées chez l'humain dans le développement des épines des neurones pyramidaux, lesquelles sont l'endroit privilégié pour la formation des synapses excitatrices. Somme toute, ces données montrent pour la première fois que différentes mutations de *GABRA1* associées à des syndromes épileptiques peuvent affecter les épines dendritiques et la formation des boutons GABAergiques d'une façon mutation-spécifique.

Abstract

About 30% of the total neuronal population in the mammalian cortex is composed by a very heterogeneous population of GABAergic interneurons. These interneurons differ in their morphology, gene expression, electrophysiological properties and subcellular targets, thus establishing a rich diversity. After birth in the ganglionic eminences these cells migrate to distinct cortical layers. Parvalbumin (PV) expressing cortical GABAergic cells which constitute the major GABAergic subtype specifically targets the soma and proximal dendrites of principal neurons and PV+ cells. These cells are often referred as Basket cells (BCs) because of the intricate morphological complexity of their axons. The maturation of the distinct connectivity of PV+ BCs, characterized by an increase of axon complexity and synapse density, occurs gradually in juvenile mice. Previous studies started to elucidate the mechanisms controlling this maturation process, including genetic factors, neuronal activity and sensory experiences. The striking increase in axonal complexity and synaptogenesis occurring during the maturation phase suggests the requirement for elevated proteins synthesis in order to sustain the developmental process. The Mechanistic Target Of Rapamycin (mTOR) pathway has been implicated in controlling several aspects of neurodevelopment by regulating protein synthesis. Mutations in the regulatory components Tsc1 and Tsc2 of mTOR-Complex1 (mTORC1) cause the disease Tuberous Sclerosis (TSC) in humans. The majority of TSC patients develop neurological problems including seizures, mental retardation and autism. Recent studies investigated the role of mTOR pathway dys-regulation in excitatory cortical cells, however its role in the development of cortical GABAergic interneurons and the specific contribution of altered GABAergic cells in disease manifestation remain largely unknown. Here, we investigated whether and how Tsc1 knockout perturbs GABAergic circuit development, both *in vitro* and *in vivo*.

To investigate the role of mTORC1 activation in BC development, we knocked out Tsc1 expression, by transfecting *Cre*-GFP driven by a promoter specific for BCs in cortical organotypic cultures prepared from Tsc1lox mice. Tsc1 knockdown *in vitro* caused a precocious increase in bouton density and terminal branching formed by mutant BCs, which was reversed by Rapamycin treatment. These data suggest that mTOR pathway hyperactivation affects the timing of BC synapse maturation. To investigate the role of mTORC1 in GABAergic cells *in vivo*, we bred Tsc1lox mice with *Nkx2.1*-Cre and *PV*-Cre mice. At P18, Tg(*Nkx2.1Cre*),$Tsc1^{flox/flox}$ mice showed both mTORC1 hyperactivation and somatic hypertrophy in BCs along with increased expression of PV in the perisomatic region of pyramidal neurons. In contrast, by P45 we found a reduction of PV-gephyrin (post-synaptic GABAergic marker) perisomatic puncta density. Study of BC morphology in organotypic cultures from the *Nkx2.1*-Cre conditional knockout confirmed the occurrence of a faster maturation rate initially which however collapsed at later stages. Additionally Tg(*Nkx2.1Cre*),$Tsc1^{flox/flox}$ mice exhibit Tsc1 dose-dependent deficits in working memory and social behaviour. All together, these results suggest that controlled mTOR activation regulates both the time course and the maintenance of BC synapses.

Dysfunction of GABAergic neurotransmission has been implicated in several disease states like epilepsy and in some patients it is associated with mutations in the $GABA_A$ receptor. How these mutations affect the BC cell maturation process remains largely unknown. To address this question, we used the Cre-lox strategy to knockout the endogenous *GABRA1* gene coding for the $GABA_A$-receptor alpha-1 subunit in single PV-expressing basket cells (BCs) in organotypic cultures. Cell-autonomous loss of *GABRA1* reduced the extent of BC innervation field suggesting changes in inhibitory inputs caused by the absence of $GABA_AR$ α1 subunit may alter BC development. Over-expression of mutant $GABA_AR$ α1 subunits (found in patients diagnosed with epilepsy) show similar effects in terms of BC target

coverage. Further studies involved the effect of these human mutations in the development of Pyramidal cell dendritic spines, which are the preferential site for excitatory synapse formation. Altogether, this data show for the first time that different *GABRA1* mutations associated with genetic epilepsy syndromes can affect dendritic spine and GABAergic bouton formation in a mutation-specific manner.

Table of contents

List of figures

Chapter 1: Introduction

Chapter 3: Single-cell genetic expression of mutant $GABA_A$ receptors causing Human genetic epilepsy alters dendritic spine and GABAergic bouton formation in a mutation-specific manner

List of tables

List of abbreviations

4E-BP1: eIF4E-binding protein 1
5HT: 5-hydroxytryptamine (serotonin)
BC: Basket cell
BDNF: brain derived neurotrophic factor
BRRS: Bannayan-Riley-Ruvacalba syndrome
BZ: Benzodiazepine
CGE: Caudal ganglionic eminence
CNS: Central nervous system
CR: Calretinin
CRMP2: Collapsing response mediator protein 2
CS: Cowden syndrome
EEG: Electroencephalogram
E_{GABA}: equilibrium potential for GABA
EGFP: Enhanced green fluorescent protein
eIF4E: Eukaryotic translation initiation factor 4E
EP: equivalent to post-natal
FIP200: Focal adhesion kinase family-interacting protein of 200 kDa
FKBP12: 12-kDa FK506-binding protein
FMRP: Fragile X mental retardation protein
FXS: Fragile X syndrome
GABA: γ-aminobutyric acid
GAD: Glutamate decarboxylase
GAP: GTPase activating protein
GDNF: glial derived neurotrophic factor
GFP: Green fluorescent protein
GGE: Genetic generalized epilepsies
GSK3-β: Glycogen synthase kinase 3 β
HCO_3^-: Bicarbonate
HEK: Human embryonic kidney
HGF/SF: hepatocyte growth factor/scatter factor
Hz: Hertz
IPSC: Inhibitory post-synaptic current
IUE: *In utero* electroporation
KCC2: K-Cl-cotransporter 2
kDa: kilo Dalton
KO: Knockout
LDD: Lhermitte-Duclos disease
LGE: Lateral ganglionic eminence
L-LTP: late-Long term potentiation
LOH: Loss of heterozygosity
LTD: Long-term depression
MAP: Mitogen activated protein kinase
MGE: Medial ganglionic eminence
MRI: Magnetic resonance imaging
mRNA: messenger Ribonucleic acid
mSin1: MAP kinase–interacting protein 1
mTOR: Mechanistic target of Rapamycin

mTORC1/2: mTOR complex 1/2
Na^+: Sodium
Narp: Neuronal activity-regulated pentraxin
NCAM: Neural cell adhesion molecule
NF1: Neurofibromatosis
NGS: Next-generation sequencing
NKCC1: Na-K-Cl-cotransporter 1
NMDA: N-methyl-D-aspartic acid
NPY: Neuropeptide Y
Nrg1: Neuregulin 1
P: post-natal
PBS: Phosphate buffered saline
PFA: Paraformaldehyde
PhD: Doctor of Philosophy
PHTS: PTEN Hamartoma tumor syndromes
PI3K: Phosphatidylinositol 3-kinase
PKC-α: Protein kinase C- α
POA: Pre-optic area
PPAR-γ: Peroxisome proliferator-activated receptor γ
PRAS40: proline-rich Akt substrate 40 kDa
PSA: Polysialic acid
PTEN: Phosphatase and tensin homolog
PV: Parvalbumin
Rheb: Ras homolog enriched in brain
RNAi: RNA interference
rRNA: ribosomal Ribonucleic acid
S6K1: S6 kinase 1
SEGA: Subependymal giant cell astrocytoma
SEM : Standard error of the mean
SGK1: Serum- and glucocorticoid-induced protein kinase 1
SREBP1/2: Sterol regulatory element-binding protein 1/2
SST: Somatostatin
SVZ: Sub-ventricular zone
SYT2: Synaptotagmin 2
TIF-1A: tripartite motif-containing protein-24
TrkB: Tropomyosin receptor kinase B
tRNA: transfer Ribonucleic acid
TSC: Tuberous Sclerosis complex
TTX: Tetrodotoxin
ULK1: unc-51-like kinase 1Atg13: mammalian autophagy- related gene 13
vGAT: Vescicular GABA transporter
VIP: Vasoactive intestinal peptide
WES: Whole exome sequencing
WGS: Whole genome sequencing
WT: wild-type

Acknowledgements

Pursuing my doctoral degree has been a fascinating journey to say the least right from its inception. The success of my PhD training comes with the inner awakening of a curious learner who wants to carry on with this interesting sojourn for the rest of his life. It was a 'dream come true' moment when Dr. Di Cristo interviewed me and had accepted me (I was a foreign student then) although I was neither literate in neuroscience nor was proficient to work in a francophone environment.

Dr. Di Cristo's constant supervision and guidance played the most crucial role to make me realize my own potential. Her patience, honest criticisms and financial support has been vital in realizing and supporting my goals as a young researcher. I will be indebted to her for this valuable training for the rest of my life.

Even before I came to Canada, the greatest support came from my parents and Indrani (my wife) for believing in me and instilling the confidence to face the unknown future that was waiting. Indrani has been the friend who stood by me through the darkest hours during this phase. My labmates, Elie, Patty, Marisol and Martin demand a special mention who became more than colleagues over time as we went through similar challenges on a daily basis. Josianne (we call her JoJo) was my first teacher in the lab from whom I learnt several techniques. Her patience, sincerity and organizational skills have been a great source of inspiration. Bidisha always provided valuable inputs to my project during our Wednesday lab meetings. The opportunity to share a few words in our native tongue (Bengali) with Bidisha was a sheer bonus. Other researchers at HSJ from the Michaud's, Carmant's , Zoha's and Rossignol's lab have been amazing colleagues and have added value to the quality of lab life. A special mention to Ankush and Ciprian who provided interesting discussions (on science, politics, religion and almost everything) which stimulated my grey cells as well as the nicotine receptors in them.

I would like to thank our collaborators Dr. Patrick Cossette and Dr. Pamela Lachance-Touchette for providing a great opportunity to diversify my PhD experience. Ana and Arianne demands a special mention for their assistance in my projects.

I am grateful to Dr. Elsa Rossignol and Dr. Lionel Carmant for their valuable feedbacks while discussing my project. I also express my gratitude towards my committee members Dr. Parker and Dr. Vande Velde who have provided inputs to give shape to my project during the initial years.

Finally, my heartfelt gratitude for the members of the Bengali diaspora in Montréal whose blessings and support have been phenomenal during this phase.

Chapter 1: Introduction

The mammalian cortex is made up of a multitude of neurons of which the vast majority are excitatory cells. Conversely, inhibitory cells (interneurons) constitute only ~20-30% of neurons. These interneurons synthesize and release GABA which is the major inhibitory neurotransmitter in the adult CNS. The main focus of my PhD work is on the mechanisms regulating inhibitory circuit development. From a clinical perspective, growing evidence suggests that maldevelopment of the inhibitory circuits can lead to severe neuro-developmental disorders. In this doctoral dissertation, I look into the role of two distinct genes namely, (a) spell it out the first time *TSC1* and (b) spell it out the first time *GABRA1* in GABAergic cell development in the cortex, using mouse genetics, organotypic cultures, confocal imaging and behavioural analysis. Further, this work shows that single-cell genetics may be a powerful tool to study neurodevelopmental disorders.

1.1 Development of GABAergic cells in the cortex

Probably, the most striking feature of the inhibitory neuronal population is its diversity, due to differences in terms of gene expression, electrophysiological properties and connectivity. For example, Parvalbumin (PV)-expressing basket cells in the cortex are fast-spiking (short action potential and high frequency of firing) and target the somata and proximal dendrites of neighbouring cells (**Figure.1.1**). Condensing this large and heterogeneous population into finite groups of interneurons based on the above mentioned features has been a challenging task. However, with the advent of new genetic tools recent studies have been able to dissect this diverse population into more generalized groups. A second striking feature of GABAergic cells lies in its long developmental time window which extends to several weeks after birth in rodents. Both of these aspects have been discussed in length in the following

two sections and primarily try to throw light on "from where they came" and "who they became" through intricate cellular and molecular mechanisms.

1.1.1 Spatial and temporal origins of cortical inhibitory neurons

The answer to understanding the basis of interneuron diversity in the post-natal cortex lies in the underlying mechanisms of gene expression of progenitor cells during embryonic stages in sub-cortical proliferative zones. In the embryonic brain, the telencephalon (which later forms the cortex in the adult brain) has three distinct zones which host the sub-cortical progenitor cells, namely the medial ganglionic eminence (MGE) and caudal ganglionic eminence (CGE) along with the preoptic area (POA) (**Figure.1.2**).

The medial ganglionic eminence is the major contributor of the cortical inhibitory cell population (~50-60%) and is the birthplace of large population of inhibitory progenitor cells in mice. The major populations of MGE-derived GABAergic interneurons are exclusively PV (Parvalbumin) and SST (Somatostatin)-expressing cells while a smaller diaspora of cells also express Reelin, NPY (Neuropeptide Y) or CR (Calretinin) along with SST. The *Dlx* class of genes have been the earliest genes to be correlated with interneuron migration from sub-pallium to cortex[1]. Both PV- and SST- expressing interneurons greatly depend on the transcription factor *Nkx2.1* for their generation. Previous studies have shown that *Nkx2.1* mutants lacked their ability to generate more than half of these two interneuron populations in the cortex[2]. Later studies involving both *in vitro* experiments[3,4] as well as *in vivo* transplantation analysis[3,5] showed that MGE-derived cells in the cortex consist of ~65% of PV- and remaining ~35% of SST-expressing interneurons. The *Nkx2.1* transcription factor has both activator and repressor functions[6]. While it represses the expression of CGE-specific genes, it activates the *Lhx6* gene in PV- and SST-expressing interneurons. *Lhx6* in turn also activates other genes like *Sox6* and *Satb1* which further influences the post-natal

developmental process of the cortical interneurons[7, 8]. Interestingly, the ventricular zone in the MGE has different domains of progenitor cells and based on their spatial location, this region can be subdivided into five zones designated as pMGE1 to pMGE5[9].

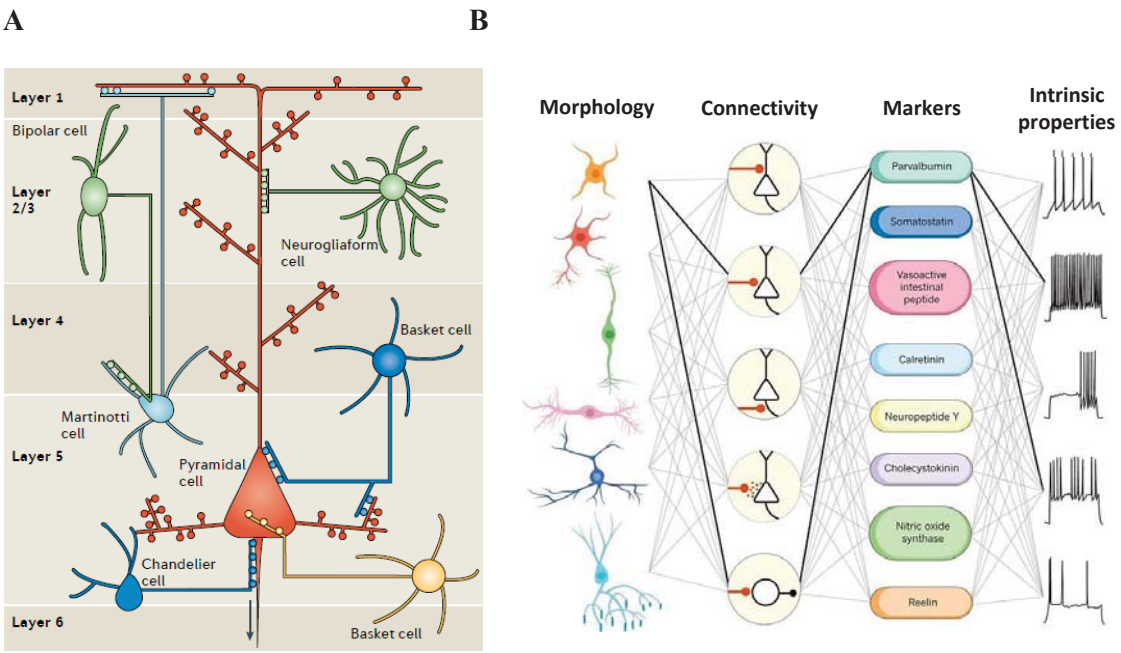

Figure.1.1 ***A***, Different classes of interneuron in the cortical layers showing distinct pattern of connectivity based on the cellular region of target (adapted from Marin, 2012)[216]. ***B***, Diversity of interneurons based on morphology, connectivity pattern, marker expression and intrinsic firing properties (adapted from Kepecs and Fishell, 2014)[11].

The role of the CGE in its contribution to the cortical interneuron population is slowly emerging and has been recently estimated that ~30-40% cortical interneurons originate from CGE. The CGE region is a caudal fusion of the MGE and LGE (Lateral Ganglionic Eminence) which begins at the coronal level of the mid-thalamus. Using *in utero* transplantation techniques, Nery and co-workers showed for the first time that CGE progenitor cells migrated to the cortex where they gave rise to a robust population of interneurons[12]. Further studies involving both *in vitro* and *in vivo* studies have corroborated this finding demonstrating that cortical interneurons with bipolar and double-bouquet

morphology are derived from the CGE and express CR (but not SST) and/or VIP[5,13]. Further studies show that the transcription factor *CoupTF2* is richly expressed in CGE progenitors and experimental evidence support their role in migration of CGE-derived interneurons to the cortex. Almost, all CGE-derived interneurons express the $5HT_{3a}$ receptor[14].

Finally, the POA is the third region that contributes to the cortical interneuron diversity[15]. Located ventrally to the MGE, the POA progenitor cells also express *Nkx2.1* transcription factor but none of them express *Lhx6*[9]. A small proportion of these POA cells express *Nkx5.1* and have electrophysiological properties similar to fast adapting neurons. However, they do not express PV, SST, CR or VIP making them distinctly different from interneurons derived from the MGE and CGE.

These progenitors trudge through a long migratory path from subcortical ventral telencephalon to the cortex (**Figure.1.2**). This sojourn is guided by a variety of chemorepulsion, chemoattraction, migratory substrates and motogens[16]. These precursor cell show a strong migratory drive and express various motogens like hepatocyte growth factor/scatter factor (HGF/SF), glial derived neurotrophic factor (GDNF), brain derived neurotrophic factor (BDNF) and NT4 promoting tangential migration[17-19]. Chemorepulsive guidance cues provided by Eph-ephrin and Slit- Robo signalling have been well characterized in earlier[20-22]. Chemoattractrants involved in this guidance process include ErbB4-Neuroligin 1 signalling and netrin[23, 24]. Therefore a variety of cues work in concert to ensure the passage of cortical interneurons to their final destination.

A **B**

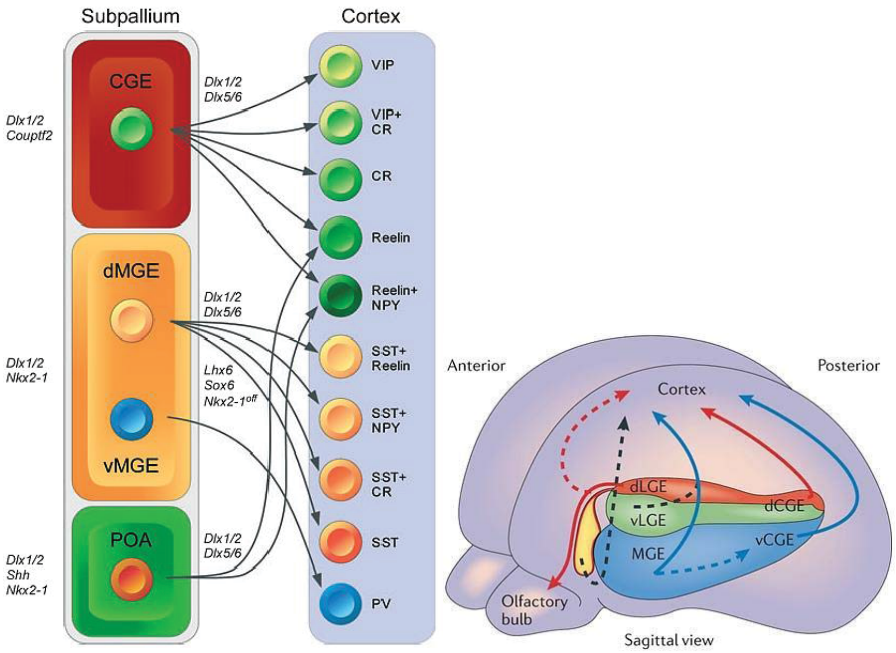

Figure 1.2. ***A***, Distinct transcriptional profiles of spatially segregated progenitor cells give rise to cortical interneuron diversity (adapted from Gelman *et al*, 2010)[10].***B***, Migration pathways of cortical interneuron subgroups from the ventral telencephalon (adapted from Wonders and Anderson, 2006)[25].

1.1.2 Post-natal development of Parvalbumin (PV) cells in the cortex

1.1.2.1 PV cell identity and function

After migrating to the cortex, the majority of MGE-derived interneurons become fast-spiking and start to express the calcium binding protein Parvalbumin (PV) by post-natal day 14(P14). This is achieved through the consorted action of several genes which includes *Nkx2.1*, *Dlx5*, *Dlx6*, *Lhx6* and *Sox6*. Conversely, these genetic factors are not the only facets that shape the post-natal development of these cells. Multiple studies have focussed on the role of neuronal activity and sensory experience in shaping the connectivity of these cells. But before we try

to understand “how” they mature, it is important to know “what” a mature PV neuron is in terms of morphology and function.

Parvalbumin (PV) expressing cells constitute about ~50% of the total interneuron population in the rodent cortex and even lesser in humans[26]. The majority of these cells are PV-expressing basket cells (BC) which target the soma and proximal dendrites of principal excitatory cells while a less-abundant population consists of axon initial segment targeting Chandelier cells. The PV-expressing BCs can be further subdivided based on their morphology into large BCs, small BCs and nest BCs. The electrophysiological properties make these cells unique and the most reliable source of inhibition in the cortex. PV-expressing BCs exhibit fast membrane kinetics, brief action potentials with large after hyperpolarisation , low input resistance and can sustain high frequency of firing rate[27,28]. The high expression of K_v3 voltage gated potassium channels essentially allows fast repolarization and termination of action potential rendering them capable of displaying such fast kinetics[29, 30]. Additionally, the BC’s express P/Q type of presynaptic Ca^{2+} channels which facilitates the coupling of neurotransmitter release after an action potential[31, 32]. Also, the rich abundance of Ca^{2+} binding proteins like PV and Calbindin allows efficient buffering of Ca^{2+} inside the cell which in turn may shield it from Ca^{2+}-induced excitotoxicity following fast-spiking activity.

Our past understanding on the role of interneurons was reduced to providing local inhibition to excitatory cells through release of GABA, which serves as a guard against excess excitation[33]. However, the role of inhibition has been shown to be far more sophisticated since these interneurons form microcircuits at the local level and allows flow-control of information in the network in response to specific behavioural events. These microcircuit motifs can provide both feedforward and feedback inhibition. In feedforward inhibition, afferent excitatory axons activate both principal cells and interneurons in parallel. Feedback

inhibition occurs in a circuit when afferent excitatory axons activate principal cells which in turn activate interneurons forming a series. This type of inhibition can be further classified into recurrent and lateral feedback inhibition (**Figure.1.3**).

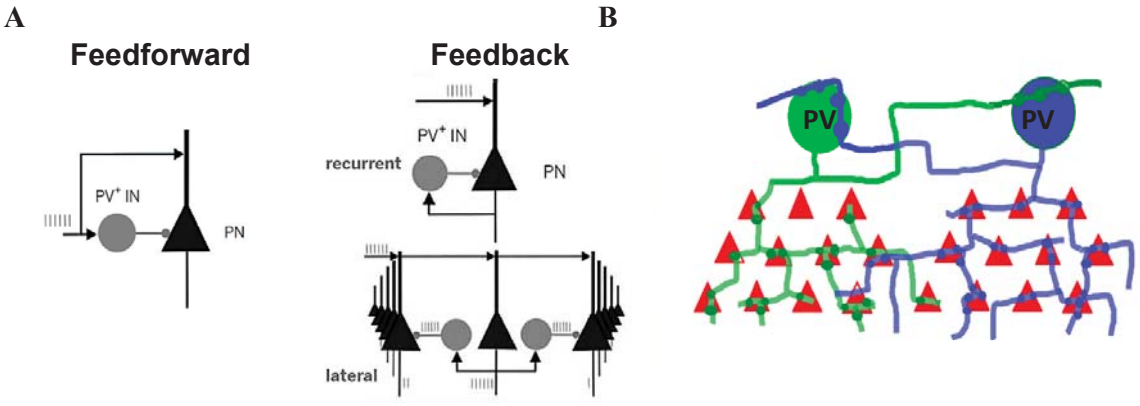

Figure 1.3. ***A***, Inhibitory microcircuits can provide both feedforward and feedback inhibition. Feedback inhibition can be further divided into recurrent and lateral inhibition. ***B*****,** Disinhibition of interneurons by inhibition of one interneuron by another (adapted from Hu *et al*, 2014)[34].

PV-expressing BCs perisomatically connect hundreds of neighbouring pyramidal cells and this allows them to control the excitability of the target cells. In this way BCs are able to provide feed-forward inhibition and execute temporal control of summation of excitatory inputs and spike generation within populations of pyramidal cells[35 ,36]. Interestingly, these PV-expressing BCs are highly connected with each other through both chemical and electric synapses (gap junctions) thereby creating a network of synchronously active BCs. This vast network of BCs is capable of triggering and maintaining gamma oscillations (high frequency waves of 30-90 Hz) in the cortex[37, 38]. Specifically, when fast-spiking BCs in the barrel cortex were activated using optogenetic techniques, gamma oscillations were amplified[39]. In contrast, specific activation of pyramidal cells only generated low frequency oscillations thereby dissociating the role of BCs in generation of gamma oscillations. In a separate study

this finding has been recapitulated when light-driven (optogenic) inhibition of BC activity supressed gamma oscillations *in vivo* whereas activation of BCs generated emergent gamma-frequency rhythmicity[40]. PV cells can also form disinhibitory microcircuits which have been recently implicated in controlling ocular dominance plasticity (permanent cortical unresponsiveness to one eye after loss of vision). Recent studies have shown that excitatory pyramidal cells through less activation of PV cells can in turn reduce inhibitory effects resulting higher excitation in them[41].

1.1.2.2 PV cell development

The plethora of functional paradigms PV expressing BC cells are involved (both in singularity and as a network) resides in its capability to provide inhibition to a vast population of target neurons. This probably justifies the long duration of their post-natal maturation process in order to innervate and form synapses on a finite number of neurons.

Various factors that shape maturation of PV-expressing BCs have come to light over the past two decades. GABA, apart from being the main inhibitory neurotransmitter in the vertebrate brain, also serves as a trophic factor that guides neuronal migration and neurite growth both during embryonic and post-natal development. New born pyramidal cells express $GABA_A$ receptors and receive GABAergic inputs on them even before excitatory synapses are formed[42]. In fact, GABA has a depolarizing effect and essentially acts as an excitatory neurotransmitter in immature neurons allowing efflux of Cl^- through $GABA_A$ receptors; which promotes Ca^{2+} influx and signalling[43, 44]. The physiological basis of the excitatory function of GABA was correlated with high level of *NKCC1* (Na-K-Cl-cotransporter 1) expression in the immature neurons. *NKCC1* causes increase in Cl^- inside the cell which in turn shifts the equilibrium potential for GABA (E_{GABA}) towards more depolarized values[45]. Therefore $GABA_A$ receptor activation leads to efflux of Cl^- and causes depolarization of the

cell. A developmental switch occurs when the level of *KCC2* (K-Cl-cotransporter 2) expression increases leading to reduced levels of Cl^- inside the cell. This causes a shift of the E_{GABA} towards more negative values allowing GABA to have an inhibitory effect in mature neurons[46, 47]. Overall, it is well established that GABA plays an important role in the development of the immature brain.

However, the synaptogenesis and refinement of the innervation pattern of PV-expressing BCs continues till late adolescence both in rodents and primates[48-50] Chattopadhyaya and co-workers have reported the innervation pattern of BCs during post-natal weeks in organotypic culture system. This work has segregated the developmental time windows into various phases where BC innervation and target coverage is progressively enhanced between EP14 to EP32[48] (**Figure.1.4**).

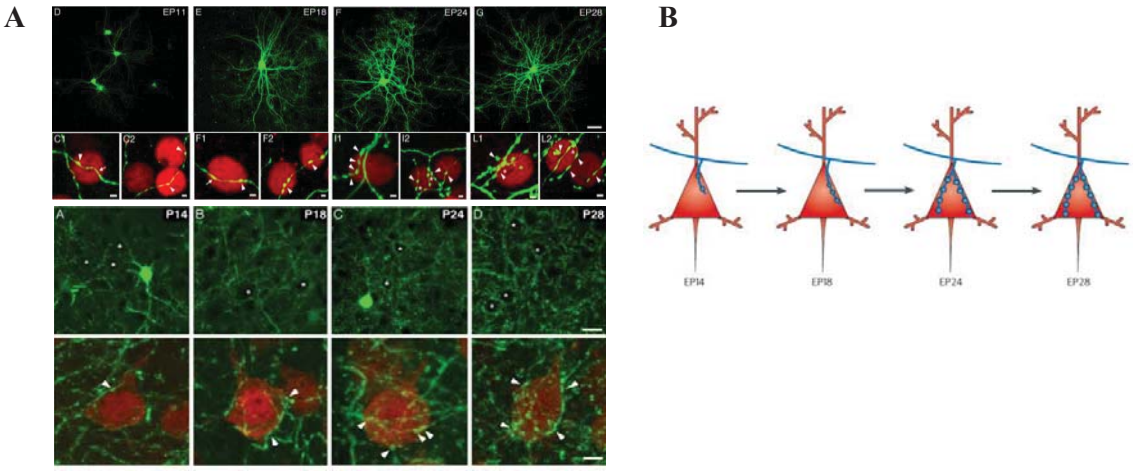

Figure 1.4. ***A***, PV-expressing basket cells show increase in innervation field of target cells, axonal arborisation and synaptic density on target excitatory cells both in organotypic cultures and in vivo during the second and fourth post-natal weeks (adapted from Chattopadhayaya *et al*, 2004)[48]. ***B***, Schematic representing increased branching and synaptic density on target cells during this phase (adapted from Huang *et al*, 2007)[51].

The cellular and molecular mechanisms involved in this maturation process are slowly emerging and implicates genetic factors, neuronal activity and sensory experiences working in concert to shape up their precise connectivity. Deprivation of sensory experience in the visual cortex either through dark rearing or intra-ocular TTX injection leads to reduced innervation of BCs[48,49]. Also sensory deprivation through whisker trimming alters the maturation process of PV cells in the somatosensory cortex[52]. Some molecules have been identified whose expression levels are activity and/or sensory experience dependent. One of the first molecules identified to be involved in GABAergic interneuron maturation process is Brain Derived Neurotrphic Factor (BDNF), which is expressed mainly by pyramidal cells. BDNF is upregulated following light stimulation in the visual cortex[53,54] and is implicated in inhibitory synapse formation in hippocampal and cortical cultures[55,56].

Interestingly, GABA is another molecule that plays a strong role in regulating synapse maturation apart from its role as a trophic factor. GABA is produced by two enzymes, the GAD_{67} (Glutamate decarboxylase) which is the rate limiting enzyme and accounts for ~90% of GABA content and GAD_{65}, which accounts for the remaining ~10%. Unlike GAD_{67}, GAD_{65} is primarily localized at the pre-synaptic terminals[57]. Manipulating the level of GABA synthesis and release at different time points of developmental have yielded interesting insights. Deletion of GAD_{67}, the chief GABA producing enzyme in single BCs during the peak of maturation phase resulted in reduced connectivity however did not affect connectivity when removed at later stages[58]. Germline reduction in single copy of GAD_{67} recapitulates aberrant reduction in perisomatic synapse maturation. Additionally, these deficits were rescued by agonists of $GABA_A$ and $GABA_B$ receptors suggesting a receptor-specific effect of GABA-mediated signalling during GABAergic synapse maturation. Separate studies have shown that transcription of *Gad1* gene which leads to GAD_{67} expression are both activity-dependent[59] and sensitive to experience[60]. More recent study has shown that when GABA

neurotransmission is modulated by lowering excitability to fire action potentials it negatively affects global target coverage of single BCs at various time points in the developmental time window[61]. However, affecting synaptic vesicle release had opposing effects depending on the developmental stage of the BC. Wu and co-workers showed that complete removal of GABA synthesis by knocking out both GAD_{67} and GAD_{65} or removing vGAT leads to over-proliferation of small synapse and overgrowth of axons[62]. This finding is corroborated by Baho and Di Cristo where disruption of GABA release lead to hyper-connectivity of target somas in single BCs. In summary, these results indicate that GABA *per se* is not essential for inhibitory synapse formation however GABAergic neuronal activity is necessary for validation and stabilization of synapses.

(PSA) is another molecule which is a negative regulator of synapse formation in the developing visual cortex. PSA is a long, linear homopolymer of α-2, 8-linked sialic acid that attaches almost exclusively to the neural cell adhesion molecule (NCAM) in vertebrates[63]. NCAMs exist as three different isoforms, NCAM120, NCAM140 and NCAM180.The levels of PSA in the visual cortex declines with eye opening and conversely this decline is impaired by visual deprivation. Enzymatic removal of PSA leads to premature increase in innervation of target cells by BCs[64]. Further study has shown that NCAM removal specifically in BCs during the maturation phase of their synaptic connections causes reduction in both the percentage of innervated pyramidal cells and density of synapses formed by BC onto them. This reduction can be rescued by addition of NCAM120 and NCAM140, but not NCAM180[65].

So far, a handful of genetic factors have been identified which is involved in shaping the developmental process of cortical PV cells. However, future studies will reveal more such genes that shape this process and how the expression and function of these genes are affected in neurodevelopment disorders.

Chapter 1.2 $GABA_A$ receptors in cortical synapse development

GABA is the major inhibitory neurotransmitter in the adult CNS and acts by binding to post-synaptic GABA receptors. GABA receptors are of 3 types, (1) $GABA_A$ receptors (ionotropic) (2) $GABA_B$ receptors (metabotropic) and (3) $GABA_C$ receptors (ionotropic). $GABA_A$ is most abundantly expressed in the adult mammalian cortex. GABA action mediated by $GABA_A$ receptors plays an important role in cortical development. This section briefly describes the genetics, structure and expression of $GABA_A$ receptors in the cortex and its subsequent role in epilepsy.

1.2.1 $GABA_A$ receptors in the developing brain

$GABA_A$ receptors are pentameric channels composed of different combination of subunits which differ in kinetic, pharmacological and localization properties (**Figure 1.5**). $GABA_A$ receptors are ionotropic receptors. These receptors open upon binding of the neurotransmitter GABA, thus allowing passage of anions (Cl^- and HCO_3^-) through them. $GABA_A$ receptors are also targets of several pharmacological agents like benzodiazepine-site (BZ-site) ligands, barbiturates, neurosteroids, intravenous anaesthetics (e.g. propofol and etomidate), inhalation anaesthetics (e.g. Isoflurane) and alcohol. In mature neurons, under normal conditions, the activation of $GABA_A$ receptors leads to hyperpolarization of cell membrane potential and inhibition of neuronal activity. $GABA_A$ receptors are not only present at postsynaptic sites, but also in extra-synaptic membranes. Earlier studies using whole-cell voltage-clamp recordings in developing neurons have shown that these extra-synaptic $GABA_A$ receptors are responsible for tonic inhibition[66,67], while synaptic $GABA_A$ receptors mediate phasic inhibition.

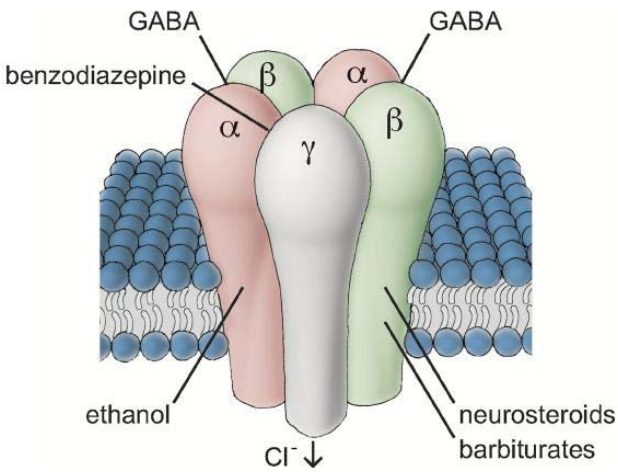

Figure 1.5. Schematic illustration of the $GABA_A$ receptor and its associated binding sites (adapted from Uusi-Oukari and Korpi, 2010)[68].

1.2.1.1 $GABA_A$ receptor genetics

A complex set of genes comprising of 19 genes codes for different $GABA_A$ subunits in mammals. These genes encode for a total of 8 subunit classes, namely α1–α6, β1–β3, γ1– γ3, δ, ε, θ, π, ρ1- ρ3[69]. Further gene mapping studies showed that most genes are clustered in vertebrate chromosomes[70,71]. Fourteen of the 19 human $GABA_A$ receptor genes are clustered on four chromosomes, 4p12-p13, 5q31-q35, 15q11-q13 and Xq28[71]. Two clusters of four genes encode two α subunits, one β subunit, and one γ subunit (*GABRA2, GABRA4, GABRB1*, and *GABRG1* on chromosome 4, and *GABRA1, GABRA6, GABRB2*, and *GABRG2* on chromosome 5). Chromosome 15 contain a cluster of three genes which comprises one α subunit gene (*GABRA5*), one β subunit gene (*GABRB3*), and one γ subunit gene (*GABRG3*). Another cluster in X chromosome consists of one α subunit gene (*GABRA3*), the θ subunit gene (*GABRQ*), and the ε subunit gene (*GABRE*). The θ and ε subunits have 50% identity similar to β and γ respectively. In mice, $GABA_A$ receptor genes are clustered similar to humans[69]. This clustering of GABA receptors which is evolutionary favoured could be because of in-built mechanisms that regulate the coordination of their expression.

Alternatively, it is also possible that this clustering arose from an ancestral αβγ receptor set by a series of duplications, sequence divergences, and chromosomal translocations[72].

1.2.1.2 $GABA_A$ receptor subunit composition and localization

The most common subunit stoichiometry for a $GABA_A$ receptor is thought to be 2α/2β/γ. Sometimes the γ subunit is substituted by δ or θ[69,73]. Studies from other groups have reported the existence of different stoichiometry comprising of only α and β, 2α/β/2γ and 2α/β/2ε[74]. It is still not properly understood how these pentameric assemblies are formed. In the regular pentameric composition 2α/2β/γ, γ2 is more frequent than γ1 or γ3 and both the α and β subunits can be either identical or different. These combinatorial possibilities allow for at least 36 distinct $GABA_AR$ subtypes in CNS neurons. A handful of studies using *in situ* hybridization have revealed that the six α subunit variants largely correspond to distinct $GABA_A$ receptor subtypes, each with a specific distribution pattern that overlaps only partially with that of other α subunits[75]. On the other hand, according to the Allen Brain Atlas, the ρ1 and ρ2 subunit mRNAs (corresponding to $GABA_C$ receptors) are restricted to the superficial layers of the superior colliculus, and the π subunit mRNA is undetectable in the adult mouse brain. The presence of so many different $GABA_A$ receptors, which differ in kinetics properties, allow for a fine-tuning of inhibition in CNS.

1.2.1.3 Maturation of $GABA_A$ receptors in cortical interneurons and pyramidal cells

$GABA_A$ receptors are present in the brain from a very early stage in neuronal precursor cells. Earlier study in the rodent brain reported the presence of $GABA_A$ receptors in neural stem cells[76,77] as well as migrating neuroblasts[78]. Interestingly, $GABA_A$ receptor is expressed in these precursor cells long before GABAergic synapses are formed. $GABA_A$ receptors composition undergoes a gradual change over the course of neuronal maturation. In the rat brain, the expression of α3, α5, and β3 mRNAs starts at late embryonic stages and peaks

during early postnatal development. Over time the expression of these three genes lowers and correspondingly there is increase in expression of α1, α4, β2, and δ during postnatal development in cortical neurons. The adult brain predominantly expresses these subunits. Also the expression of α2 and γ2 remain fairly constant during development[79]. These developmental changes in subunit expression are strongly correlated with decrease in decay time constant (τ) of GABAergic IPSC (inhibitory post-synaptic current). MGE-derived PV-expressing cells in the neocortex acquire mature IPSC properties only after the third or fourth postnatal week which parallels with the decrease in τ_{IPSC} in these cells[80,81]. Similarly, CGE-derived $5HT_3R$-expressing cortical neurons also display a sharp decrease in τ_{IPSC}[82]. These developmental changes in terms of subunit expression also occur in excitatory cells. In cortical pyramidal cells, a similar decrease in IPSC decay kinetics is associated with upregulation of α1 and α4 and downregulation of α3 and α5 $GABA_A$ receptor subunits[83-86]. Altogether, it seems the changes in α subunit expression are a common phenomenon across all cortical neurons (both inhibitory and excitatory). Indeed, the increase in α1 subunit expression during development is observed both in rodents and primates, suggesting this are an evolutionary conserved process in mammals[87,88]. The α subunits also differ in their sub-cellular distribution. While the α1 is uniformly distributed in the axosomato-dendritic domains, α2 is mainly located in the axon initial segment[89,90]. In summary, these observations suggest that $GABA_A$ receptor properties are finely regulated both in time and location, thus increasing the versatility of GABA-mediated inhibition.

1.2.1.4 Specific roles of $GABA_A$ receptors subtypes

Several studies involving constitutive deletion of $GABA_A$ receptor subunit genes indicate that deletion of one subunit can lead to changes in distribution and expression pattern of remaining subunits. For example, *GABRA*1-KO (α1-KO) mice show upregulation of α2-containing $GABA_A$ and α3-containing $GABA_A$ receptors in regions where the a1 subunit is

abundant[91,92]. Also, δ-KO mice show increased α4 subunit expression as well as altered subcellular distribution, where α4 is usually associated with γ2 subunit[93]. However, most of the work clearly indicates that deletion of a particular subunit does not lead to a mere replacement by another type in the same cell. This is true especially in neurons, which have both post-synaptic and extra-synaptic receptors. Deletion of α subunit variants leads to loss of postsynaptic receptors and subsequent loss in post-synaptic currents, but extra-synaptic receptors are either unaffected or increased[91,94]. This increase in extra-synaptic receptors could be a compensation for the loss of post-synaptic receptors but needs further explanation. The *GABRA1*-KO (α1-KO) mice survived and displayed only moderate changes in behaviour[91].

Development of knock-in mice has shed more light to our understanding of the role of $GABA_A$ receptor subunits. The H101R knock-in mice, engineered to remove the diazepam-binding site located at the α/γ interface of the pentameric complex have highlighted the role of each of the 4 α subunits[95-98]. In fact, this histidine to arginine mutation did not affect assembly, cell surface trafficking, regulation or gating of the $GABA_A$ receptors. Therefore, these studies allowed classification of the contribution of each subtype to the spectrum of diazepam's effects in terms of behaviour. For example, while α1-containing $GABA_A$ receptors regulate sedation, anxiety-related behaviours are affected by allosteric modulation of α2-containing $GABA_A$ receptors[99]. These results indicate that, due to their subunit composition, $GABA_A$ receptor subtypes are unique entities defined to play specific functional roles, which cannot be interchanged in a specific neuronal type.

1.2.2 $GABA_A$ receptor α1 subunit mutations in seizures and epilepsy

The primary source of inhibition in the cortex is comprised by GABA action mediated through $GABA_A$ receptors and disturbances in inhibition lead to abnormal neuronal activity. Seizures are defined as clinical manifestations of excessive/and or hyper-synchronous activity of neurons. Seizures can arise in different parts of the brain based on pathological conditions (e.g. a head injury). However, when seizures occur in a recurrent and unprovoked fashion chronically, the condition is termed epilepsy. Genetic generalized epilepsies (GGE) constitute ~50% of all epilepsy cases, the cause of which can be attributed to genetic mutations[100] Mutations in $GABA_A$ receptors have been associated with GGE and primarily affect either (1) biogenesis or (2) function of $GABA_A$ receptors.

$GABA_A$R mutation	**Cell surface $GABA_A$R composition**	**Channel gating properties**
A322D	Reduced surface expression	Reduced whole cell current, altered gating kinetics
D219N	unaffected	Altered gating kinetics
K353delins18X	Complete reduction	n/a

Table.1.1 Effect of different $GABA_A$R mutations on cell surface composition and channel gating properties.

As discussed earlier, α1 is the most common and widely expressed $GABA_A$ receptor subunit and several mutations in α1subunit have been identified in epileptic patients[101,102] (**Figure. 1.6**). One important question is how specific $GABA_A$ receptor subunit mutations contribute to the generation of epileptic brain circuits. One popular hypothesis in the field is that pathogenic mutations affect $GABA_A$ currents, therefore acutely altering network activity. On the other hand, many studies demonstrate that GABA actions regulate several steps of circuit development, including synapse formation. Altered GABAergic transmission during critical

development steps may this altered neural circuit formation. Part of my PhD work focussed on understanding the role of specific mutations in α1subunit of $GABA_A$ in morphological synapse development. In the next section I will briefly explain the identity of these specific mutations.

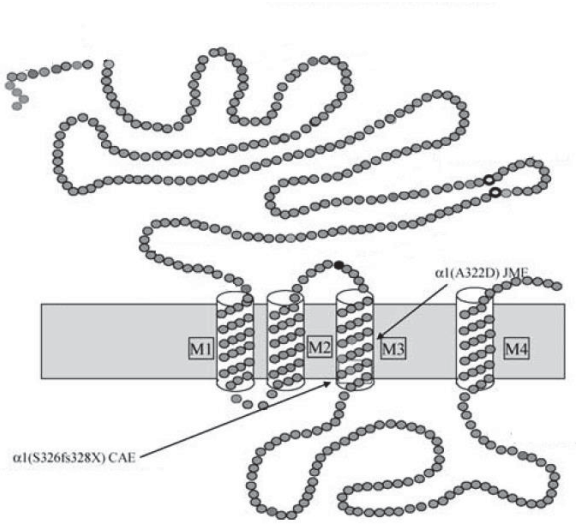

Figure 1.6. Schematic representation of the $GABA_A$ receptor subunit topology, showing the location of autosomal dominant epilepsy mutations associated with 2 reported cases of α1 subunit mutations (adapted and modified from Macdonald and Kang, 2009)[103].

1.2.2.1 $GABA_A$ receptor α1 subunit missense mutations

Missense mutations alter codon nucleotide sequences, which results in incorporation of a different amino acid into the subunit. If the altered amino acid is identified only in patients with the disease, it is classified as a mutation, but if the alteration is also identified in the general population, it is termed susceptibility variant. The $GABA_A$ receptor α1 subunit mutation (A322D) introduces a negatively charged aspartate into the middle of the M3 transmembrane helix of the α1 subunit at residue A322 and is associated with autosomal dominant juvenile myoclonic epilepsy[101]. Co-expression of α1 subunit (A322D) with wild-

type β2 and γ2 subunits reduced both total and surface α1 subunit levels. This mutation also leads to reduction in peak GABA-evoked currents both in heterozygous and homozygous condition. Gallagher and co-workers showed that this mutation lies in a transmembrane domain, which destabilized M3 α helix formation and impaired α1 subunit folding and pentamer assembly[104]. Endoplasmic Reticulum mediated cellular quality control processes are involved in the degradation of the misfolded proteins[104]. Another study reported a D219N missense mutation in a French Canadian family, which lead to reduced expression of $GABA_A$ receptors in the surface along with altering gating kinetics[102].

1.2.2.2 $GABA_A$ receptor α1 subunit frameshift mutations

Frameshift mutations occur because deletion or insertion of one or two nucleotides causes a change in downstream codons, with or without a change in the frameshifted codon. Frameshift mutations alter amino acid sequence and can often lead to a pre-termination codon, which results in altered protein product. One mutation has been identified in the $GABA_A$ α1 receptor (975delC), which is autosomal dominant and is associated with childhood absence epilepsy (brief duration seizures occurring with high frequency). This frameshift mutation was predicted to create a premature stop codon at S326fs328X. Indeed, this frameshift mutation results in a premature translation–termination codon in exon 8 and in 84 base pairs upstream of intron 8, which elicit nonsense mediated decay. Comparison of expression of wild-type and mutant α1 subunits tagged with EGFP (enhanced green fluorescent protein) revealed that this mutation does not allow integration of mutant α1 subunits in the membrane. This was confirmed by confocal studies, which indicated the presence mutant α1 subunits only in the cytoplasm contrary to wild-type α1 subunits present in the membrane. Touchette-Lachance and co-workers found another α1 subunit mutation where an insertion of 25 nucleotides occurred in the intron close to the splice acceptor site of

exon 11(K353delins18X)[102]. Further analysis revealed that this mutation altered $GABA_A$ receptor function by a complete reduction of surface expression.

So far, several mutations in the α1 subunit have been discovered in patients who suffer from milder to severe form of epilepsies. How these mutations affect both excitatory and inhibitory cell connectivity during cortical development is still unclear.

1.3 The role of mTOR pathway in neurodevelopment

The process of post-natal development of neurons requires integration of neuronal activity and synaptic inputs that correspondingly affect several basic cellular processes in order to maintain growth and attain functional maturity. In mammals, the mTOR (originally termed '**m**ammalian' **T**arget **O**f **R**apamycin but now officially termed '**m**echanistic' **T**arget **O**f **R**apamycin) kinase is a protein which provides anchorage to a signalling network called the mTOR pathway. The mTOR pathway (**Figure. 1.7**) integrates a large amount of environmental cues and mainly controls cellular processes that generate or use nutrients and energy. It is gradually becoming clear that the mTOR signalling affects most cellular functions (e.g. protein synthesis, lipid biosynthesis and autophagy); therefore play a central role in controlling basic cell behaviours like growth and proliferation. Consequently, dysregulation of the mTOR pathway has been implicated in several neurodevelopmental disorders like Tuberous Sclerosis (*TSC1* and *TSC2*), PTEN hamartoma tumour syndromes (*PTEN*), Neurofibromatosis (*NF1*) and Fragile X Syndrome (*FMRP*).

1.3.1 The biology of mTOR signalling pathway

The TOR pathway is an evolutionarily conserved signalling pathway and the TOR protein was initially discovered in a genetic screen in budding yeast aimed to identify the target of

the antiproliferative drug Rapamycin[105]. Interestingly, the drug Rapamycin was isolated from the bacteria *Streptomyces hygroscopicus* found in the Easter Island (Rapa nui) by a Canadian scientific exploration team in 1964. The mammalian counterpart of TOR (mTOR), found by three independent research groups, is a protein serine/threonine kinase that belongs to the phosphatidylinositol 3-kinase (PI3K)-related kinase family[106-108]. The mTOR protein can exist as two complexes namely the mTORC1 and mTORC2 (**Figure. 1.8**). The mTORC1 has 6 separate components apart from mTOR, of which the most defining are Raptor (regulatory associated protein of mTOR) and PRAS40 (proline-rich Akt substrate 40 kDa). The mTORC2 is even larger with 7 other components; of these, Rictor (rapamycin-insensitive companion of TOR), the mammalian stress-activated MAP kinase–interacting protein 1 (mSin1), and Protor-1 and Protor-2 (protein observed with Rictor 1and 2) are unique to this complex. The effects of Rapamycin on the two complexes is still not well understood, however it is clear that Rapamycin forms a gain-of-function complex with the intracellular 12-kDa FK506-binding protein (FKBP12)[106,107]. Although it was originally thought that the mTORC2 was insensitive to Rapamycin, recent studies have proved otherwise, as chronic treatment can suppress its assembly and activity[109,110].

Upstream regulation of mTORC1 and mTORC2

mTORC1, the better characterized of the two complexes, can sense a diverse range of intracellular and extracellular cues like growth factors, stress, energy status, oxygen, amino acids, and further controls many major processes, which include protein and lipid synthesis and autophagy. Synaptic signals that activate the mTORC1 involve glutamate activation of NMDA receptors and TrkB receptor activation by neurotrophins (in particular by Brain Derived Neurotrophic Factor, BDNF). These signals converge onto mTORC1 through the PI3K and tuberous sclerosis complex proteins Tsc1 and Tsc2. Tsc1 (also known as hamartin) and Tsc2 (also known as tuberin) form a complex, which is a key upstream regulator of

mTORC1. The Tsc1-Tsc2 complex functions as a GTPase-activating protein (GAP) for the Ras homolog enriched in brain (Rheb) GTPase. The GTP bound Rheb directly interacts with mTORC1 and enhances its kinase activity. PI3K activates Akt (also known as protein kinase B, PKB) which directly phosphorylates *TSC2* rendering it inactive. This leads to activation of Rheb and consequently mTORC1.

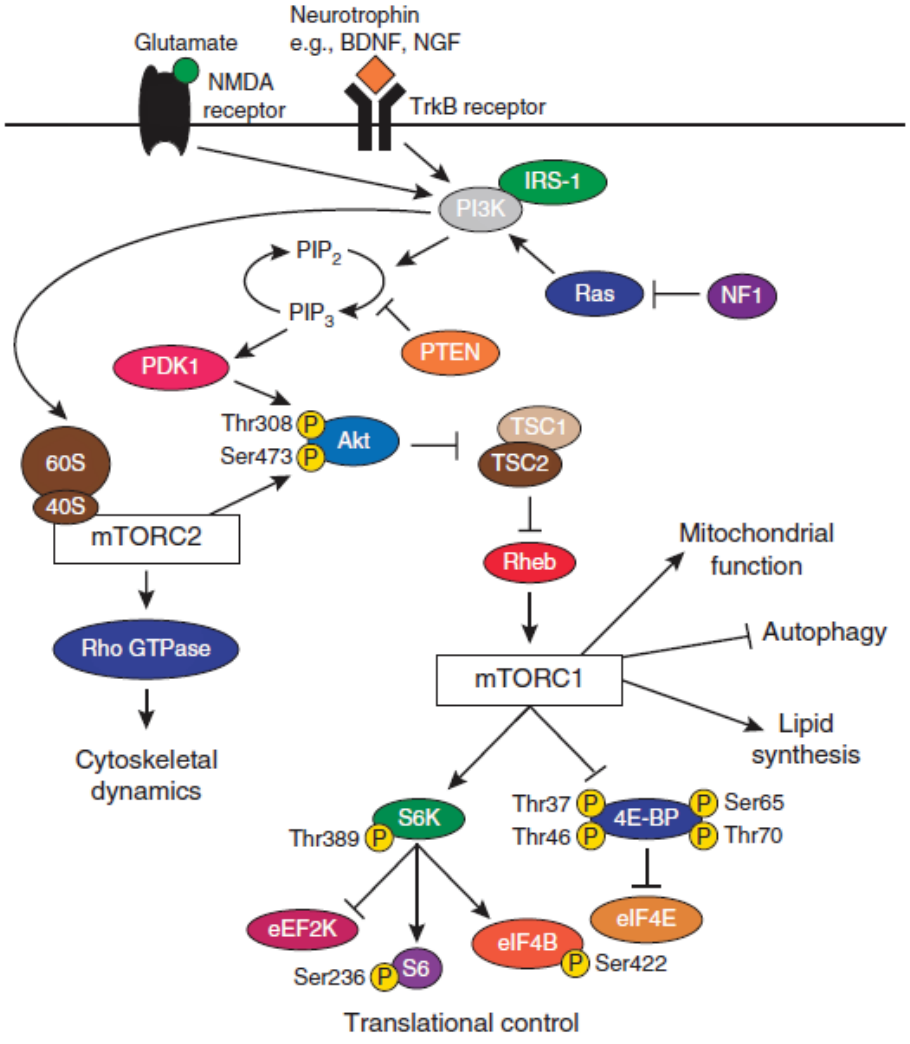

Figure 1.7. The mTOR signalling network in the brain (adapted from Costa-Matiolli and Monteggia, 2013)[111]

Akt can also control mTORC1 in a TSC-independent manner by phosphorylating the PRAS40, which is an endogenous inhibitor of mTORC[111]. PTEN (phosphatase and tensin homolog) is another negative regulator of this pathway, which through its lipid phosphatase activity directly counteracts the kinase function of PI3K and the activation of Akt and mTORC1[112]. Contrary to mTORC1, mTORC2 is more recently discovered and not much is known about its upstream regulation. However, it is known that Akt can regulate mTORC2 by phosphorylating at Ser473. Akt activation through NMDA, glutamate, neurotrophins as well long lasting changes in synaptic strength like L-LTP (late-Long term Potentiation) can converge onto mTORC2[113]. It's a paradox that although mTORC2 does not play a role in protein synthesis *per se*, a reverse suppressor genetic screen in yeast revealed that assembled ribosomes directly bind to and activate mTORC2 in a PI3K-dependent manner[114]. This finding opens the possibility that chronic effects of Rapamycin on mTORC2 could be at least in part mediated through attenuation of ribosome biogenesis controlled by mTORC1.

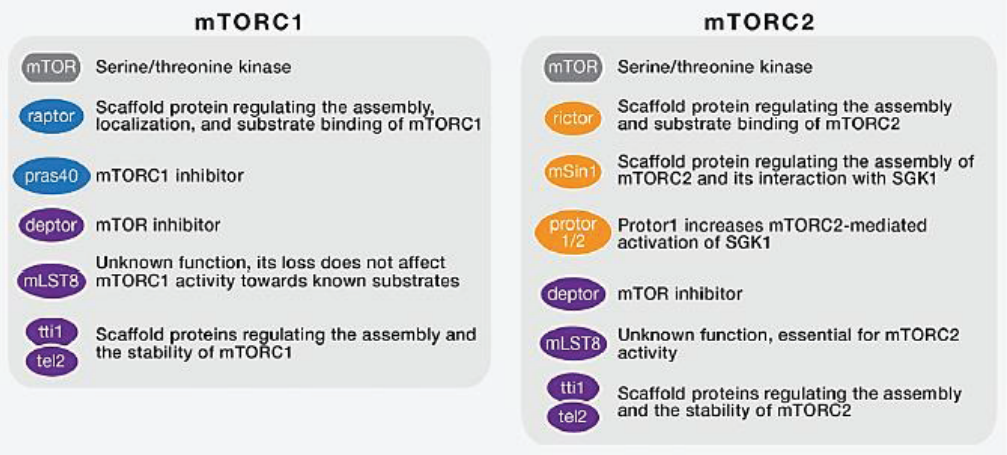

Figure 1.8. The components of mTORC1 and mTORC2 (adapted from Laplante and Sabatini, 2012)[115].

Downstream regulation of mTORC1 and control of cellular processes

Control of protein synthesis has been so far the most well studied process regulated by the mTORC1 both in neurons and other cell types. mTORC1 directly phosphorylates the translational regulators eukaryotic translation initiation factor 4E (eIF4E)-binding protein 1 (4E-BP1) and S6 kinase 1 (S6K1), which separately controls the rate of translation. 4E-BP1 functions as a translational inhibitor, but upon phosphorylation by mTOR it can no more bind to the cap-binding protein eIF4E, enabling it to participate in the formation of the eIF4F complex that is required for the initiation of cap-dependent translation. It was originally thought that S6K1 which phosphorylates the ribosomal S6 protein was involved in the translation of a special class of mRNA called 5'TOP mRNAs (mRNAs characterized by an oligopyrimidine tract at the 5' end). It was later found that although mTOR is responsible for the translation of 5'TOP mRNAs, S6 protein is not involved in the process[116]. So, how mTORC1 controls the translation of these mRNAs still remains unknown. Apart from 4E-BP1 and S6K1, mTORC1 regulates two other downstream effectors that can promote protein synthesis. mTOR activates the regulatory element tripartite motif-containing protein-24 (TIF-1A), which facilitates its interaction with RNA Polymerase I (Pol I) and allows ribosomal RNA (rRNA) expression[117]. mTOR phosphorylation of Maf1 (a Pol III repressor) induces 5S rRNA and transfer RNA (tRNA) transcription[118,119]. Other studies have further clarified the role of mTOR in mRNA translation using inhibitors to block mTOR active sites which consequently reduced the rate of protein synthesis in proliferating cells in culture[120,121] Altogether, these studies suggest that mTOR activation enhances the translational capacity of the cell through activation of several molecules involved in the translational machinery.

Apart from its role in regulating protein synthesis, mTORC1 is also involved in the regulation of lipid biosynthesis. mTOR regulates the sterol regulatory element-binding protein 1/2 (SREBP1/2) transcription factors that control the expression of numerous genes involved in

fatty acid and cholesterol synthesis[122]. mTOR also promotes the expression and activity of peroxisome proliferator-activated receptor γ (PPAR-γ), the master regulator of adipogenesis[123].

Not only does mTOR promote growth by positively regulating anabolic processes (biosynthesis of macromolecules) but also does so by negatively regulating autophagy, a catabolic process. Autophagy is required for degradation of damaged sub-cellular organelles which occurs during nutrient deficiency for cell survival. Inhibition of mTOR leads to activation of autophagosomes, which engulf cytoplasmic organelles and proteins and then fuse with lysosomes leading to degradation of cell components and recycling of cellular proteins. mTOR negatively regulates autophagy by directly phosphorylating ULK1/Atg13/FIP200 (unc-51-like kinase 1/mammalian autophagy- related gene 13/focal adhesion kinase family-interacting protein of 200 kDa)[124,125].

The mTORC2 signalling network

As mentioned earlier, mTOR forms two complexes, mTORC2 is less well characterized of the two. Initially, it was believed that the mTORC2 was insensitive to Rapamycin. Since acute Rapamycin treatment did not affect mTORC2 signalling and FKBP2-Rapamycin complex did not bind to mTORC2, these two observations supported this hypothesis. However, later studies showed that chronic Rapamycin treatment affected mTORC2 signalling by disrupting mTORC2 assembly[109,126]. mTORC2 controls several molecular players downstream to it like Akt, serum- and glucocorticoid-induced protein kinase 1 (SGK1), and protein kinase C- α (PKC-α) (**Figure. 1.9**). mTORC2 activates Akt by phosphorylation at the Ser473 position[127] . Depletion of mTORC2 leads to defective Ser-473-Akt phosphorylation, which in turn affects forkhead box O1/3a (FoxO1/3a) phosphorylation (downstream target of Akt). Interestingly, other targets of Akt like *TSC2* or GSK3-β are

unaffected[128,129]. This indicates that Akt activity is not exclusively regulated by mTORC2. Another target of mTORC2 is SGK1 whose activity is completely abolished upon mTORC2 ablation[130]. Other studies have identified PKC-α as the third target of mTORC2. Activation of PKC-α along with other effectors like paxilin and Eho-GTPases can affect the actin cytoskeleton and hence regulate cell-shape in a cell-autonomous fashion[131,132]. Dysregulation of mTORC1 elicits a feedback response by negatively regulating Akt activity[110,133]. mTOR hyperactivity following Tsc1 inactivation leads to decreased levels of phosphorylated Ser473-Akt. These findings are reversed upon Rapamycin treatment[110] suggesting that attenuation of Akt activity is indeed a feedback effect of mTORC1 dysregulation.

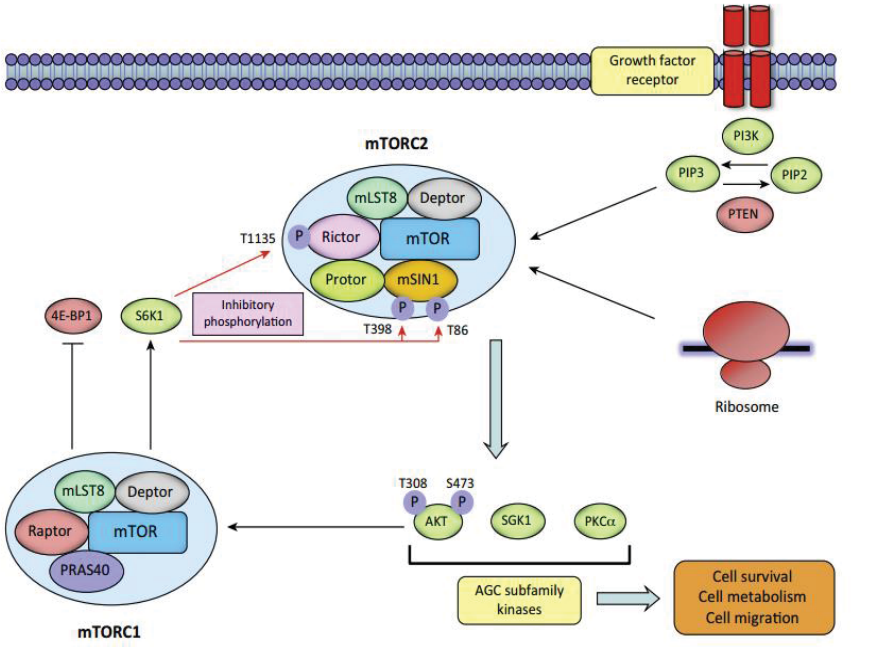

Figure 1.9. The components of mTORC2 signalling pathway (adapted from Masui *et al*, 2014)[134].

1.3.2 Dysregulated mTOR signalling in Tuberous Sclerosis Complex

Given that mTOR plays a central role in the regulation of several fundamental cellular processes, it is not surprisingly the dysregulation of the mTOR pathway leads to several disorders in humans, which are overall termed as 'mTORopathies'. One of the most well-studied genetics mTORopathy is Tuberous Sclerosis Complex (TSC), which is associated with mutations in the genes *TSC1* and *TSC2*, encoding for the proteins hamartin and tuberin, respectively[135].

1.3.2.1 Tuberous Sclerosis

Tuberous Sclerosis Complex (TSC) is an inheritable developmental disease where discrete lesions or growths are observed in several organs of body which includes heart, kidney, lungs, skin and brain[136]. TSC affects 1 in 6000 individuals worldwide. The three major neuropathological features associated with TSC are epilepsy (approximately 90% of patients), intellectual disability (approximately 50%), and autism (approximately 50%). Other neuropsychiatric morbidities may range from sleep disruption, attention-deficit hyperactivity disorder, and anxiety[137]. One of the key pathological features of TSC is the presence of tumor-like cortical malformations called 'tubers'. Various types of human mutations inactivating *TSC1* or *TSC2* can independently lead to hyperactivity of the mTOR pathway. Mutations in TSC2 tend to have more severe phenotypes in patients[138]. Most patients are born with one mutation while a second mutation in the other functional allele occurs during early development in a subset of cells[139,140]. This process is called loss of heterozygosity (LOH) and has been often detected in peripheral and brain lesions[141,142].

It has been more than two decades since mutations in the two genes *TSC1* and *TSC2* have been associated with TS. The genetic inheritance of TSC is autosomal dominant (*TSC1* located on chromosome 9 and *TSC2* on chromosome 16) and follows typical Mendelian

distribution. Mutations in a third gene *TBC1D7* have been hypothesized to cause TSC but have not been associated with patients so far[143]. A broad spectrum of neurological symptoms along with lesions in brain, kidney and skin suggests the genetic mechanism of TSC is rather complicated. The vast majority of genetically diagnosed TSC patients fall under three categories: (1) ~33% of patients have inherited the mutations from their parents[144], (2) 2-3% of patients have *de novo* mutations arising from germline mosaicism[145] and (3) the rest of the patients are thought to have sporadic mutations in early somatic cells, which do not affect all organs to the same extent[146]. The widespread variability in phenotypes is attributed to the timing and spatial origin of these mutations which could be germline, somatic or inherited. Also, because mTOR has a complex biology, various mutations in *TSC1/2* genes could affect different structural and functional domains of these proteins, thus differentially altering cellular localization, protein stability, and integration of upstream signals or regulation of GAP activity. These different effects could underlie the variability in disease manifestations observed in humans[117, 146,147]. Knudson and co-workers had proposed a two-hit hypothesis which results in LOH during development[148]. According to this hypothesis, lesions or tumors are formed when patients with inherited mutations suffer a second, somatic mutation. In fact, other studies have been able to support this hypothesis as they found two hits in the TSC alleles resulting in cortical tubers and subependymal giant cell astrocytoma (SEGA)[149,150]. However, it should be also taken into account that single mutations resulting in loss of function of *TSC1* or *TSC2* can give rise to lesions and tubers in absence of LOH. In summary, it is commonly observed that most TSC patients have one functional allele of *TSC1* or *TSC2* at birth but a second hit can arise in somatic cells of certain patients.

Epileptic seizures are a common phenotype in TSC patients and are often unresponsive to common drug-based therapies[151,152]. In most cases these seizures start very early in the form of infantile spasms which are epileptic spasms arising between three to twelve months after

birth. Although, most children can survive these spasms, over time they acquire other forms of seizures. In many patients, cortical tubers have been strongly correlated with seizure activity in the brain (**Fig 1.10,** ***A***). These tubers are characterized by gliosis, loss of lamination, presence of giant cells and cytomegalic neurons that are dysmorphic and ectopically located[153,154]. In some patients, magnetic resonance imaging (MRI) scans of cortical tubers and focal inter-ictal discharges recorded by EEG suggest a similar spatial origin paving the option for surgical removal of cortical tubers[155,156]. Surgical removal of these tubers has been able to resolve seizures in this sub population of patients[157]. Further, autistic traits in terms of social responsiveness and cognition have been correlated with epileptiform activity. Therefore surgical removal of these tubers is a viable option for treatment in children with TSC[158] at least to prevent epilepsy. On the other hand, it still remains a debate if epilepsy leads to autism in all affected individuals. How cortical tubers contribute to seizure activity still remains unclear. Major and co-workers found them to be electrically silent[159] suggesting cortical tubers *per se* do not contribute to seizure initiation. However, it is possible that nascent tubers are epileptogenic, giving rise to short- and long-distance seizure generations in a progressive fashion[160]. A few molecular evidences have been in favour of this hypothesis. One study found $GABA_A$ receptor expression is low in these tubers but conversely GABA levels were found to be low[161]. This reduction in $GABA_A$ receptors could be a compensatory mechanism to achieve adequate amount of inhibition in the pretext of low GABA availability. Additionally, cortical giant cells or cytomegalic cells (**Fig 1.10B,*C1-D2***) display an immature complement of glutamate receptors which could underlie immature and hyperexcitable electrophysiological properties[162]. Another additional possibility is that the tissue surrounding the tubers is hyperexcitable and, thus responsible for seizure generation. In support of this hypothesis, the neuronal population surrounding these

tubers although histologically normal show an increased excitatory synaptic drive[163]. These observations were made in a cohort of 20 patients diagnosed with TSC.

Finally, impairments in neuropsychological functions, including deficits in memory, attention and executive functions[165-167], are very common in TSC patients. Whether these problems are caused by a direct effect of TSC mutations on synaptic and circuit-based formation and plasticity, or by indirect alterations caused by seizures, are still hotly debated. Likely, both factors can contribute depending on seizure severity and age-onset.

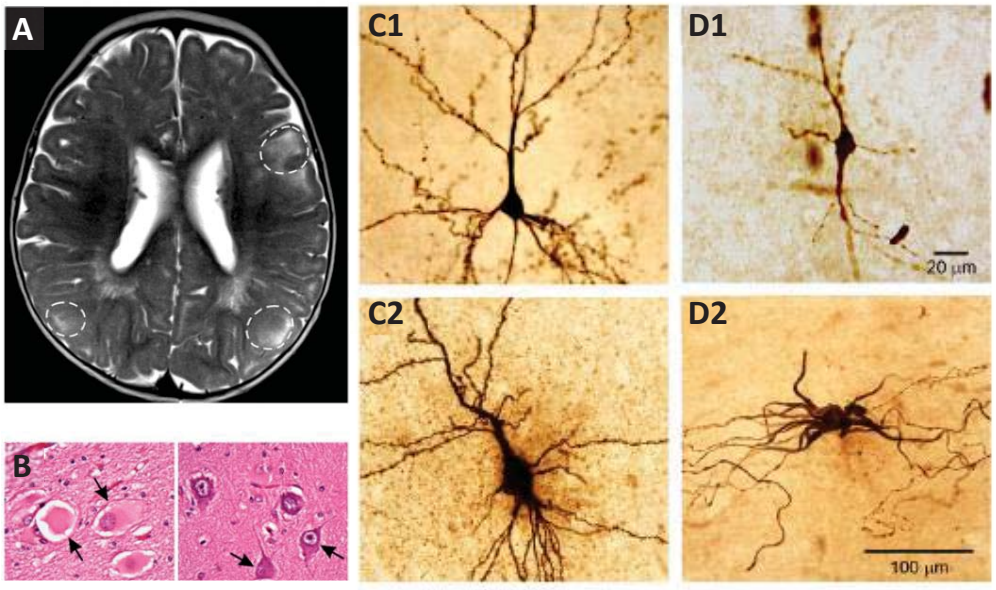

Figure 1.10. ***A***, Representative axial MRI scans of children with refractory epilepsy from TSC. ***B***,Section of a tuber showing abundant giant cells and disorganized collections of dysmorphic neurons. ***C1-D2***, Morphology of TSC cell types revealed by biocytin labeling showing four types of cell namely Pyramidal (***C1***), cytomegalic (***C2***), interneuron (***D1***), and (***D2***) giant cells (adapted from Cepeda *et al*, 2012)[163].

1.3.2.2 Mouse models of TSC

In order to gain a deeper insight into the cellular and molecular basis of TSC pathophysiology, several transgenic mice lines have been developed. For the sake of convenience, this section focusses only on germline (constitutive) and cell-type specific (conditional) knockout models of Tsc1 in mice. One of the key objectives behind the creation of these models is to recapitulate the disease phenotypes seen in humans and also to investigate the efficacy of various mTOR inhibitors in their reversal. The availability of various *Cre*-driver lines has facilitated the study of the specific contribution of different cell populations (excitatory, inhibitory and glial) in TSC disease manifestation.

1.3.2.2.1 Germline knockout of Tsc1 in mice

Goorden and co-workers generated a heterozygous germline knockout of Tsc1 ($Tsc1^{+/-}$ mice) to investigate the relationship between cerebral lesions, epilepsy and cognitive function[167]. Interestingly, these mice did show any spontaneous seizures, dysmorphic cells and had normal dendritic spine density in hippocampal granule cells. However, they developed cognitive impairments in terms of hippocampus based learning tasks and social behaviour. Most of other studies have used conditional knockout of Tsc1 resulting in either heterozygous or homozygous loss of the gene.

Promoter, Cre expression initiation	Phenotypes in terms of morphology, seizure activity and behavior	References
Constitutive	Impaired hippocampal-dependent tasks and social behavior.	Goorden *et al*, 2007[167].
mGFAP-Cre; E14.5	Macrocephaly, reactive gliosis, seizures.	Uhlmann *et al*, 2002[168].
SynapsinI-Cre; E12.5	Macrocephaly, mislamination, cytomegaly, hypomyelanation and seizures.	Meikle *et al*, 2007[169].
Nestin-Cre; E10.5	Macrocephaly, mislamination, cytomegaly, hypomyelanation, reactive gliosis and seizures.	Anderl *et al*, 2011[170].
Nestin-rTet-Cre; E13.5	Macrocephaly and cytomegaly.	Goto *et al*, 2011[171].
Emx1-Cre; E10.5	Macrocephaly, mislamination, cytomegaly, hypomyelanation, reactive gliosis and seizures.	Carson *et al*, 2012[172]; Margi *et al*, 2011[190].
Dlx5/6-Cre; E13.5	Macrocephaly, cytomegaly and reduced seizure threshold.	Fu *et al*, 2012[173].
L7-Cre; P6	Cytomegaly, impairment of social behavior, repetitive behavior and communication defcits.	Tsai *et al*, 2012[175].
Neonatal electroporation	Macrocephaly and cytomegaly, presence of cortical tubers and low seizure threshold.	Feliciano *et al*, 2012[176].

Table.1.2 Mice models of Tuberous Sclerosis Complex (TSC) generated by loss of Tsc1.

1.3.2.2.1 Conditional knockout of Tsc1 in mice

One of the first studies was done by Uhlmann and co-workers where the authors knocked out Tsc1 alleles in cells which express the glial fibrillary acidic protein (GFAP) promoter[168]. This promoter allowed conditional deletion of Tsc1 in astrocytes and adult neuronal progenitor cells. These mice displayed severe seizures and reduced survival rates (median life span of three to four months). Meikle and co-workers have used a similar approach where they have crossed mice carrying a mutant and conditional (floxed) Tsc1allele with mice expressing *Cre*-

recombinase under the *synapsin-1* promoter[169]. These mice started to express *Cre* around embryonic (E) 12.5 day and had a low survival rate (median life span of 35 days). Further, they displayed severe seizure activity along with enlarged and dysplastic neurons (both excitatory and inhibitory) in the cortex and hippocampus. A more recent study used mice expressing *Cre* under the *Nestin* promoter crossed with either mice containing a mutant and a conditional Tsc1 allele, or two conditional Tsc1 alleles[170,171]. This approach allowed creating loss of function of both copies of Tsc1at different time points. The mice carrying the Tsc1 mutant allele and floxed allele (*Nestin-Cre*::Tsc1$^{mutant/flox}$) died at birth. However, the *Nestin-Cre*::Tsc1$^{flox/flox}$ mice survived and displayed several hallmark features of TSC. Other mice models have used Cre-driver lines under promoters, which target different progenitor cells. For example, in *Emx-Cre*::Tsc1$^{flox/flox}$ mice, where Tsc1 is deleted in glutamatergic cells and astrocytes has reduced survival rates and display common TSC phenotypes[172]. Therefore different groups have studied the loss of Tsc1 in various progenitor cells that give rise to excitatory and/or glial cells Interestingly, most of the these studies indicate that only homozygous loss of Tsc1 in these conditional knockouts lead to development of TSC phenotypes although the disease condition in human is heterozygous with growing evidence that LOH occurs at some point. Many of these mice have reduced life span and develop spontaneous seizures. Contrary to these mice models, TSC in humans does not reduce life span severely although the quality of life is significantly impaired. Moreover, reduced life span of these mice poses a challenge to identify any correlation between Tsc1 loss in the targeted cell population with behavioural deficits diagnosed in humans.

The effects of Tsc1 deletion in GABAergic circuits on seizures and life span are less well investigated. In fact, only one study has focused on the role of Tsc1 in GABAergic cells using the *Dlx5/6* promoter to drive *Cre* expression in all types of inhibitory interneurons (**Table.1.1**). These mice had reduced life span (60% mice die by two months), decreased total

inhibitory cell count and clustering of ectopic inhibitory cells in cortex. Although these mice did not show spontaneous seizures, exposure to a proconvulsant (flurothyl) revealed decreased seizure threshold[173].

Interestingly, ~30% of TSC patients have cerebellar abnormalities but the pathophysiology of these lesions is not well understood[174]. To explore this issue, Tsai and co-workers generated a mouse where Tsc1 is knocked out specifically in Purkinje cells starting from P6 using which *L7*-Cre line. Both heterozygous and homozygous loss of Tsc1 in mouse cerebellar Purkinje cells results in autistic-like behaviours, including abnormal social interaction, repetitive behaviour and deficits in vocalizations, in addition to decreased Purkinje cell excitability[175]. This study highlights the contribution of the cerebellum in the manifestation of autistic phenotypes. However, how the cerebellum modulates the social behaviour and other cognitive processes is subject to further investigation.

A big drawback of these rodent models lies in its inability to recapitulate the presence of cortical tubers which is a hallmark of TSC. In a seminal work by Feliciano and co-workers, the authors used *in utero* electroporation (IUE) to incorporate plasmids expressing *Cre* at embryonic stages in mice with a mutant copy of Tsc1[176]. By this approach, *Cre* expression was able to create LOH at an early stage of brain development. The resulting mice had ectopic neurons in the cortex and generated large clusters of cells in and above the corpus callosum (white matter). These 'white matter nodules' in cortex are probably the equivalent of the cortical tubers seen in TSC patients.

TSC in humans is mainly characterized by presence of cortical tubers, epileptic seizures and autistic phenotypes. Constitutive or conditional deletion of one/two copies of Tsc1 is unable to reproduce tuberous malformations in the cortex although giant cells are common. Many of these models exhibit either spontaneous seizures or increased susceptibility to seizures.

Reduced life span in most of these models has been a challenge to adequately investigate the cellular and molecular basis of cognitive deficits associated with autism in TSC. It is perhaps impossible to create an exact model of the human condition in mice for a complex disease like TSC.

1.3.2.3 Altered connectivity in TSC

It has been suggested that tuber burden and seizures may contribute to cognitive deficits and neuropsychiatric problems in TSC. However, many of the above mentioned animal models hint at more subtle changes in synaptic connectivity as an underlying basis of these deficits as cognitive impairment persists in absence of tubers. The structural underpinnings of neuronal connectivity and communication in the CNS are constituted by dendrites, synapses and axons. For an individual neuron, the dendrites serve as antennae for receiving signalling inputs which is processed and sent down the axon to relay the output to connected cells. Therefore studying the morphology of axon, dendrite and synapses serves as a good proxy for analysing the development and maintenance of connectivity in the brain. This allows us to understand the changes that occur during development both in healthy and disease conditions.

Several studies have tried to establish the role of mTOR pathway in the development of dendritic arborisation[177,178]. By using RNAi-based approaches, Urbanska and co-workers knocked down Rictor and Raptor and showed that both mTORC1 and mTORC2 play a role in the development of hippocampal pyramidal neuron dendritic morphology. However, post-natal (P14-P16) deletion of Tsc1 by viral injection (encoding CreEGFP fusion protein) in hippocampal pyramidal neurons did not affect dendritic morphology[179]. *Syn1-Cre*-Tsc1$^{mut/flox}$ mice, described previously, exhibited increased apical dendritic thickness and abnormal polarity in sporadic cortical pyramidal cells[110,169]. Further, the authors observed a similar increase in structural complexity of basal dendrites in pyramidal neurons and olfactory bulb

granule neurons in the subventricular zone (SVZ)[176]. Altogether these studies indicate that the timing of Tsc1 ablation and subsequent dysregulation of the mTOR pathway has different effects on dendritic arborisation depending on the developmental time window.

Spines are microscopic protrusions found on the membranes of most dendrites and are the post-synaptic site of ~90% of excitatory synapses[180]. Dendritic spines exhibit a high degree of structural plasticity whereby they undergo changes in shape and size driven by neural activity and experience. Alterations in spine density and spine morphology have been correlated with mental retardation and autistic phenotypes in humans and animal models[181]. Further, analysis of post-mortem brains from TSC patients revealed the presence of fewer spines on abnormally shortened dendrites of principal projection neurons, in cortical tubers[182,183].

Knockout of both Tsc1 alleles in pyramidal cells from hippocampal slice cultures resulted in fewer spines and increased spine length and head width[184]. The authors used mice at P5-P7 for culture which were transfected after two days and the cells were analysed six days after transfection. Knocking out only one allele resulted in similar but less pronounced phenotype suggesting these effects are gene-dosage dependent. All these effects were reversible by Rapamycin treatment suggesting a strong role of mTOR hyperactivity. Contrary to these findings, when both copies of Tsc1 were knocked out *in vivo* in post-mitotic pyramidal cells of the CA1 region of the hippocampus no changes were seen in terms of spine number and morphology[179] using viral delivery of *Cre* at P14-P16. Meikle and co-workers found consistent results in ectopic and dysplastic cortical neurons in $Tsc1^{flox/mutant}$ mice which showed reduction in spine density without affecting spine length[110]. Contrary to the loss of spines in hippocampal pyramidal cells, loss of Tsc1in cerebellar Purkinje cells lead to increase in spine density[175]. Therefore the effect of Tsc1 loss on spine density varies greatly depending both on the timing of knockout and the cell-type being targeted.

Brain scans using diffusion tensor imaging suggest TSC patients have abnormalities in axonal structures including poor myelination[185, 186]. The development of axonal architecture depends on both cell internal factors as well as external cues in order to determine how many cells it will contact and how many synapse will form on each target. In one of the early studies, neurons deficient in Tsc1 showed ectopic axon formation in dissociated hippocampal cultures as well as in vivo in the *SynI*-Cre-Tsc1$^{flox/flox}$ mice[187]. Conversely, over-expression of Tsc1 resulted in reduced axon formation along with lower mTOR activity in cultured neurons 6 *days in vitro* after E17. The authors then investigated the molecules whose expression changes upon mTOR dysregulation and identified SAD Kinase as an interesting player. SAD kinase has implicated in axon development in *C. elegans*[188]. In separate studies, mTOR has been shown to regulate expression of other molecules which determines cell polarity and axon specification like Tau and collapsing response mediator protein 2(CRMP2)[189]. In Tg(*Emx1*-Cre);Tsc1$^{flox/mut}$ mice, pyramidal neurons showed abnormal projections and dis-arranged neurites and axons[190].

Certain questions still remains unanswered regarding how Tsc1/Tsc2 regulates connectivity in the developing brain. For example, it remains unknown if loss of Tsc1 in a wild-type background is different compared to a mutant background in terms of connectivity. Also how connectivity is affected due to heterozygous loss of Tsc1 prior to birth compared to acquiring an inactivating mutation in post-natal development is still unclear. The molecular mechanisms downstream of mTOR need to be further screened to assess how expression, activity and sub-cellular localization of candidate proteins may change following Tsc1 loss.

1.3.3 Dysregulated mTOR signalling in other neurodevelopmental disorders

1.3.3.1 PTEN Hamartoma tumor syndrome

The phosphatase and tensin homolog (PTEN) protein acts as a phosphatase, which can inhibit the mTOR pathway[191]. Germline mutations in the *PTEN* gene cause a group of rare disorders often termed as PTEN Hamartoma tumor syndromes (PHTS)[192,193]. These include Cowden syndrome (CS), Lhermitte-Duclos disease (LDD), and Bannayan-Riley-Ruvacalba syndrome (BRRS). CS is characterized by macrocephaly and benign hamartomas of the breast, thyroid, or endometrium, as well as malignant tumours. A minority of patients are also diagnosed with intellectual disability. In LDD, the cerebellum is severely affected and is characterized by dysplastic gangliocytomas, which clinically cause ataxia, seizure, or increased intracranial pressure[192]. BRRS is another disorder that comes under the umbrella of PHTS where patients suffer from macrocephaly, developmental delay and/or intestinal polyps[194]. Interestingly, all of these disorders (CS, LDD, and BRRS), arise following mutations in the *PTEN* gene clearly suggesting that additional factors are involved in causing specific phenotypes[193,195]. About 1% of sporadic cases of autism have been linked with *PTEN* mutations, therefore in a clinical context, *PTEN* gene testing is often recommended when macrocephaly and autism features overlap[196]. In a mouse model where PTEN was knocked out in mature neuronal subpopulations in cortex and hippocampus using $PTEN^{flox/flox}$ mice with *Nse*-Cre mice, macrocephaly was observed along with deficits in social behaviour[197]. *Cre* expression was seen in ~30-60% of neurons by fourth post-natal week. The affected neurons had larger somas, exuberant dendritic arborisation and increased dendritic spine density. In a very recent study, the loss of *PTEN* in GABAergic cells lead to reduction of SST+ cells but not PV+ cells of the cortex. Further, in these mice PV cells showed ectopic projections in cortical layer I. These mice also exhibit deficits in social behaviour[198]. Mice models of PTHS indicate the role of *PTEN* in cellular connectivity. *PTEN* is also a negative regulator of mTOR pathway

like *TSC1/TSC2* and therefore could be a potential target to understand the pathophysiology involved in mTORpathies.

1.3.3.2 Neurofibromatosis

Neurofibromatosis (NF1) is a neurocutaneous disorder characterized by both benign and malignant tumours affecting both the central and peripheral nervous system. Similar to TSC, NF1 is autosomally inherited and the incidence rate is 1 in 2500-3000 live births. It primarily affects tissues originating from the neural crest. Clinical features of NF1 include the brain (glial tumors, macrocephaly), skin (cafe´ au lait spots, freckling, neurofibromas), kidney (renal artery stenosis), bone (sphenoid wing dysplasia) and endocrine systems. Most common symptoms include learning disabilities, attention-deficit hyperactivity disorder, sleep disruption and anxiety. Only ~10% of patients are diagnosed with epilepsy in NF1 and similar to PTHS macrocephaly is common too[199]. NF1 is caused by mutations in the *NF1* gene that encodes a GTPase-activating protein which suppresses the activity of the proto-oncogene Ras. Mice deficient in *Nf1* gene have Schwann cells with increased Ras activity and growth rate. Ras signalling is important for activation of the mTOR pathway[200]. Although NF1 loss leads to hyperactivation of mTORC1 which leads to tumorigenesis[201], the regulation of mTORC1 by NF1 appears to be independent of TSC-Rheb[202].

1.3.3.3 Fragile X syndrome

Fragile X syndrome is associated with dysfunction of the Fragile X mental retardation protein 1 (*FMRP*) gene. FMRP1 protein functions as a translational repressor of mRNAs. Recently, it was discovered that the silencing of FMR1 is mediated by the formation of a DNA-mRNA duplex between the promoter and the trinucleotide repeat region of the mRNA[203]. Fragile X syndrome (FXS) is most commonly associated with mental retardation, occurring in about 1:5000 males and roughly half as many females. Males diagnosed with FXS suffer from

intellectual disability along with motor abnormalities, speech delay, hyperactivity and anxiety. Many mice models have been developed to study FXS but only the studies relevant to this thesis work have been discussed in this section. Fmrp mutant mice exhibit elevated mTOR activity and protein synthesis. mGluR-dependent long term depression (LTD) which refers to a form of synaptic plasticity where weakening of synapses occur is exaggerated in these mice[204,205]. Genetic deletion of S6K1, one of the downstream effectors of the mTORC1 involved in regulation of protein synthesis, was able to reduce the elevated level of protein synthesis and reversed neurophysiological and behavioural defects[206]. In a very interesting study, Bear and colleagues found that $Tsc2^{+/-}$ mice had hyperactivity of mTORC1 but did not favour protein synthesis of components involved in mGluR-LTD (long term changes in synaptic plasticity mediated through metabotropic glutamate receptors). Strangely, when these mice were crossed with the $Fmrp1^{y/-}$ mice, the resulting double mutants demonstrated normalization of mGluR-LTD, protein synthesis rates and cognitive behaviour[204].

Many studies involving animal models of several neurodevelopmental disorders strongly established the role of a dysregulated mTOR pathway. Therefore, these observations hold the promise for a common treatment. However, recent failures in clinical trials suggest that pathophysiological mechanisms could be different and unique to the disease condition. Treatment of neurodevelopmental disorders with Rapamycin and its analogues has a promising future. In this work, *in vitro* application of Rapamycin was able to reverse the cellular phenotypes which have been discussed elaborately in chapter 4. However, the study of *in vivo* effects has been beyond the scope of this doctoral work and remains to be explored in the future.

1.4 Objectives of research

1.4.1 Rationale

Development of the inhibitory circuits in the neocortex is a long process and extends to the third or fourth post-natal weeks in rodents. There are several factors that influence how a single PV-expressing basket cell innervate a large number of neighbouring cells and to what extent they can form, mature and maintain a finite number of synapses on these target cells. A developing neuron requires a large amount of proteins in order to achieve the structural complexity attributed to mature neurons. There is accumulating evidence that mutations or dysfunctions in two groups of genes encoding proteins involved in, (1) control of protein synthesis and (2) synaptic function lead to developmental disorders and epilepsy. Altering the relative numbers, functions, and/or connectivity between excitatory neurons and inhibitory interneurons can lead to imbalances in excitation/inhibition ratio in the brain causing epilepsy and autism in humans. How the loss of these genes affects the development of inhibitory circuits and contributes to disease manifestation is not well understood. In my PhD work, I have investigated the role of Tsc1 (involved in translational control by regulating mTORC1) and $GABA_A$ receptor (inhibitory synaptic protein) in PV cell connectivity.

1.4.2 Broader objectives

- The role of Tsc1 in development of PV cell circuitry in the cortex.
- The role of different $GABA_A$ receptor mutations in regulation of cortical excitatory and inhibitory cell connectivity.

1.4.3 Specific objectives

- Study of mTORC1 activity during different ages during development in wild-type mice.
- Study the effect on PV cell connectivity upon Tsc1 knockdown in single PV cells.
- Study the effect on PV cell connectivity upon Tsc1 knockdown at the network level.
- Study the effect of Tsc1 gene dosage and timing of knockout on behaviour and PV cell connectivity in conditional mouse models.
- Effect of different $GABA_A$ receptor mutations in cortical PV cell connectivity.
- Effect of different $GABA_A$ receptor mutations in cortical pyramidal cell connectivity.

Chapter 2. Materials and methods

2.1 Animals

Mice with *loxP* sites flanking exon 17 and 18 of Tsc1gene ($Tsc1^{flox/flox}$) was purchased from Jackson Laboratories. The $Tsc1^{flox/flox}$ mice were bred with wild type mice of Sv129 background to generate $Tsc1^{flox/wt}$ mice. Both $Tsc1^{flox/flox}$ and $Tsc1^{flox/wt}$ mice have been used for organotypic cultures to study Tsc1 knockout in single cells. Two separate transgenic mice lines expressing Cre recombinase, (1) Tg(*Nkx2.1*-Cre) and (2)Tg(*PV*-Cre) were maintained as pure colonies. The Tg(*PV*-Cre) mice was a kind gift from Dr. Elsa Rossignol. Tg(*Nkx2.1*-Cre) was purchased from Jackson laboratories and have been previously described (Xu et al, 2008)[27]. Backcross between $Tsc1^{flox/flox}$ mice and Tg(*Nkx2.1*-Cre) produced $Tsc1^{flox/flox}$ or $Tsc1^{flox/+}$ (referred as $Tsc1^{Ctrl}$), Tg(*Nkx2.1*-Cre);$Tsc1^{flox/+}$ and Tg(*Nkx2.1*-Cre);$Tsc1^{flox/flox}$ mice. A similar breeding strategy was used to cross $Tsc1^{flox/flox}$ and Tg(*PV*-Cre) mice. All mice were housed under standard pathogen-free conditions in a 12h light/dark cycle with *ad libitum* access to sterilized laboratory chow diet. Animals were treated in accordance with Canadian Council for Animal Care and protocols were approved by the Animal Care Committee of CHU Ste-Justine Research Center.

2.2 Genotyping of mice:

DNA was extracted from mice tails and was genotyped to detect the presence of Cre alleles and Tsc1 alleles. Polymerase chain reaction (PCR) of the wild-type and conditional alleles of Tsc1 was performed using primers F4536 (5' AGGAGGCCTCTTCTGCTACC -3') ,R4830 (5'- CAGCTCCGACCATGAAGTG -3') and R6548 (5′-TGGGTCCTGACCTATCTCCTA-3′) with band sizes of 295 bp for the wild-type and 480 bp for the floxed allele. Primers for characterizing Cre in Tg(*Nkx2.1*-Cre) breeding were F1 (5'-AAGGCGGACTCGGTCCA CTCCG-3'), F2(5'-AAGGCGGACTCGGTCCACTCCG-3') and R1 (5'-TCGGATC

CGCCGCATAACCAG-3') which generated 550bp and 220bp mutant and wild-type bands.Primers for characterizing Cre in Tg(*PV*-Cre) breeding were F1 (5'-CAGCCTCTGT TCCACATACACTCC-3'), F2(5'-GCTCAGAGCCTCCATTCCCT-3') and R1 (5'-TCACTCGAGAGTACCAAGcAGGCAGGAGATATC-3') which generated 400bp and 526bp mutant and wild-type bands.

2.3 DNA constructs

P_{G67}-GFP was generated by subcloning of a10kb region of *Gad1* gene promoter by gap repair in front of the GFP coding region in pEGFP(Clontech) as previously described(Chattopadhyaya et al.,2004)[48]. Cre, *GABRA1*-A322D, *GABRA1*- D219N, *GABRA1*-K353delins18X constructs (Cossette et al., 2002; Lachance-Touchette et al., 2011)[101,102], were subcloned inPG_{67} vector by using restriction site *Pme1*via sequence and ligation–independent cloning method (SLIC) (Li and Elledge,2007). All constructs were sequenced to confirm the presence of the mutations and to exclude any other variants that may have been introduced during PCR amplification.

2.4 Slice culture and biolistic transfection

Slice culture preparation was done as described by Stoppini et *al.*, 1991. Postnatal day 4 or 5 (P4 or P5) mouse pups from $Tsc1^{flox/flox}$, $Tsc1^{flox/wt}$, $Tsc1^{Ctrl}$ $Tsc1^{flox/+}$, Tg(*Nkx2.1*-Cre; $Tsc1^{flox/+}$ or Tg(*Nkx2.1*-Cre; $Tsc1flox^{/flox}$) mice were decapitated, and brains were rapidly removed and immersed in ice-cold culture medium (containing DMEM, 20% horse serum, 1 mM glutamine, 13 mM glucose, 1 mM $CaCl_2$, 2 mM $MgSO_4$, 0.5 μm/ml insulin, 30 mM HEPES, 5 mM $NaHCO_3$, and 0.001% ascorbic acid). Coronal brain slices of the occipital cortex, 400 μm thick, were cut with a Chopper (Stoelting, Wood Dale, IL). Slices were then placed on transparent Millicell membrane inserts (Millipore, Bedford, MA), usually three slices/insert, in 30 mm Petri dishes containing 0.75 ml of culture medium. Finally, the slices

were incubated in a humidified incubator at 34°C with a 5% CO_2-enriched atmosphere and the medium was changed three times per week. All procedures were performed under sterile conditions. Constructs to be transfected were incorporated into "bullets" that were made using 1.6 μm gold particles coated with a total of ~60 μg of the DNA(s) of interest. These bullets were used to biolistically transfect slices by Gene gun (Bio-Rad, Hercules, CA) at high pressure (180 ψ), and the transfected slices were incubated for 8 days *in vitro* under the same conditions as described above, before imaging. For each experimental group, cortical slices were prepared from at least three mice. On average 6-7 neurons were transfected per cortical organotypic slice. The majority of neurons labeled by this promoter were parvalbumin-positive basket cells (as described in Chattppadhyaya et al., 2004, 2007)[48,58], while a minority (~10%) were pyramidal cells. Pyramidal cells were recognized by the complexity of their dendritic arbor, including an apical dendrite, and the presence of numerous dendritic spines.

2.5 Immunohistochemistry and confocal imaging:

Mice were perfused transcardially with 1X PBS AND 4% PFA. Brains were postfixed with 4% PFA overnight followed by 30% sucrose solution in PBS. The brains were frozen with OCT and sagittal sections of 40 μm were produced using a cryostat. The following primary antibodies were used for immunohistochemistry on mice cryosections or organotypic cultures: rabbit phospho-S6 (1:1000, Cell Signaling), mouse NeuN (1:400, Millipore), mouse PV (1:1000, Millipore), rabbit PV(1:1000, Swant), guinea pig PV (1:1000,Synaptic Systems), rabbit vGAT (1:1000, Synaptic Systems), mouse gephyrin (1:500, Synaptic Systems). Secondary antibodies were used to visualize primary antibodies which include Alexa-fluor 488,555,594,633, and 647 (Life technologies). Images were taken on a Leica confocal microscope with a camera using the same exposure and acquisition settings for each section unless specified.

2.6 Image quantification in organotypic cultures and *in vivo*:

For organotypic cultures, at least two confocal stacks of each basket cell axon arbor in the first 150μm from the basket cell soma using a 63X glycerol objective(NA1.3, Leica) and a Leica TCS SPE confocal microscope. Pyramidal neurons were imaged using a Leica confocal microscope SPE (63X glycerol immersion objective; NA1.3). Atleast 6 labeled pyramidal neurons, characterized by the presence of a well-defined apical dendrite, were randomly selected from cortical layers 2/3 and 5. Image stacks of basal dendrites were acquired with a z-step of 0.5μm and then reconstructed in 3D with Neurolucida (MicroBrightField) software. Cortical pyramidal cells from at least four animals were used for each experimental condition. Dendritic length,total spine density,spine morphology and spine length were quantified using NeuroExplorer software (MicroBrightField).Mushroom spines were defined as spine with a neck and bearing a head,which was at least twice as large as the neck. Thin spines were defined as dendritic protrusions shorter than 5μm and lacking a clearly defined head. Basket cells were analysed as discussed in Chattopadhyaya et al, 2013[65]. For *in vivo* analysis, images were acquired on the same day using identical confocal parameters and either using 20x water immersion objective (for analysis of % of PV cells colocalizing with pS6+ cells) or 63x glycerol objective(for analysis of PV,vGAT,pS6, gephyrin intensity and/or puncta counting). Layer V of somatosensory cortex was imaged confocally with z-step size 1μm and images were exported in TIFF format. Cell area of PV soma was counted using Image J (1.47v, NIH) or Neurolucida (MBF Softwares). Fluorescence intensity of pS6 signal in PV cells was calculated using Image J for the mean gray value. Intensity of PV and vGAT was calculated on a traced cross-sectional area around NeuN somas. Puncta quantification of PV, gephyrin and vGAT was done at both P18 and P45. PV, vGAT, gephyrin and PV/vGAT-gephyrin colocalized punctas were identified visually around periphery NeuN+ soma and punctas located only at the confocal plane with the highest soma circumference (± 1μm) was

calculated manually on Neurolucida software. User was blind to genotype during the analysis.

2.7 Western Blot :

Western blots were performed on samples from four mice per group and from two separate experiments. Protein lysates were prepared by homogenizing tissue from rat hippocampus in 50 mM Tris–HCl (pH 7.6), 2 mM EDTA, 1% Igepal CA-630 (Sigma-Aldrich), and one tablet of protease inhibitor cocktail (Roche, Mississauga, ON, Canada). Tissues were disrupted using needles and a syringe, and centrifuged at 10000 g for 10 min at 4°C; the supernatant was then collected. Protein levels were quantified by Bradford Protein Assay (Bio-Rad, Mississauga, Ontario, Canada), and their concentrations were adjusted with deionized water. Samples were mixed with an equal volume of 2x Laemmli buffer, boiled for 5 min, and used immediately or stored at 80°C. Proteins were separated using 6.5% polyacrylamide separation gels and 5% stacking gels (Bio-Rad); equal amounts were loaded in each lane, and then transferred onto Immobilon-P Transfer Membrane, a poly(vinylidene difluoride) microporous membrane (Millipore, Temecula, California, USA). These membranes were then blocked by incubation in Tris-buffered saline blocking buffer with 5% dried milk and 0.1% Tween-20 solution. Membranes were probed with the following primary antibodies: anti-pS6 (Ser 240/244)1:10000, Cell Signalling) and anti-β actin (1:3000,Novus Biologicals). Rabbit or mouse HRP-conjugated secondary antibody used for detection of primary antibodies was purchased from Sigma-Aldrich. Immunoreactive bands were detected with Western Lightning Chemiluminescence Reagent Plus (PerkinElmer), and the signal was visualized by exposing the membrane to BioFlex MSI film for autoradiography, maximum sensitivity (InterScience). Bands for every sample were used for quantification, using imageJ software.

2.8 Analysis of rodent behaviour:

2.8.1 Open Field

A mouse was placed at the centre of the open-field arena and the movement of the mouse was recorded by a video camera for 10 min. The recorded video file was later analysed with Smart video tracking system (v3.0, Harvard Apparatus). Total distance travelled during the 10 minute period was calculated to measure exploratory behaviour. The open field arena was cleaned with 70% ethanol and wiped with paper towels between each trial. Investigators were blind to genotype during both recording and scoring of videos.

2.8.2 Elevated plus maze

A mouse was placed at the junction of the two open and closed arms. Apparatus consisted of two open arms without walls across from each other and perpendicular to two closed arms with walls with a centre platform. Experiment was performed as described in Vogt et al, 2015[198]. Exploration time in this apparatus was recorded for 5 min with a video camera. Recorded video was scored to measure time spent in open arms, closed arms and centre regions respectively.

2.8.3 T-maze

The T-maze apparatus consists of a T-shaped walled chamber where mice (aged P43) are tested for two trials in order to assess working memory. An individual mouse was placed at the middle arm of the T-maze which walks was allowed to make a free choice to enter an arm at the T-junction. Once the mouse made a decision to go in left/right direction it was blocked in that chamber for 10 seconds and was taken out from the apparatus. It was allowed to rest in an empty cage for a period of 50 seconds and put back again in the middle arm to score if it

altered its choice for choosing the arm once at the junction. Each mouse was scored for one trial for three consecutive days.

2.8.4 Three chambered social novelty test

A three-chamber arena was used to assess the social recognition performance of the mice (Silverman *et al.,* 2010)[30]. The tested animal (P38-P42) was placed in the middle of the central chamber and allowed to explore all the chambers for 10 min. During this habituation session, small wire cages were present, one in each opposite chamber. After habituation, an unfamiliar conspecific of the same sex and age (Stranger 1) was placed inside a small wire cage whereas the other remained empty. The tested animal was allowed to freely explore the three chambers of the apparatus for 10 min. At the end of this 10min, a new unfamiliar mouse of the same sex and the same age (Stranger 2) was placed in the previously unoccupied wire cage and the tested mouse was examined for an additional 10 min to assess preference for social novelty. Stanger 1 and stranger 2 animals originated from different home cages and had never been in physical contact with the tested mice or between each other. Social recognition was evaluated by quantifying the time spent by the tested mice in each chamber during the third 10 min session.

Chapter 3. Single-cell genetic expression of mutant $GABA_A$ receptors causing Human genetic epilepsy alters dendritic spine and GABAergic bouton formation in a mutation-specific manner

Pamela Lachance-Touchette[1*], Mayukh Choudhury[2*], Ana Stoica[1], Graziella Di Cristo[2$] & Patrick Cossette[1$]

[1]Centre d'Excellence en Neuromique de l'Université de Montréal (CENUM), Centre de recherche CHUM, Montréal, QC, Canada
[2]Centre Hospitalier Universitaire Sainte-Justine, Université de Montréal, Montréal, QC, Canada

*Both authors contributed equally to this study

Correspondence:
$-Graziella Di Cristo, CHU Ste-Justine, 3175, Chemin de la Côte-Ste-Catherine, Montréal (Quebec), H3T 1C5.
$-Dr. Patrick Cossette, CHUM-Hôpital Notre-Dame, 1560 Sherbrooke est, Montréal, Québec, H2L 4M1.

Keywords: Channelopathy, epilepsy, bouton formation, human genetics, $GABA_A$ receptor, organotypic slice culture.

3.1 Abstract

Mutations in genes encoding for $GABA_A$ receptor subunits are a well-established cause of genetic generalized epilepsy. GABA neurotransmission is implicated in several developmental processes including neurite outgrowth and synapse formation. Alteration in excitatory/inhibitory synaptic activities plays a critical role in epilepsy, thus here we investigated whether mutations in α1 subunit of $GABA_A$ receptor may affect dendritic spine and GABAergic bouton formation. In particular, we examined the effects of three mutations of the *GABRA1* gene (D219N, A322D and K353delins18X) that were found in a cohort of French Canadian families with genetic generalized epilepsy. We used a novel single-cell genetic approach, by preparing cortical organotypic cultures from *GABRA1*$^{flox/flox}$ mice and simultaneously inactivating endogenous *GABRA1* and transfecting mutant α1 subunits in single glutamatergic pyramidal cells and basket GABAergic interneurons by biolistic

transfection. We found that *GABRA1*$^{-/-}$ GABAergic cells showed reduced innervation field, which was rescued by co-expressing α1-A322D and α1-WT but not α1-D219N. We further found that the expression of the most severe *GABRA1* missense mutation (α1-A322D) induced a striking increase of spine density in pyramidal cells along with an increase in the number of mushroom-like spines. In addition, α1-A322D expression in GABAergic cells slightly increased perisomatic bouton density, whereas other mutations did not alter bouton formation. All together, these results suggest that the effects of different $GABA_AR$ mutations on GABAergic bouton and dendritic spine formation are specific to the mutation and cannot be always explained by a simple loss-of-function gene model. The use of single cell genetic manipulation in organotypic cultures may provide a better understanding of the specific and distinct neural circuit alterations caused by different $GABA_A$ receptor subunit mutations and will help define the pathophysiology of genetic generalized epilepsy syndromes.

3.2 Introduction

Genetic factors play a key role in the development and severity of genetic generalized epilepsy (GGE). Epilepsy-causing mutations have been identified in several $GABA_A$ receptor ($GABA_AR$) subunits, including α1, β3, γ2, and δ subunits (Baulac *et al*., 2001;Wallace *et al*., 2001;Cossette *et al*., 2002;Harkin *et al*., 2002;Kananura *et al*., 2002;Dibbens *et al*., 2004;Audenaert *et al*., 2006;Maljevic *et al*., 2006;Sun *et al*., 2008;Tanaka *et al*., 2008;Dibbens *et al*., 2009;Lachance-Touchette *et al*., 2010;Shi *et al*., 2010;Klassen *et al*., 2011;Lachance-Touchette *et al*., 2011;Carvill *et al*., 2013;Epi *et al*., 2013;Tian *et al*., 2013;Carvill *et al*., 2014;Hancili *et al*., 2014;Ishii *et al*., 2014;Johnston *et al*., 2014). $GABA_ARs$ are ligand-gated ion channels that are permeable to chloride and bicarbonate anions and mediate most of cortical inhibitory neurotransmission. Their molecular structure comprises of a heteropentameric protein complex assembled from 19 different subunits (α1-

6, β1-3, γ1-3, δ, ε, π, θ, and ρ1-3). Although there is the potential for a high variability of combinations, the α1β2γ2 is the most abundant and represents approximately 60% of all $GABA_A$Rs in adult brain (Sieghart and Sperk, 2002). Mutations in the *GABRA1* gene are linked to a spectrum of endophenotypes of GGE syndromes as well as more severe forms of epilepsy associated with intellectual disability (Carvill *et al*., 2014). We previously reported D219N, A322D, K353delins18X mutations in families with autosomal dominant genetic generalized epilepsy (Cossette *et al*., 2002;Lachance-Touchette *et al*., 2011). Whether these mutations cause protein inactivation and thus loss of function is still unclear. Deletion of α1 in mice produced EEG spike-wave discharges and absence-like seizures (Arain *et al*., 2012). This mouse model recapitulates some of the epilepsy phenotypes that were reported in human carriers of *GABRA1* mutations (Cossette *et al*., 2002;Maljevic *et al*., 2006;Klassen *et al*., 2011;Lachance-Touchette *et al*., 2011). *In vitro* investigations in heterologous cells demonstrated that *GABRA1* mutants could affect mRNA transcript stability, cell surface $GABA_A$R composition and channel gating properties (Cossette *et al*., 2002;Gallagher *et al*., 2004;Krampfl *et al*., 2005;Maljevic *et al*., 2006;Gallagher *et al*., 2007;Lachance-Touchette *et al*., 2011;Carvill *et al*., 2014). By expressing wild type or mutant α1 in heterologous cells, we previously showed that A322D and K353delins18X mutations reduced GABA-evoked currents amplitude by impairing α1β2γ2 receptor surface expression due to endoplasmic reticulum retention (Krampfl *et al*., 2005;Lachance-Touchette *et al*., 2011). In addition, two *GABRA1* mutations (A322D, D219N) exhibited altered gating kinetic properties (Lachance-Touchette *et al*., 2011). Further, studies in cultured neurons revealed that α1-A322D mutation altered the kinetics and the amplitude of miniature inhibitory postsynaptic currents (mIPSCs) in pyramidal neurons (Ding *et al*., 2010). These data support the hypothesis that reduced inhibition underlies network hyperexcitability in GGE associated with $GABA_A$R mutations.

On the other hand, $GABA_AR$ mutations may also alter specific developmental processes. Alterations in the number and strength of inhibitory and excitatory synapses are thought to contribute to epilepsy (Bernard, 2012). In addition, GABA transmission have been shown to play a key role during brain development, influencing virtually all developmental steps from neurogenesis to the establishment of neuronal connectivity (Gaiarsa and Porcher, 2013;Kilb *et al*., 2013). Focusing in particular on synaptogenesis, recent studies demonstrated in organotypic cortical slices that endogenous GABA regulates axonal branching and synapse formation of cortical basket cells- a prominent class of GABAergic neurons- through the activation of $GABA_A$ and $GABA_B$ receptors (Chattopadhyaya *et al*., 2007;Baho and Di Cristo, 2012;Wu *et al*., 2012). GABAergic transmission can also play a critical role in excitatory synapse development. In pyramidal neurons of the cerebral cortices, excitatory synaptic inputs are made on small dendritic protrusions, called dendritic spines. Hayama and collaborators (2012) showed that dendritic spine shrinkage and elimination can be promoted either by uncaging of a caged GABA compound that mimics IPSCs or by tonic application of a $GABA_A$ agonist, muscimol (Hayama *et al*., 2013). Whether and how *GABRA1* mutations affect dendritic spines and GABAergic bouton formation, thus contributing to the epilepsy phenotype has not been so far examined.

So far, the vast majority of mutations in $GABA_AR$ subunits causing Human epilepsy are associated with loss-of-function, when assessing gating properties of the GABA-evoked currents *in vitro* (Macdonald and Kang, 2009). However, review of functional studies on GABRA mutations in heterologous cell system revealed controversial findings between different groups (reviewed in (Cossette *et al*., 2012)). For example, for long time no consensus was reached regarding the impact of *GABRG2* missense mutations on GABA currents amplitude or kinetics as well as cell surface expression by using heterologous cell

culture. Only the generation of a mouse model harbouring the γ2 point mutation (R82Q) dissipated all these ambiguities (Tan *et al*., 2007). The emergence of massive gene-sequencing studies will generate an enormous amount of data, on the other hand developing mouse knock-in models for each new GABRA mutations is unrealistic, both because it is time consuming and far too expansive.

Here, we propose of using single cell genetic manipulation to investigate the effects of different mutations of $GABA_A$ α1 subunit on both dendritic spine and GABAergic bouton formation in cortical organotypic slices, which maintain the three dimensional structure of the brain tissue and the tight spatial relationships between different cell types. In particular, we analyzed the density and morphology of pyramidal cell dendritic spines, which are the preferential postsynaptic site of glutamatergic synapses. We also examined the axon morphology and bouton density of basket cells, which are the most prominent type of GABAergic interneurons in the cortex.

3.3 Materials and methods

Mice

Funder mice B6.129(FVB)-*Gabra1*^{tm1Geh}/J, first described in Vicini *et al*. (2001), were kindly gifted by Dr. Rudolph (McLean Hospital, Harvard Medical School) (Vicini *et al*., 2001). They were bred to establish a colony in the animal facility at the *Centre de recherche du Centre hospitalier de l'Université de Montréal* (CRCHUM). All mice were housed under standard pathogen–free conditions in a 12-hour light/dark cycle with *ad libitum* access to sterilized laboratory chow diet. Animals were treated in accordance with Canadian Council for Animal Care and protocols were approved by the Animal Care Committee of the CRCHUM and of CHU Ste-Justine Research Center. B6.129(FVB)-*Gabra1*^{tm1Geh}/J mice were previously produced in a mixed background. The background was characterized with a

microsatellite panel consisting of 110 markers spread across the genome at about 15 cM intervals and was confirmed to be 99.08% congenic to C57BL/6J background (Charles River, NY). B6.129(FVB)-*Gabra1*^{tm1Geh}/J mice possess three *loxP* sites on both sides of the α1 exon encoding an essential transmembrane domain of $GABA_A$ receptor.

DNA constructs

P_{G67}-GFP was generated by subcloning of a 10 kb region of *Gad1* gene promoter by gap repair in front of the GFP coding region in pEGFP (Clontech) as previously described (Chattopadhyaya *et al*., 2004). We subcloned CRE, *GABRA1*-A322D, *GABRA1*-D219N, *GABRA1*-K353delins18X constructs (Cossette *et al*., 2002;Lachance-Touchette *et al*., 2011) in P_{G67} vector by using restriction site Pme1 via sequence and ligation–independent cloning method (SLIC) (Li and Elledge, 2007). All constructs were sequenced to confirm the presence of the mutations and to exclude any other variants that may have been introduced during PCR amplification.

Slice culture and biolistic transfection

Slice culture preparation was done as described by (Stoppini *et al*., 1991). Postnatal day 4 or 5 (P4 or P5) mouse pups were decapitated, and brains were rapidly removed and immersed in ice-cold culture medium (containing DMEM, 20% horse serum, 1 mM glutamine, 13 mM glucose, 1 mM $CaCl_2$, 2 mM $MgSO_4$, 0.5 μm/ml insulin, 30 mM HEPES, 5 mM $NaHCO_3$, and 0.001% ascorbic acid). Coronal brain slices of the occipital cortex, 400 μm thick, were cut with a Chopper (Stoelting, Wood Dale, IL). Slices were then placed on transparent Millicell membrane inserts (Millipore, Bedford, MA), usually three slices/insert, in 30 mm Petri dishes containing 0.75 ml of culture medium. Finally, the slices were incubated in a humidified incubator at 34°C with a 5% CO_2-enriched atmosphere and the medium was changed three times per week. All procedures were performed under sterile conditions.

Constructs to be transfected were incorporated into "bullets" that were made using 1.6 μm gold particles coated with a total of ~60 μg of the DNA(s) of interest. These bullets were used to biolistically transfect slices by Gene gun (Bio-Rad, Hercules, CA) at high pressure (180 ψ), and the transfected slices were incubated for 8 days *in vitro* under the same conditions as described above, before imaging. For each experimental group, cortical slices were prepared from at least three mice. On average 6-7 neurons were transfected per cortical organotypic slice. The majority of neurons labeled by this promoter were parvalbumin-positive basket cells (as described in (Chattopadhyaya *et al*., 2004;Chattopadhyaya *et al*., 2007)), while a minority (~10%) were pyramidal cells. Pyramidal cells were recognized by the complexity of their dendritic arbor, including an apical dendrite, and the presence of numerous dendritic spines.

Imaging and spine analysis of pyramidal cells

Pyramidal neurons were imaged using a Leica confocal microscope SPE (63X glycerol immersion objective; NA 1.3). At least 6 labeled pyramidal neurons, characterized by the presence of a well-defined apical dendrite, were randomly selected from cortical layers 2/3 and 5. Image stacks of basal dendrites were acquired with a z-step of 0.5 μm and then reconstructed in 3-D with Neurolucida (MicroBrightField) software. Cortical pyramidal cells from at least four animals were used for each experimental condition. Dendritic length, total spine density, spine morphology and spine length were quantified using NeuroExplorer software (MicroBrightField). Mushroom spines were defined as spine with a neck and bearing a head, which was at least twice as large as the neck. Thin spines were defined as dendritic protrusions shorter than 5 μm and lacking a clearly defined head. All quantifications were done blind to the treatment.

Analysis of basket cell innervation

We quantified two aspects of basket cell axon innervation field – 1) the extent of perisomatic innervation around single neuronal somata (terminal branching and perisomatic GFP-positive bouton density) and 2) the percentage of potentially innervated cells in the field (percentage of innervation). We have previously shown that the vast majority of GFP-labeled boutons in our experimental condition most likely represent presynaptic terminals, by localization of pre- and post-synaptic markers and electron microscopy (Chattopadhyaya *et al*., 2004;Chattopadhyaya *et al*., 2007;Wu *et al*., 2012). For each experimental group, we took care to acquire an equal number of basket cells localized in layers 2/3 and 5/6 of the cortex. We acquired at least two confocal stacks of each basket cell axon arbor in the first 150 μm from the basket cell soma using a 63X glycerol objective (NA 1.3, Leica) and a Leica TCS SPE confocal microscope. The typical confocal stack size was 116.4 X 116.4 μm with an average depth of 40–70 μm and a z-step of 1 μm. Analysis of basket cell perisomatic innervation and bouton size was performed essentially as described by Chattopadhyaya *et al.* (2013). Briefly, in our Three-Dimensional Sholl analysis, Sholl spheres with a 1 μm increment from the center of a pyramidal soma were used to quantify basket axon terminal branch complexity and bouton density around the pyramidal cell soma. Axon branch complexity around a single pyramidal cell soma was quantified by the average number of intersections between basket cell axons and the Sholl spheres in the first 9 μm from the center of the pyramidal cell soma. We choose 9 μm as the limiting radius for a Sholl sphere because it approximates the average pyramidal cell soma diameter measured from pyramidal neurons immunostained with NeuN antibody. Between 10 and 15 pyramidal neurons were analyzed for each basket cell. Bouton density around each pyramidal cell soma was measured within the same set of Sholl spheres and averaged among pyramidal neurons for each condition. Only pyramidal cell somata with Sholl spheres, which intersected the basket cell axon in the

first 9 μm from the center of their soma, were taken for analysis. Using this approach, we obtained an unbiased estimate of the number of presumptive boutons on individual labeled pyramidal cell soma. The percentage of neuron somata innervated by a basket cell was defined in a confocal stack by the number of NeuN-positive cells contacted by at least one GFP-positive-bouton divided by the total number of NeuN-positive cells. This was repeated over all the fields of each basket axon and the results were averaged (Chattopadhyaya *et al*., 2013).

All data were first averaged per basket cell; statistical analysis was then done using the number of basket cells as *n*.

Statistical analysis

Differences between groups were assessed with one-way ANOVA followed by post-hoc Holm-Sidak test for normally distributed data or one-way ANOVA followed by post-hoc Kruskal-Wallis test for not-normally distributed data. The cells analyzed derived from at least three different sets of experiments. Data are expressed in term of mean ± standard error of mean (SEM).

3.4 Results

GABRA1 is broadly expressed in the nervous system and $GABA_AR$-mediated signalling plays multiple roles during development (Rossignol, 2011). In order to examine how different *GABRA1* mutants may affects the formation of dendritic spine and GABAergic bouton formation, we used a transgenic mouse carrying a conditional allele of *GABRA1* (Vicini *et al*., 2001), which allows cell-type and developmental-stage restricted knockdown of *GABRA1* synthesis. In this floxed-*GABRA1* mouse ($GABRA1^{flox/flox}$), Cre-mediated recombination

results in excision of exon 8, causing a shift in reading frame and premature termination of translation.

To inhibit *GABRA1* expression in isolated pyramidal neurons and GABAergic basket cells and simultaneously label their dendritic and axonal arbors at high resolution, we used a previously characterized promoter region P_{G67} (Chattopadhyaya *et al*., 2004) to express either Cre recombinase together with GFP (P_{G67}-GFP/Cre) or GFP alone (P_{G67}-GFP) in cortical organotypic cultures of *GABRA1*$^{flox/flox}$ mice (Figure 1). For pyramidal neurons, we focussed our analysis on dendritic spines, because dendritic spine alterations have been observed both in experimental animal models of epilepsy (Wong, 2005;Ma *et al*., 2013) and in human epilepsy patients (Multani *et al*., 1994;Isokawa, 2000). GABAergic basket cells (BCs), which represent about 40% of all cortical GABAergic cells in rodents, form synapses onto the somata and proximal dendrites of excitatory pyramidal cells. Because of the perisomatic localization and strength of their synapses, BCs strongly control the firing output of pyramidal cells and are thought to be important contributors to the maintenance of the overall excitation/inhibition balance in the cortex (Haider and McCormick, 2009). Further, BCs could act as a gate to prevent runaway excitation, which underlies the propagation of epileptiform activity (Trevelyan *et al*., 2007). Previous studies have shown that the basic features of dendritic spine formation and of the maturation of perisomatic innervation by BCs onto pyramidal cells are retained in cortical organotypic cultures (Dunaevsky *et al*., 1999;Chattopadhyaya *et al*., 2004;Di Cristo *et al*., 2004). We genetically manipulated pyramidal cells and BCs between the third and fourth postnatal week during which a significant and stereotyped maturation of BCs perisomatic innervation occurs (Chattopadhyaya *et al*., 2004;Chattopadhyaya *et al*., 2007;Di Cristo *et al*., 2007). Pyramidal cells from *GABRA1*$^{flox/flox}$ cultures transfected with P_{G67}*-GFP/*Cre (referred here on as *GABRA1*$^{-/-}$ cells) from equivalent postnatal day 16 (EP16, P4 + 12 days *in vitro*) to EP24 showed no

significant alterations in the overall spine density and morphology compared to age-matched control transfected only with P_{G67}-*GFP* (Figure 2G-H; Suppl Figure 1; total spine density *GABRA1*$^{+/+}$ vs *GABRA1*$^{-/-}$; 0.63 ± 0.04 vs 0.71 ± 0.05 spine/µm; p>0.05). *GABRA1*$^{-/-}$ BCs showed a significant reduction in the number of contacted target cells (Figure 3H; *GABRA1*$^{+/+}$ vs *GABRA1*$^{-/-}$; 61 ± 2% vs 41 ± 3%; p<0.05). In turn, the perisomatic innervations they formed around contacted neurons did not differ from those formed by control age-matched BCs, in term of bouton density or terminal branching (Figure 3F; *GABRA1*$^{+/+}$ vs *GABRA1*$^{-/-}$; 9.1 ± 0.5 vs 9.6 ± 0.7 boutons/soma; p>0.05). The axon density and average internode axon length were also not significantly different between these two groups (Suppl. Figure 2), thus suggesting that knockdown of *GABRA1* in this developmental time window did not affect overall axon growth.

To explore whether and how specific *GABRA1* mutants associated with GGE affect pyramidal cell spine and BCs GABAergic bouton formation, we inactivated the endogenous *GABRA1* alleles and simultaneously re-introduced either *GABRA1*$^{WT/WT}$ or each of the *GABRA1* mutant separately in single pyramidal and BCs from EP16-24. We choose this approach because global *GABRA1* manipulations may alter the excitation/inhibition balance of the whole slice, therefore making it difficult to distinguish between specific effects of distinct *GABRA1* mutants and unspecific, generalized effects of altered neuronal activity. In our experimental model, *GABRA1* was deleted only in sparse neurons in an otherwise wild-type background. It is therefore unlikely that the overall excitation levels in the slices was altered. A second critical advantage of our single-cell labeling/genetic manipulation approach is that we could visualize, reconstruct and quantify at high-resolution the dendritic and axonal arbours of single neurons with their putative boutons.

GABRA1$^{WT/WT}$ expression in *GABRA1*$^{-/-}$ pyramidal cells did not alter overall spine density (Figure 2G; *GABRA1*$^{+/+}$ vs *GABRA1*$^{WT/WT}$; 0.63 ± 0.04 vs 0.74 ± 0.05 spine/µm p>0.05),

although we observed a slight increase in the density of thin spines (Figure 2H; $GABRA1^{+/+}$ vs $GABRA1^{WT/WT}$; 0.02 ± 0.005 vs 0.09 ± 0.02 thin spines/µm; $p<0.001$). Importantly, $GABRA1^{WT/WT}$ expression rescued the number of target cells contacted by each $GABRA1^{-/-}$ BC (Figure 3H*;* $GABRA1^{+/+}$vs $GABRA1^{WT/WT}$; 61 ± 2% vs 59 ± 4%; $p>0.05$ and Figure 3H; $GABRA1^{-/-}$ vs $GABRA1^{WT/WT}$; *41* ± 3% vs 59 ± 4%; $p<0.001$) suggesting that biolistic transfection of $GABRA1^{WT/WT}$ under the P_{G67} promoter can drive the expression of enough protein to rescue *GABRA1* deficits in single cells.

Interestingly, we found that α1-A322D expression in $GABRA^{-/-}$ pyramidal cells specifically and significantly increased both total spine density (Figure 2G; $GABRA1^{+/+}$ vs $GABRA1^{AD/AD}$; 0.63 ± 0.04 vs 0.9 ± 0.1 spines/µm; $p<0.05$) and the proportion of mushroom-like spines on pyramidal cells basal dendrites (Figure 2H; Suppl Figure 1; $GABRA1^{+/+}$ vs $GABRA1^{AD/AD}$; 0.48 ± 0.05 vs 0.8 ± 0.1 mushroom spines/µm; $p<0.05$). As dendritic spines are the preferential site for glutamatergic synapse formation and mushroom spines in particular tend to show larger EPSCs compared to other spine types (Lee *et al*., 2012), these data suggest that α1-A322D expression may increase both the number and strength of excitatory synapses. In parallel, we found that α1-A322D expression in $GABRA1^{-/-}$ BCs rescued the loss of innervated targets caused by *GABRA1* deletion (Figure 3H; $GABRA1^{+/+}$ vs $GABRA1^{AD/AD}$; 61 ± 2% vs 51 ± 2%; $p>0.05$) and further increased the number of GABAergic boutons formed by BCs onto target cell somata compared to age-matched controls (Figure 3F; $GABRA1^{+/+}$ vs $GABRA1^{AD/AD}$; 9.1 ± 0.5 vs 13 ± 1 boutons/soma; $p<0.05$), suggesting that α1-A322D expression can increase the formation of GABAergic boutons.

Finally, we found that the expression of the other mutants, α1-D219N or α1-K353delins18X, had no effects on spine density and morphology in $GABRA1^{-/-}$ pyramidal cells. On the other hand, α1-D219N expression failed to rescue the loss of innervated targeted cells caused by *GABRA1* deletion (Figure 3H; $GABRA1^{+/+}$ vs $GABRA1^{DN/DN}$; 61 ± 2% vs 46 ± 5%; $p<0.001$)

and showed a trend towards reduced bouton density, which however did not reach significance (Figure 3F; *GABRA1*$^{+/+}$ vs *GABRA1*$^{DN/DN}$; 9.1 ± 0.5 vs 7.5 ± 0.8 boutons/soma; $p>0.05$). In summary, our data show a remarkably *GABRA1* mutant-specific effects on both dendritic spine and GABAergic bouton formation.

3.5 Discussion

Altogether, our data show for the first time that different *GABRA1* mutations associated with familial autosomal dominant GGE can affect dendritic spine and GABAergic bouton formation in a mutation-specific manner. Interestingly, *GABRA1* deletion in single pyramidal neurons did not affect their dendritic spine density or morphology, likely due to the compensatory action of other α1 subunits of $GABA_AR$. Consistently, α2 and α3 proteins were expressed at higher-level in the cerebral cortex of *GABRA1*-KO mice (Bosman *et al*., 2005;Zeller *et al*., 2008). In the same mouse model, global deletion of the α1 subunit triggered an increase in the density of postsynaptic sites expressing α3 subunit in the molecular layer of the cerebellum, which has been interpreted as a reorganization of cerebellar networks (Kralic *et al*., 2006). On the other hand, *GABRA1* deletion reduced the extent of BC innervation field in a cell-autonomous fashion (Figure 3), indicating that compensatory expression of other alpha subunits may not occur in GABAergic cells or that changes in inhibitory inputs caused by the presence of $GABA_AR$ lacking the α1 subunit may alter BC development. In fact, it has been shown that the maturation of the innervation field of GABAergic BCs is exquisitely dependent on neuron excitability and GABA release (Chattopadhyaya *et al*., 2007;Baho and Di Cristo, 2012;Wu *et al*., 2012). Consistent with this hypothesis, Purkinje cells from *GABRA1*$^{-/-}$ mice lacked spontaneous and evoked IPSCs (Fritschy and Panzanelli, 2006). In addition, stellate cell synapses on Purkinje cells dendrites were reduced by 75% in the same mouse model (Fritschy and Panzanelli, 2006). Unexpectedly, the expression of α1-WT in a knock-out background (*GABRA1*$^{-/-}$ pyramidal

neurons) increased the formation of thin spines, which are generally thought to represent immature/new synapses. One possibility is that the overexpression of α1-WT causes excess inhibition, which in turn promotes the formation of new excitatory synapses (Queenan *et al*., 2012). Quantitative analysis of inhibitory and excitatory inputs onto transfected neurons will be necessary to clarify this issue and will be the focus on future studies.

Surprisingly, we found that different α1 mutants have very different impacts on the development of GABAergic boutons and dendritic spines. The *GABRA1* mutant that showed the most dramatic effects on both pyramidal cell spines and basket cell innervation field was α1-A322D. This observation is consistent with previous electrophysiological studies showing that this mutation has more severe effect *in vitro* on the gating properties of the GABA-evoked currents, compared to other *GABRA1* missense mutations (Macdonald *et al*., 2010;Lachance-Touchette *et al*., 2011). One possibility is that α1-A322D may act as dominant negative. Using cell cultures, Ding and collaborators (2010) showed that α1-A322D reduced the overall surface expression of $GABA_AR$ by associating with the wild type subunits within the endoplasmic reticulum and preventing them from trafficking to the cell surface (Ding *et al*., 2010;Lachance-Touchette *et al*., 2011). Reduction in cell surface expression of $GABA_AR$ resulted in decreased postsynaptic inhibition (Ding *et al*., 2010), which may in turn facilitate long-term potentiation (LTP) of excitatory synapses (Carlson *et al*., 2002). One of the main effects of LTP is the increase in AMPA-receptor density at postsynaptic sites on dendritic spines (Liu *et al*., 2005;Whissell *et al*., 2013), which correlate with the presence of more mature mushroom spines characterized by large heads (Luscher *et al*., 2000), consistently to what we observed (Figure 2). Similarly, reduction of inhibition onto BCs could promote GABA release and, subsequently, formation of GABAergic boutons (Chattopadhyaya *et al*., 2007;Baho and Di Cristo, 2012). Therefore, these results suggest that

altered excitatory/inhibitory synaptic balance may be partially responsible for the increased excitability of cortical networks in human carriers of α1-A322D.

Interestingly, α1-D219N expression in *GABRA1*$^{-/-}$ BC was unable to rescue the deficits in their innervation field, while it did not affect dendritic spine density. Our prior studies showed that $GABA_A$Rs containing α1-D219N were trafficked to the membrane and that mutation altered $GABA_A$ receptor gating kinetics. In particular, $GABA_A$Rs containing α1-D219N have slower desensitization rates and faster off-kinetics compared to wild-type receptors (Lachance-Touchette *et al*., 2011). It is therefore possible that reduced inhibition may be partially responsible for both altered development of GABAergic cells and increased excitability of neuronal circuits in human carriers of α1-D219N. Finally, the expression of α1-K353delins18X did not affect any of the developmental events we analyzed. We have previously reported that this frameshift mutation altered the downstream amino acid sequence and resulted in the introduction of a premature translation–termination codon (PTC) (Lachance-Touchette *et al*., 2011). The premature translation termination is likely to cause mRNA degradation by a process called nonsense-mediated mRNA decay (Baker and Parker, 2004), thereby explaining why expression of α1-K353delins18X did not affect the phenotype of *GABRA1*$^{-/-}$ neurons.

Altogether, our data suggest that a "loss-of-function" model may not always explain the effects of *GABRA1* mutations on dendritic spines and GABAergic bouton formation. For example, reduced inhibition is most often mentioned as a cause of epileptic syndromes. Here, our data suggest that α1-A322D may instead increase the number of dendritic spines, which are the preferential site of excitatory synapse formation, an event that may result in higher cortical excitation. These potential effects on developing neuronal networks need to be

further explored by recording miniature inhibitory (mIPSCs) and excitatory (mEPSCs) postsynaptic currents in transfected neurons.

With the advance in the technology of large-scale multiplex sequencing or next-generation sequencing (NGS), it is now possible to obtain the sequence of the whole exome (WES) and even the whole genome (WGS) for a given individual. These methodological approaches are very powerful and are already opening new frontiers of genomics research. However, by sequencing many more genomes, we will need *in vitro* models to determine the functional biological role of all new variants that we will find. The use of heterelogous models such as HEK cells and xenopus oocytes may not be the best systems to test the impact of mutations in $GABA_AR$ subunits. For example, despite a large number of studies, the functional alterations caused by missenses mutations identified in *GABRG2* in epileptic patients are still not well understood. In fact, there is no consensus about the effect of the mutations R82Q, P83S, R177G and K328M on the GABA currents amplitude (Baulac *et al*., 2001;Wallace *et al*., 2001;Bianchi *et al*., 2002;Bowser *et al*., 2002;Kang and Macdonald, 2004;Hales *et al*., 2005;Audenaert *et al*., 2006;Kang *et al*., 2006;Eugene *et al*., 2007;Frugier *et al*., 2007;Goldschen-Ohm *et al*., 2010;Lachance-Touchette *et al*., 2011;Huang *et al*., 2014;Todd *et al*., 2014). As another example, it is still debated whether β3-P11S, β3-G32R and γ2-P83S altered surface expression of the $GABA_AR$ or of the subunit itself (Tanaka *et al*., 2008;Delahanty *et al*., 2011;Lachance-Touchette *et al*., 2011;Gurba *et al*., 2012). In addition, the exclusive use of non-neuronal cells will not answer the question on how biophysical alterations in mutated receptor properties may alter brain development and ultimately lead to hyperexcitable networks. Here, we suggest that organotypic slice cultures may provide an accessible system for investigating the specific effects of GABA receptor mutants on neuronal development. Moreover, in contrast to what occur in dissociated neuronal cultures,

organotypic slice cultures retain complex 3-dimensional interactions between different cell types as they occur *in vivo*. Therefore, we believe that the single cell genetic manipulation described here is a novel tool to understand how $GABA_A$ receptor mutants disrupt neuronal circuit formation and will help define the pathophysiology of genetic epilepsy syndromes.

3.6 Acknowledgement

We are grateful to Caroline Meloche, Marylise Piché and Denise Carrier for animal handling and technical support. We thank also Dr. Devendra Amre for help with statistical analysis. This work was supported by operating grants to P. Cossette from the Canadian Institutes for Health Research, the Savoy Foundation and Genome Canada. G. Di Cristo is supported by a Canada Research Chair and Savoy Foundation. P. Lachance-Touchette is supported by a doctoral fellowship from FRQS. We are grateful to Dr. Jean-Claude Lacaille (Université de Montréal) for data discussion.

3.7 Figures

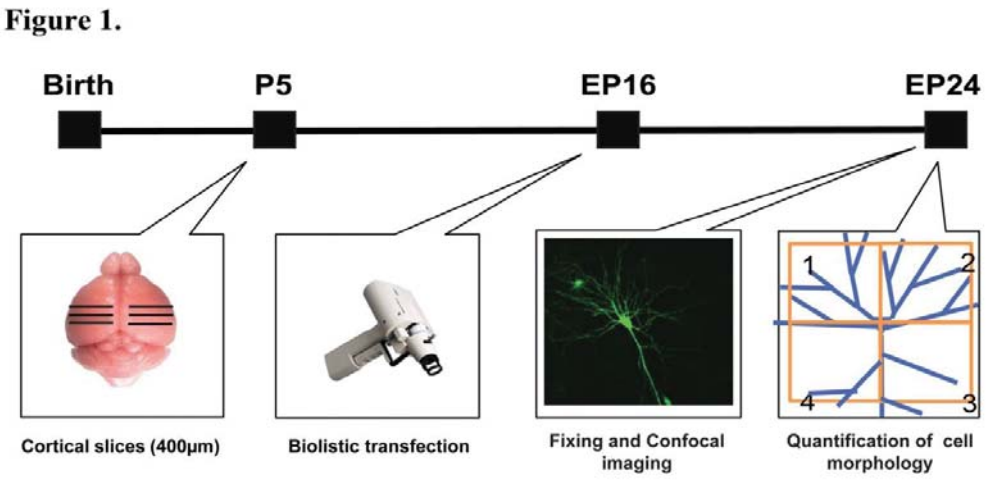

Figure 3.1 Figure 1.Schematic of the experimental approach. Single cell transfection strategy avoids altering the overall activity level in the cortex.

Figure 2.

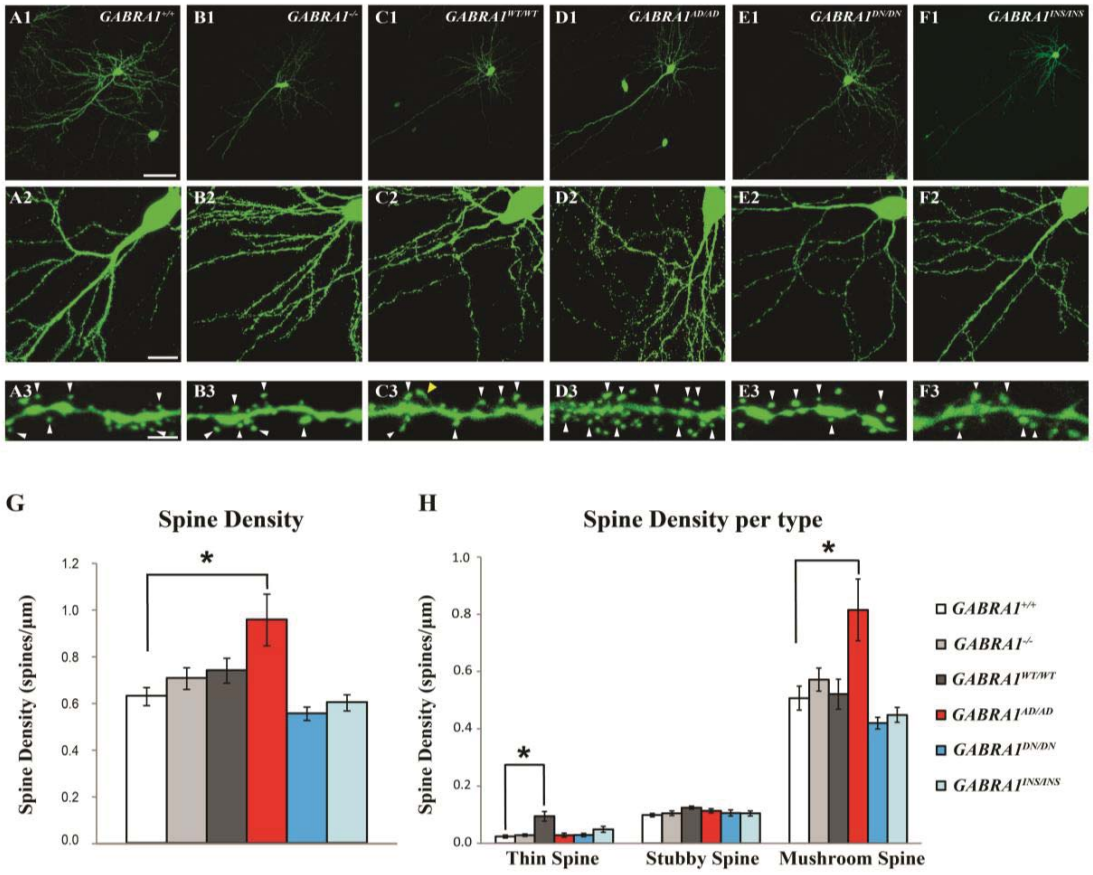

Figure 3.2 Figure 2.α1-A322D expression induces a significant increase in the number and maturation of dendritic spines in cortical pyramidal cells. (**A1-A3**) Confocal images showing pyramidal cells transfected with GFP (green) alone (control, *GABRA1*$^{+/+}$ cells) or ***(B1-B3)*** GFP and CRE (*GABRA1*$^{-/-}$) to knockdown endogenous α1 subunits, or GFP-CRE and either one of the wild-type or mutants α1 ***(C1-F3)*** to investigate the effects of different α1 mutants on spine density and morphology, in organotypic cultures. (**A3-F3**) High magnification images of dendrites from pyramidal cells in ***A2-F2***. White arrowheads indicates mushroom spines, yellow arrowhead indicate a thin spine. (**G, H**) α1-A322D mutant pyramidal cells show significantly increased density of total (***G***) and mushroom-like spines (***H***) compared to control age-matched pyramidal cells (1-way ANOVA; *p<0.05). α1-WT expression induces a significant increase in thin-like spines (***H***, 1-way ANOVA; *p<0.05). GFP n=7; GFP-CRE n=9; GFP-CRE-WT n=7; GFP-CRE-A322D n=7; GFP-CRE-D219N n=6; GFP-CRE-K353delins18X n=7 pyramidal cells. Scale bars: ***A1-F1***, 50 µm; ***A2–F2***, 10µm; ***A3-F3***, 5 µm.

Figure 3.

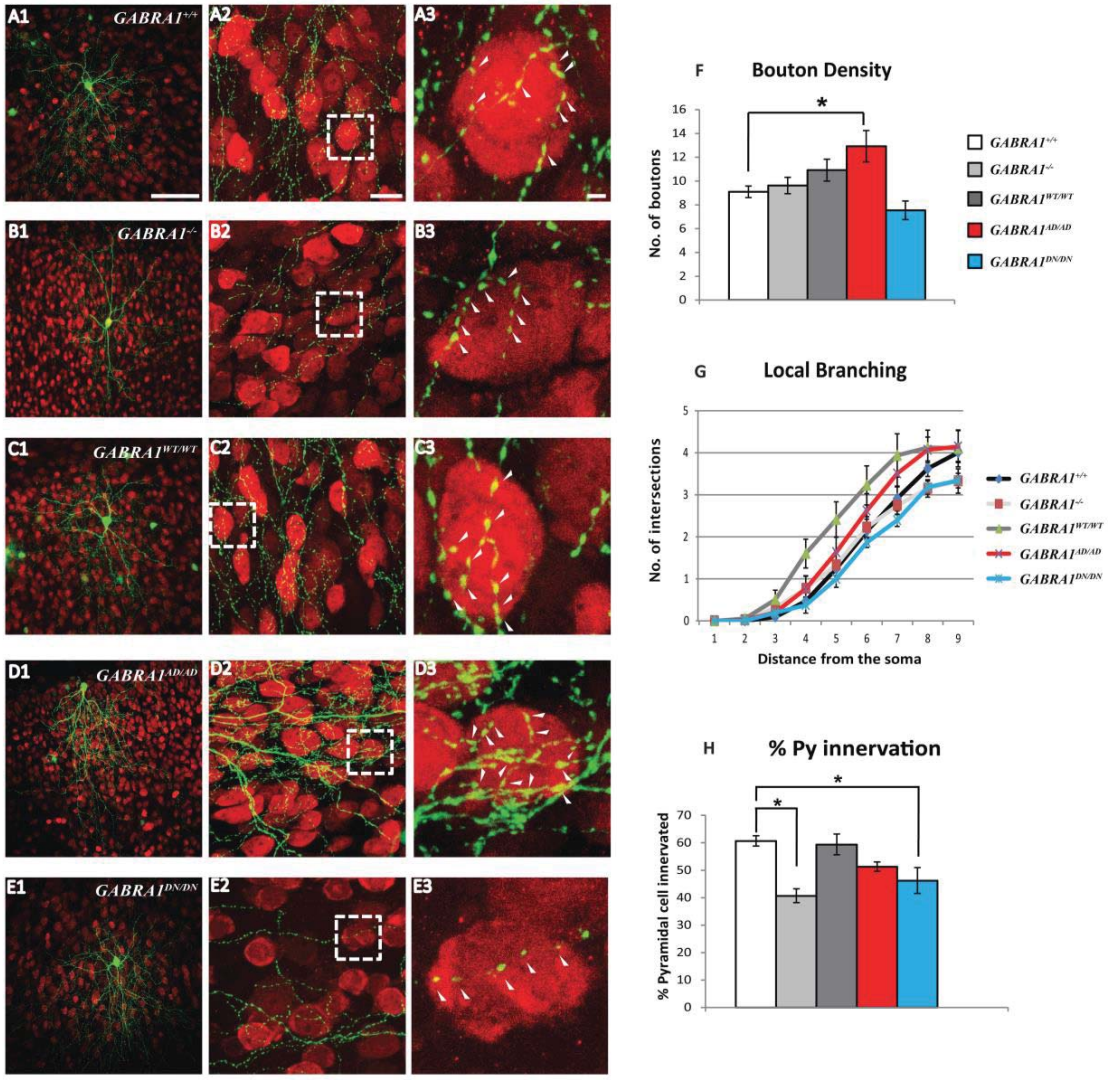

Figure 3.3 Figure 3.α1-A322D expression induces a significant increase in boutons formed by GABAergic cortical basket cells. (A-E) Low (***A1-E1***) and high magnification (***A2-E2***) confocal images showing basket cells transfected with GFP (green) alone (***A,*** *GABRA1*$^{+/+}$cells) or GFP and CRE (***B,*** *GABRA1*$^{-/-}$ cells), or GFP-CRE and either one of the wild-type or mutants α1 subunits (***C-E***). Basket cells form terminal axon branching bearing numerous presynaptic boutons around NeuN (red)-positive somata (arrowheads). **A3-E3** are high-magnification images from boxed areas in **A2-E2**. (**F**) *GABRA1*$^{-/-}$ basket cells transfected with α1-A322D show significant increase in bouton density (***F***). Local branching (***G***) does not differ across the groups. (**H**) *GABRA1*$^{-/-}$ basket cells contact less pyramidal somata compared to age-matched basket cells. This deficit is rescued by the expressions of α1-wild-type or α1-A322D but not of α1-D219N (1-way ANOVA; *p<0.05). GFP n=6; GFP-CRE, n=6; GFPCRE- WT, n=6; GFP-CRE-A322D, n=6; GFP-CRE-D219N, n=4 basket cells. Scale bars: ***A1–E1***, 50 μm; ***A2–E2***, 10 μm; ***A3–E3***, 5 μm.

Supplemental Figure 1.

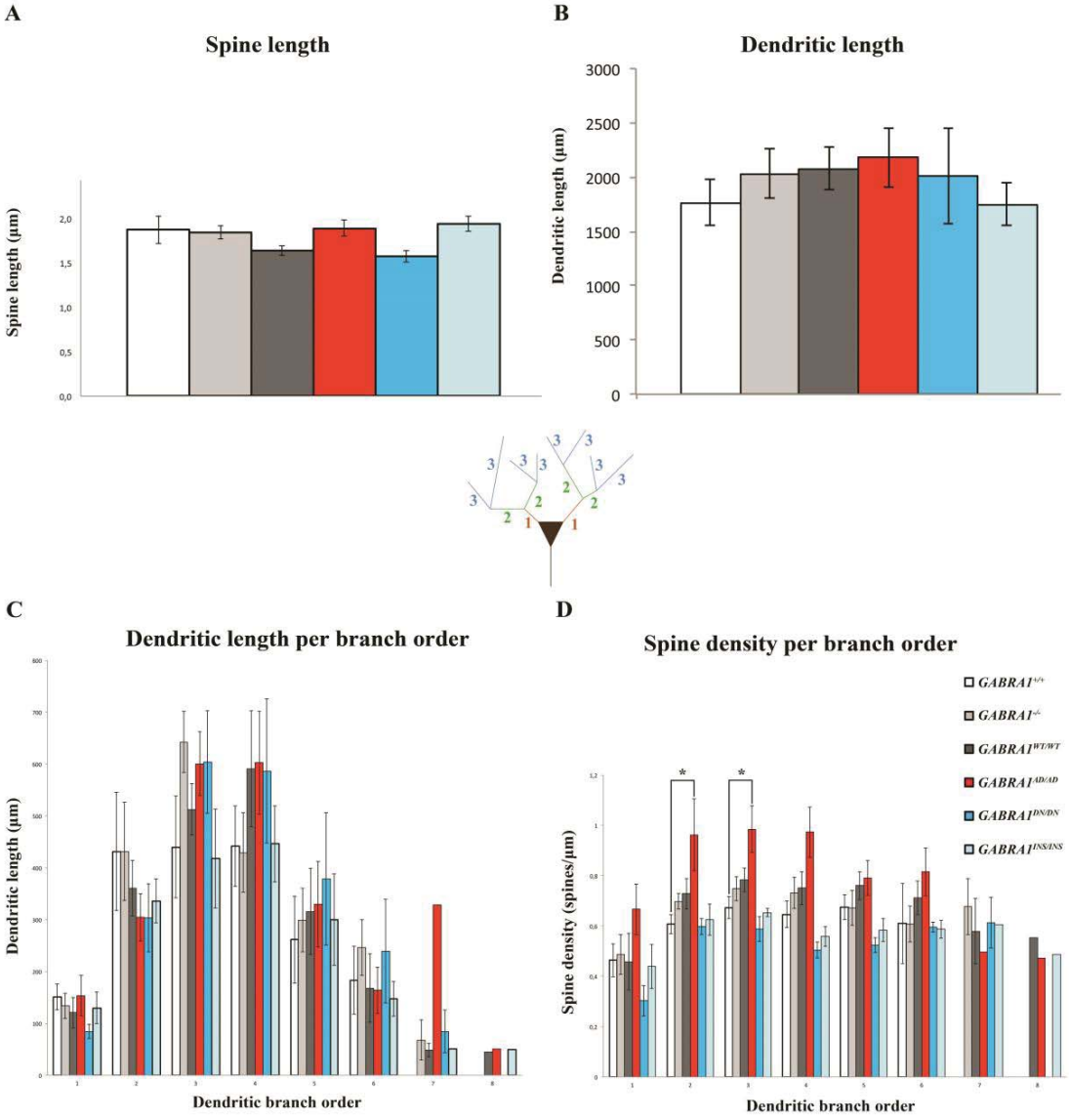

Figure 3.4 Supplementary Figure 1. α1-A322D expression induces a significant increase in spines density in cortical pyramidal cells. (**A**) Spine length, (**B**) dendritic length and (**C**) dendritic length per branch order do not differ across the groups. (**D**) *GABRA1*$^{AD/AD}$ mutant pyramidal cells show significantly increased density of spines in dendritic branch order two and three compared to control age-matched pyramidal cells *GABRA*$^{+/+}$ (1-way ANOVA; *p<0.05). GFP n=7; GFP-CRE n=9; GFP-CRE-WT n=7; GFP-CRE-A322D n=7; GFP-CRE-D219N n=6; GFP-CRE-K353delins18X n=7.

Supplemental Figure 2.

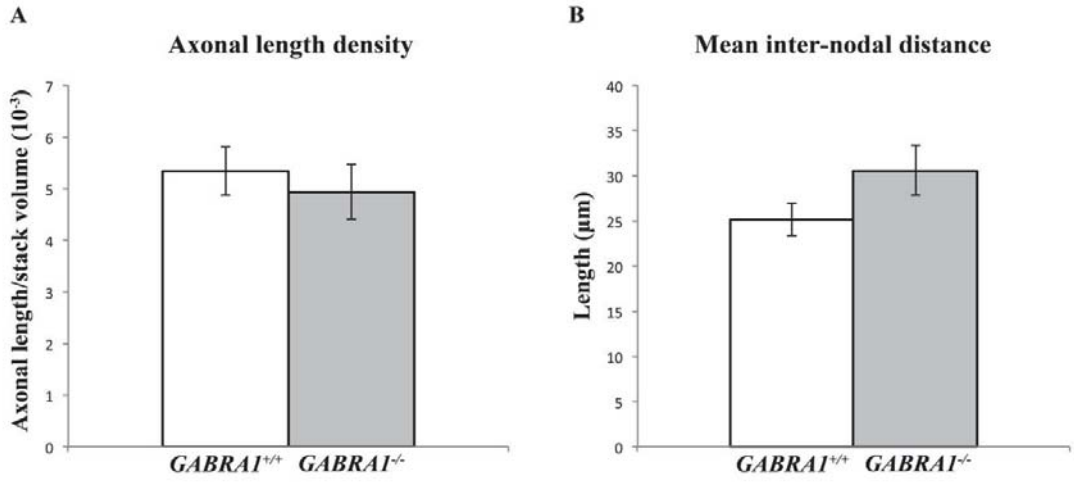

Figure 3.5 Supplementary Figure 2. *GABRA1* knockdown does not alter the overall axon growth basket cells. (A) Axonal density and (B) inter-node axon length are not significantly different between *GABRA1*$^{-/-}$ and *GABRA1*$^{+/+}$ basket cells. GFP n=6; GFP-CRE, n=6 basket cells.

3.8 References

Arain, F.M., Boyd, K.L., and Gallagher, M.J. (2012). Decreased viability and absence-like epilepsy in mice lacking or deficient in the GABAA receptor alpha1 subunit. *Epilepsia* 53**,** e161-165. doi: 10.1111/j.1528-1167.2012.03596.x.

Audenaert, D., Schwartz, E., Claeys, K.G., Claes, L., Deprez, L., Suls, A., Van Dyck, T., Lagae, L., Van Broeckhoven, C., Macdonald, R.L., and De Jonghe, P. (2006). A novel GABRG2 mutation associated with febrile seizures. *Neurology* 67**,** 687-690. doi: 10.1212/01.wnl.0000230145.73496.a2.

Baho, E., and Di Cristo, G. (2012). Neural activity and neurotransmission regulate the maturation of the innervation field of cortical GABAergic interneurons in an age-dependent manner. *J Neurosci* 32**,** 911-918. doi: 10.1523/JNEUROSCI.4352-11.2012.

Baker, K.E., and Parker, R. (2004). Nonsense-mediated mRNA decay: terminating erroneous gene expression. *Curr Opin Cell Biol* 16**,** 293-299. doi: 10.1016/j.ceb.2004.03.003.

Baulac, S., Huberfeld, G., Gourfinkel-An, I., Mitropoulou, G., Beranger, A., Prud'homme, J.F., Baulac, M., Brice, A., Bruzzone, R., and Leguern, E. (2001). First genetic evidence of GABA(A) receptor dysfunction in epilepsy: a mutation in the gamma2-subunit gene. *Nat Genet* 28**,** 46-48.

Bernard, C. (2012). "Alterations in synaptic function in epilepsy," in *Jasper's Basic Mechanisms of the Epilepsies,* eds. J.L. Noebels, M. Avoli, M.A. Rogawski, R.W. Olsen & A.V. Delgado-Escueta. 4th ed (Bethesda (MD)).

Bianchi, M.T., Song, L., Zhang, H., and Macdonald, R.L. (2002). Two different mechanisms of disinhibition produced by GABAA receptor mutations linked to epilepsy in humans. *J Neurosci* 22**,** 5321-5327. doi: 20026554

22/13/5321 [pii].

Bosman, L.W., Heinen, K., Spijker, S., and Brussaard, A.B. (2005). Mice lacking the major adult GABAA receptor subtype have normal number of synapses, but retain juvenile IPSC kinetics until adulthood. *J Neurophysiol* 94**,** 338-346. doi: 10.1152/jn.00084.2005.

Bowser, D.N., Wagner, D.A., Czajkowski, C., Cromer, B.A., Parker, M.W., Wallace, R.H., Harkin, L.A., Mulley, J.C., Marini, C., Berkovic, S.F., Williams, D.A., Jones, M.V., and Petrou, S. (2002). Altered kinetics and benzodiazepine sensitivity of a GABAA receptor subunit mutation [gamma 2(R43Q)] found in human epilepsy. *Proc Natl Acad Sci U S A* 99**,** 15170-15175. doi: 10.1073/pnas.212320199

212320199 [pii].

Carlson, G., Wang, Y., and Alger, B.E. (2002). Endocannabinoids facilitate the induction of LTP in the hippocampus. *Nat Neurosci* 5**,** 723-724. doi: 10.1038/nn879.

Carvill, G.L., Heavin, S.B., Yendle, S.C., Mcmahon, J.M., O'roak, B.J., Cook, J., Khan, A., Dorschner, M.O., Weaver, M., Calvert, S., Malone, S., Wallace, G., Stanley, T., Bye, A.M., Bleasel, A., Howell, K.B., Kivity, S., Mackay, M.T., Rodriguez-Casero, V., Webster, R., Korczyn, A., Afawi, Z., Zelnick, N., Lerman-Sagie, T., Lev, D., Moller, R.S., Gill, D., Andrade, D.M., Freeman, J.L., Sadleir, L.G., Shendure, J., Berkovic, S.F., Scheffer, I.E., and Mefford, H.C. (2013). Targeted resequencing in epileptic encephalopathies identifies de novo mutations in CHD2 and SYNGAP1. *Nat Genet* 45**,** 825-830. doi: 10.1038/ng.2646.

Carvill, G.L., Weckhuysen, S., Mcmahon, J.M., Hartmann, C., Moller, R.S., Hjalgrim, H., Cook, J., Geraghty, E., O'roak, B.J., Petrou, S., Clarke, A., Gill, D., Sadleir, L.G.,

Muhle, H., Von Spiczak, S., Nikanorova, M., Hodgson, B.L., Gazina, E.V., Suls, A., Shendure, J., Dibbens, L.M., De Jonghe, P., Helbig, I., Berkovic, S.F., Scheffer, I.E., and Mefford, H.C. (2014). GABRA1 and STXBP1: Novel genetic causes of Dravet syndrome. *Neurology* 82**,** 1245-1253. doi: 10.1212/WNL.0000000000000291.

Chattopadhyaya, B., Baho, E., Huang, Z.J., Schachner, M., and Di Cristo, G. (2013). Neural cell adhesion molecule-mediated Fyn activation promotes GABAergic synapse maturation in postnatal mouse cortex. *J Neurosci* 33**,** 5957-5968. doi: 10.1523/JNEUROSCI.1306-12.2013.

Chattopadhyaya, B., Di Cristo, G., Higashiyama, H., Knott, G.W., Kuhlman, S.J., Welker, E., and Huang, Z.J. (2004). Experience and activity-dependent maturation of perisomatic GABAergic innervation in primary visual cortex during a postnatal critical period. *J Neurosci* 24**,** 9598-9611. doi: 10.1523/JNEUROSCI.1851-04.2004.

Chattopadhyaya, B., Di Cristo, G., Wu, C.Z., Knott, G., Kuhlman, S., Fu, Y., Palmiter, R.D., and Huang, Z.J. (2007). GAD67-mediated GABA synthesis and signaling regulate inhibitory synaptic innervation in the visual cortex. *Neuron* 54**,** 889-903. doi: 10.1016/j.neuron.2007.05.015.

Cossette, P., Lachance-Touchette, P., and Rouleau, G.A. (2012). "Mutated GABAA receptor subunits in idiopathic generalized epilepsy," in *Jasper's Basic Mechanisms of the Epilepsies,* eds. J.L. Noebels, M. Avoli, M.A. Rogawski, R.W. Olsen & A.V. Delgado-Escueta. 4th ed (Bethesda (MD)).

Cossette, P., Liu, L., Brisebois, K., Dong, H., Lortie, A., Vanasse, M., Saint-Hilaire, J.M., Carmant, L., Verner, A., Lu, W.Y., Wang, Y.T., and Rouleau, G.A. (2002). Mutation of GABRA1 in an autosomal dominant form of juvenile myoclonic epilepsy. *Nat Genet* 31**,** 184-189. doi: 10.1038/ng885.

Delahanty, R.J., Kang, J.Q., Brune, C.W., Kistner, E.O., Courchesne, E., Cox, N.J., Cook, E.H., Jr., Macdonald, R.L., and Sutcliffe, J.S. (2011). Maternal transmission of a rare GABRB3 signal peptide variant is associated with autism. *Mol Psychiatry* 16**,** 86-96. doi: 10.1038/mp.2009.118.

Di Cristo, G., Chattopadhyaya, B., Kuhlman, S.J., Fu, Y., Belanger, M.C., Wu, C.Z., Rutishauser, U., Maffei, L., and Huang, Z.J. (2007). Activity-dependent PSA expression regulates inhibitory maturation and onset of critical period plasticity. *Nat Neurosci* 10**,** 1569-1577. doi: 10.1038/nn2008.

Di Cristo, G., Wu, C., Chattopadhyaya, B., Ango, F., Knott, G., Welker, E., Svoboda, K., and Huang, Z.J. (2004). Subcellular domain-restricted GABAergic innervation in primary visual cortex in the absence of sensory and thalamic inputs. *Nat Neurosci* 7**,** 1184-1186. doi: 10.1038/nn1334.

Dibbens, L.M., Feng, H.J., Richards, M.C., Harkin, L.A., Hodgson, B.L., Scott, D., Jenkins, M., Petrou, S., Sutherland, G.R., Scheffer, I.E., Berkovic, S.F., Macdonald, R.L., and Mulley, J.C. (2004). GABRD encoding a protein for extra- or peri-synaptic GABAA receptors is a susceptibility locus for generalized epilepsies. *Hum Mol Genet* 13**,** 1315-1319. doi: 10.1093/hmg/ddh146

ddh146 [pii].

Dibbens, L.M., Harkin, L.A., Richards, M., Hodgson, B.L., Clarke, A.L., Petrou, S., Scheffer, I.E., Berkovic, S.F., and Mulley, J.C. (2009). The role of neuronal GABA(A) receptor subunit mutations in idiopathic generalized epilepsies. *Neurosci Lett* 453**,** 162-165. doi: S0304-3940(09)00214-6 [pii]

10.1016/j.neulet.2009.02.038.

Ding, L., Feng, H.J., Macdonald, R.L., Botzolakis, E.J., Hu, N., and Gallagher, M.J. (2010). GABA(A) receptor alpha1 subunit mutation A322D associated with autosomal dominant juvenile myoclonic epilepsy reduces the expression and alters the

composition of wild type GABA(A) receptors. *J Biol Chem* 285**,** 26390-26405. doi: 10.1074/jbc.M110.142299.

Dunaevsky, A., Tashiro, A., Majewska, A., Mason, C., and Yuste, R. (1999). Developmental regulation of spine motility in the mammalian central nervous system. *Proc Natl Acad Sci U S A* 96**,** 13438-13443.

Epi, K.C., Epilepsy Phenome/Genome, P., Allen, A.S., Berkovic, S.F., Cossette, P., Delanty, N., Dlugos, D., Eichler, E.E., Epstein, M.P., Glauser, T., Goldstein, D.B., Han, Y., Heinzen, E.L., Hitomi, Y., Howell, K.B., Johnson, M.R., Kuzniecky, R., Lowenstein, D.H., Lu, Y.F., Madou, M.R., Marson, A.G., Mefford, H.C., Esmaeeli Nieh, S., O'brien, T.J., Ottman, R., Petrovski, S., Poduri, A., Ruzzo, E.K., Scheffer, I.E., Sherr, E.H., Yuskaitis, C.J., Abou-Khalil, B., Alldredge, B.K., Bautista, J.F., Berkovic, S.F., Boro, A., Cascino, G.D., Consalvo, D., Crumrine, P., Devinsky, O., Dlugos, D., Epstein, M.P., Fiol, M., Fountain, N.B., French, J., Friedman, D., Geller, E.B., Glauser, T., Glynn, S., Haut, S.R., Hayward, J., Helmers, S.L., Joshi, S., Kanner, A., Kirsch, H.E., Knowlton, R.C., Kossoff, E.H., Kuperman, R., Kuzniecky, R., Lowenstein, D.H., Mcguire, S.M., Motika, P.V., Novotny, E.J., Ottman, R., Paolicchi, J.M., Parent, J.M., Park, K., Poduri, A., Scheffer, I.E., Shellhaas, R.A., Sherr, E.H., Shih, J.J., Singh, R., Sirven, J., Smith, M.C., Sullivan, J., Lin Thio, L., Venkat, A., Vining, E.P., Von Allmen, G.K., Weisenberg, J.L., Widdess-Walsh, P., and Winawer, M.R. (2013). De novo mutations in epileptic encephalopathies. *Nature* 501**,** 217-221. doi: 10.1038/nature12439.

Eugene, E., Depienne, C., Baulac, S., Baulac, M., Fritschy, J.M., Le Guern, E., Miles, R., and Poncer, J.C. (2007). GABA(A) receptor gamma 2 subunit mutations linked to human epileptic syndromes differentially affect phasic and tonic inhibition. *J Neurosci* 27**,** 14108-14116. doi: 10.1523/JNEUROSCI.2618-07.2007.

Fritschy, J.M., and Panzanelli, P. (2006). Molecular and synaptic organization of GABAA receptors in the cerebellum: Effects of targeted subunit gene deletions. *Cerebellum* 5**,** 275-285. doi: 10.1080/14734220600962805.

Frugier, G., Coussen, F., Giraud, M.F., Odessa, M.F., Emerit, M.B., Boue-Grabot, E., and Garret, M. (2007). A gamma 2(R43Q) mutation, linked to epilepsy in humans, alters GABAA receptor assembly and modifies subunit composition on the cell surface. *J Biol Chem* 282**,** 3819-3828. doi: M608910200 [pii]
10.1074/jbc.M608910200.

Gaiarsa, J.L., and Porcher, C. (2013). Emerging neurotrophic role of GABAB receptors in neuronal circuit development. *Front Cell Neurosci* 7**,** 206. doi: 10.3389/fncel.2013.00206.

Gallagher, M.J., Ding, L., Maheshwari, A., and Macdonald, R.L. (2007). The GABAA receptor alpha1 subunit epilepsy mutation A322D inhibits transmembrane helix formation and causes proteasomal degradation. *Proc Natl Acad Sci U S A* 104**,** 12999-13004. doi: 10.1073/pnas.0700163104.

Gallagher, M.J., Song, L., Arain, F., and Macdonald, R.L. (2004). The juvenile myoclonic epilepsy GABA(A) receptor alpha1 subunit mutation A322D produces asymmetrical, subunit position-dependent reduction of heterozygous receptor currents and alpha1 subunit protein expression. *J Neurosci* 24**,** 5570-5578. doi: 10.1523/JNEUROSCI.1301-04.2004.

Goldschen-Ohm, M.P., Wagner, D.A., Petrou, S., and Jones, M.V. (2010). An epilepsy-related region in the GABA(A) receptor mediates long-distance effects on GABA and benzodiazepine binding sites. *Mol Pharmacol* 77**,** 35-45. doi: mol.109.058289 [pii]
10.1124/mol.109.058289.

Gurba, K.N., Hernandez, C.C., Hu, N., and Macdonald, R.L. (2012). GABRB3 mutation, G32R, associated with childhood absence epilepsy alters alpha1beta3gamma2L gamma-aminobutyric acid type A (GABAA) receptor expression and channel gating. *J Biol Chem* 287**,** 12083-12097. doi: 10.1074/jbc.M111.332528.

Haider, B., and Mccormick, D.A. (2009). Rapid neocortical dynamics: cellular and network mechanisms. *Neuron* 62**,** 171-189. doi: 10.1016/j.neuron.2009.04.008.

Hales, T.G., Tang, H., Bollan, K.A., Johnson, S.J., King, D.P., Mcdonald, N.A., Cheng, A., and Connolly, C.N. (2005). The epilepsy mutation, gamma2(R43Q) disrupts a highly conserved inter-subunit contact site, perturbing the biogenesis of GABAA receptors. *Mol Cell Neurosci* 29**,** 120-127. doi: S1044-7431(05)00009-6 [pii]
10.1016/j.mcn.2005.01.002.

Hancili, S., Onal, Z.E., Ata, P., Karatoprak, E.Y., Gurbuz, T., Bostanci, M., Pacal, Y., Nuhoglu, C., and Ceran, O. (2014). The GABAA receptor gamma2 subunit (R43Q) mutation in febrile seizures. *Pediatr Neurol* 50**,** 353-356. doi: 10.1016/j.pediatrneurol.2014.01.002.

Harkin, L.A., Bowser, D.N., Dibbens, L.M., Singh, R., Phillips, F., Wallace, R.H., Richards, M.C., Williams, D.A., Mulley, J.C., Berkovic, S.F., Scheffer, I.E., and Petrou, S. (2002). Truncation of the GABA(A)-receptor gamma2 subunit in a family with generalized epilepsy with febrile seizures plus. *Am J Hum Genet* 70**,** 530-536. doi: 10.1086/338710.

Hayama, T., Noguchi, J., Watanabe, S., Takahashi, N., Hayashi-Takagi, A., Ellis-Davies, G.C., Matsuzaki, M., and Kasai, H. (2013). GABA promotes the competitive selection of dendritic spines by controlling local Ca2+ signaling. *Nat Neurosci* 16**,** 1409-1416. doi: 10.1038/nn.3496.

Huang, X., Hernandez, C.C., Hu, N., and Macdonald, R.L. (2014). Three epilepsy-associated GABRG2 missense mutations at the gamma+/beta- interface disrupt GABA receptor assembly and trafficking by similar mechanisms but to different extents. *Neurobiol Dis* 68C**,** 167-179. doi: 10.1016/j.nbd.2014.04.015.

Ishii, A., Kanaumi, T., Sohda, M., Misumi, Y., Zhang, B., Kakinuma, N., Haga, Y., Watanabe, K., Takeda, S., Okada, M., Ueno, S., Kaneko, S., Takashima, S., and Hirose, S. (2014). Association of nonsense mutation in GABRG2 with abnormal trafficking of GABAA receptors in severe epilepsy. *Epilepsy Res* 108**,** 420-432. doi: 10.1016/j.eplepsyres.2013.12.005.

Isokawa, M. (2000). Remodeling dendritic spines of dentate granule cells in temporal lobe epilepsy patients and the rat pilocarpine model. *Epilepsia* 41 Suppl 6**,** S14-17.

Johnston, A.J., Kang, J.Q., Shen, W., Pickrell, W.O., Cushion, T.D., Davies, J.S., Baer, K., Mullins, J.G., Hammond, C.L., Chung, S.K., Thomas, R.H., White, C., Smith, P.E., Macdonald, R.L., and Rees, M.I. (2014). A novel GABRG2 mutation, p.R136*, in a family with GEFS+ and extended phenotypes. *Neurobiol Dis* 64**,** 131-141. doi: 10.1016/j.nbd.2013.12.013.

Kananura, C., Haug, K., Sander, T., Runge, U., Gu, W., Hallmann, K., Rebstock, J., Heils, A., and Steinlein, O.K. (2002). A splice-site mutation in GABRG2 associated with childhood absence epilepsy and febrile convulsions. *Arch Neurol* 59**,** 1137-1141.

Kang, J.Q., and Macdonald, R.L. (2004). The GABAA receptor gamma2 subunit R43Q mutation linked to childhood absence epilepsy and febrile seizures causes retention of alpha1beta2gamma2S receptors in the endoplasmic reticulum. *J Neurosci* 24**,** 8672-8677.

Kang, J.Q., Shen, W., and Macdonald, R.L. (2006). Why does fever trigger febrile seizures? GABAA receptor gamma2 subunit mutations associated with idiopathic generalized

epilepsies have temperature-dependent trafficking deficiencies. *J Neurosci* 26**,** 2590-2597. doi: 26/9/2590 [pii]
10.1523/JNEUROSCI.4243-05.2006.
Kilb, W., Kirischuk, S., and Luhmann, H.J. (2013). Role of tonic GABAergic currents during pre- and early postnatal rodent development. *Front Neural Circuits* 7**,** 139. doi: 10.3389/fncir.2013.00139.
Klassen, T., Davis, C., Goldman, A., Burgess, D., Chen, T., Wheeler, D., Mcpherson, J., Bourquin, T., Lewis, L., Villasana, D., Morgan, M., Muzny, D., Gibbs, R., and Noebels, J. (2011). Exome sequencing of ion channel genes reveals complex profiles confounding personal risk assessment in epilepsy. *Cell* 145**,** 1036-1048. doi: 10.1016/j.cell.2011.05.025.
Kralic, J.E., Sidler, C., Parpan, F., Homanics, G.E., Morrow, A.L., and Fritschy, J.M. (2006). Compensatory alteration of inhibitory synaptic circuits in cerebellum and thalamus of gamma-aminobutyric acid type A receptor alpha1 subunit knockout mice. *J Comp Neurol* 495**,** 408-421. doi: 10.1002/cne.20866.
Krampfl, K., Maljevic, S., Cossette, P., Ziegler, E., Rouleau, G.A., Lerche, H., and Bufler, J. (2005). Molecular analysis of the A322D mutation in the GABA receptor alpha-subunit causing juvenile myoclonic epilepsy. *Eur J Neurosci* 22**,** 10-20. doi: EJN4168 [pii]
10.1111/j.1460-9568.2005.04168.x.
Lachance-Touchette, P., Brown, P., Meloche, C., Kinirons, P., Lapointe, L., Lacasse, H., Lortie, A., Carmant, L., Bedford, F., Bowie, D., and Cossette, P. (2011). Novel alpha1 and gamma2 GABAA receptor subunit mutations in families with idiopathic generalized epilepsy. *Eur J Neurosci* 34**,** 237-249. doi: 10.1111/j.1460-9568.2011.07767.x.
Lachance-Touchette, P., Martin, C., Poulin, C., Gravel, M., Carmant, L., and Cossette, P. (2010). Screening of GABRB3 in French-Canadian families with idiopathic generalized epilepsy. *Epilepsia* 51**,** 1894-1897. doi: EPI2642 [pii]
10.1111/j.1528-1167.2010.02642.x.
Lee, K.F., Soares, C., and Beique, J.C. (2012). Examining form and function of dendritic spines. *Neural Plast* 2012**,** 704103. doi: 10.1155/2012/704103.
Li, M.Z., and Elledge, S.J. (2007). Harnessing homologous recombination in vitro to generate recombinant DNA via SLIC. *Nat Methods* 4**,** 251-256. doi: 10.1038/nmeth1010.
Liu, Q.S., Pu, L., and Poo, M.M. (2005). Repeated cocaine exposure in vivo facilitates LTP induction in midbrain dopamine neurons. *Nature* 437**,** 1027-1031. doi: 10.1038/nature04050.
Luscher, C., Nicoll, R.A., Malenka, R.C., and Muller, D. (2000). Synaptic plasticity and dynamic modulation of the postsynaptic membrane. *Nat Neurosci* 3**,** 545-550. doi: 10.1038/75714.
Ma, Y., Ramachandran, A., Ford, N., Parada, I., and Prince, D.A. (2013). Remodeling of dendrites and spines in the C1q knockout model of genetic epilepsy. *Epilepsia* 54**,** 1232-1239. doi: 10.1111/epi.12195.
Macdonald, R.L., and Kang, J.Q. (2009). Molecular pathology of genetic epilepsies associated with GABAA receptor subunit mutations. *Epilepsy Curr* 9**,** 18-23. doi: 10.1111/j.1535-7511.2008.01278.x.
Macdonald, R.L., Kang, J.Q., and Gallagher, M.J. (2010). Mutations in GABAA receptor subunits associated with genetic epilepsies. *J Physiol* 588**,** 1861-1869. doi: jphysiol.2010.186999 [pii]
10.1113/jphysiol.2010.186999.

Maljevic, S., Krampfl, K., Cobilanschi, J., Tilgen, N., Beyer, S., Weber, Y.G., Schlesinger, F., Ursu, D., Melzer, W., Cossette, P., Bufler, J., Lerche, H., and Heils, A. (2006). A mutation in the GABA(A) receptor alpha(1)-subunit is associated with absence epilepsy. *Ann Neurol* 59**,** 983-987. doi: 10.1002/ana.20874.

Multani, P., Myers, R.H., Blume, H.W., Schomer, D.L., and Sotrel, A. (1994). Neocortical dendritic pathology in human partial epilepsy: a quantitative Golgi study. *Epilepsia* 35**,** 728-736.

Queenan, B.N., Lee, K.J., and Pak, D.T. (2012). Wherefore art thou, homeo(stasis)? Functional diversity in homeostatic synaptic plasticity. *Neural Plast* 2012**,** 718203. doi: 10.1155/2012/718203.

Rossignol, E. (2011). Genetics and function of neocortical GABAergic interneurons in neurodevelopmental disorders. *Neural Plast* 2011**,** 649325. doi: 10.1155/2011/649325.

Shi, X., Huang, M.C., Ishii, A., Yoshida, S., Okada, M., Morita, K., Nagafuji, H., Yasumoto, S., Kaneko, S., Kojima, T., and Hirose, S. (2010). Mutational analysis of GABRG2 in a Japanese cohort with childhood epilepsies. *J Hum Genet* 55**,** 375-378. doi: jhg201047 [pii]
10.1038/jhg.2010.47.

Sieghart, W., and Sperk, G. (2002). Subunit composition, distribution and function of GABA(A) receptor subtypes. *Curr Top Med Chem* 2**,** 795-816.

Stoppini, L., Buchs, P.A., and Muller, D. (1991). A simple method for organotypic cultures of nervous tissue. *J Neurosci Methods* 37**,** 173-182.

Sun, H., Zhang, Y., Liang, J., Liu, X., Ma, X., Wu, H., Xu, K., Qin, J., Qi, Y., and Wu, X. (2008). SCN1A, SCN1B, and GABRG2 gene mutation analysis in Chinese families with generalized epilepsy with febrile seizures plus. *J Hum Genet* 53**,** 769-774. doi: 10.1007/s10038-008-0306-y.

Tan, H.O., Reid, C.A., Single, F.N., Davies, P.J., Chiu, C., Murphy, S., Clarke, A.L., Dibbens, L., Krestel, H., Mulley, J.C., Jones, M.V., Seeburg, P.H., Sakmann, B., Berkovic, S.F., Sprengel, R., and Petrou, S. (2007). Reduced cortical inhibition in a mouse model of familial childhood absence epilepsy. *Proc Natl Acad Sci U S A* 104**,** 17536-17541. doi: 0708440104 [pii]
10.1073/pnas.0708440104.

Tanaka, M., Olsen, R.W., Medina, M.T., Schwartz, E., Alonso, M.E., Duron, R.M., Castro-Ortega, R., Martinez-Juarez, I.E., Pascual-Castroviejo, I., Machado-Salas, J., Silva, R., Bailey, J.N., Bai, D., Ochoa, A., Jara-Prado, A., Pineda, G., Macdonald, R.L., and Delgado-Escueta, A.V. (2008). Hyperglycosylation and reduced GABA currents of mutated GABRB3 polypeptide in remitting childhood absence epilepsy. *Am J Hum Genet* 82**,** 1249-1261.

Tian, M., Mei, D., Freri, E., Hernandez, C.C., Granata, T., Shen, W., Macdonald, R.L., and Guerrini, R. (2013). Impaired surface alphabetagamma GABA(A) receptor expression in familial epilepsy due to a GABRG2 frameshift mutation. *Neurobiol Dis* 50**,** 135-141. doi: 10.1016/j.nbd.2012.10.008.

Todd, E., Gurba, K.N., Botzolakis, E.J., Stanic, A.K., and Macdonald, R.L. (2014). GABAA receptor biogenesis is impaired by the gamma2 subunit febrile seizure-associated mutation, GABRG2(R177G). *Neurobiol Dis* 69**,** 215-224. doi: 10.1016/j.nbd.2014.05.013.

Trevelyan, A.J., Baldeweg, T., Van Drongelen, W., Yuste, R., and Whittington, M. (2007). The source of afterdischarge activity in neocortical tonic-clonic epilepsy. *J Neurosci* 27**,** 13513-13519. doi: 10.1523/JNEUROSCI.3005-07.2007.

Vicini, S., Ferguson, C., Prybylowski, K., Kralic, J., Morrow, A.L., and Homanics, G.E. (2001). GABA(A) receptor alpha1 subunit deletion prevents developmental changes of inhibitory synaptic currents in cerebellar neurons. *J Neurosci* 21**,** 3009-3016.

Wallace, R.H., Marini, C., Petrou, S., Harkin, L.A., Bowser, D.N., Panchal, R.G., Williams, D.A., Sutherland, G.R., Mulley, J.C., Scheffer, I.E., and Berkovic, S.F. (2001). Mutant GABA(A) receptor gamma2-subunit in childhood absence epilepsy and febrile seizures. *Nat Genet* 28**,** 49-52.

Whissell, P.D., Eng, D., Lecker, I., Martin, L.J., Wang, D.S., and Orser, B.A. (2013). Acutely increasing deltaGABA(A) receptor activity impairs memory and inhibits synaptic plasticity in the hippocampus. *Front Neural Circuits* 7**,** 146. doi: 10.3389/fncir.2013.00146.

Wong, M. (2005). Modulation of dendritic spines in epilepsy: cellular mechanisms and functional implications. *Epilepsy Behav* 7**,** 569-577. doi: 10.1016/j.yebeh.2005.08.007.

Wu, X., Fu, Y., Knott, G., Lu, J., Di Cristo, G., and Huang, Z.J. (2012). GABA signaling promotes synapse elimination and axon pruning in developing cortical inhibitory interneurons. *J Neurosci* 32**,** 331-343. doi: 10.1523/JNEUROSCI.3189-11.2012.

Zeller, A., Jurd, R., Lambert, S., Arras, M., Drexler, B., Grashoff, C., Antkowiak, B., and Rudolph, U. (2008). Inhibitory ligand-gated ion channels as substrates for general anesthetic actions. *Handb Exp Pharmacol***,** 31-51. doi: 10.1007/978-3-540-74806-9_2.

Chapter 4. Loss of Tsc1 in GABAergic PV cells impairs their connectivity and causes cognitive deficits

Mayukh Choudhury[1,2], Clara A. Amegandjin[1,2], Josianne Nunes Carrico[2], Ariane Quintal[1], Martin Berryer[1,2], Jean-Claude Lacaille[1], Graziella Di Cristo[1,2,*]

Neuroscience Department, Université de Montréal[1]; CHU Ste.Justine Research Center[2]

*Corresponding authors

Graziella Di Cristo

Research Center, CHU Ste-Justine/Université de Montréal

3175, Côte-Sainte-Catherine, Montréal, QC H3T 1C5, Canada.

The authors have declared that no conflict of interest exists.

4.1 Abstract

Properly functional cortical circuits depend on the correct development of inhibitory interneurons. In particular, the axonal arborisation and synapse density of parvalbumin (PV)-positive interneurons undergo striking changes in the young brain. The mechanisms controlling the development of PV interneuron connectivity are still not well understood. The Mechanistic Target Of Rapamycin Complex 1 (mTORC1) pathway, which is regulated by Tuberous Sclerosis (TSC) 1 and 2 proteins, has been implicated in controlling several aspects of neuronal development by integrating multiple extracellular signals to produce appropriate protein translation. How and whether mTORC1 signaling affects PV interneuron development is unknown. Here, we showed that Tsc1 knockout (KO) in single PV interneurons in cortical organotypic cultures caused a premature increase in terminal axonal branching and bouton density formed by mutant PV cells, which was reversed by Rapamycin treatment, followed by a striking loss of perisomatic innervation after the 4th postnatal week. To investigate the role of mTORC1 in PV cells *in vivo*, we bred Tsc1^{lox} with *Nkx2.1*-Cre and *PV*-Cre mice to knockout Tsc1 before and after birth, respectively. Both conditional KO mice showed mTORC1 hyperactivation and somatic hypertrophy in PV cells. Consistently to what observed following Tsc1 KO in single PV cells, PV cell perisomatic innervations were increased at P18, but decreased at P45 in *Nkx2.1*-Cre;Tsc1$^{lox/lox}$ mice compared to controls. PV cell connectivity loss was more pronounced in *PV*-Cre;Tsc1$^{lox/lox}$ mice. Finally, both conditional KO mice showed alterations in anxiety and social novelty discrimination behavior. All together, these results suggest that mTORC1 signaling regulates both the time course and the maintenance of PV cell innervations, with the direction of the regulation depending on developmental stage. Further, altered PV cell connectivity may be one of the pathological mechanisms leading to cognitive deficits in neurodevelopmental diseases characterized by mTOR dysregulation.

4.2 Introduction

Within the forebrain, GABAergic (γ-aminobutyric acid producing) interneurons possess the largest diversity in morphology, connectivity, and physiological properties (Fishell and Rudy, 2011). A fascinating hypothesis is that different interneurons may play partly distinct roles in neural circuit function and animal behavior. Cortical parvalbumin (PV)-positive basket cells (PV cells) specifically target the soma and proximal dendrites of pyramidal cells. PV cells can adjust the gain of the integrated synaptic responses and have been implicated in synchronizing the firing of neuronal populations and the generation of gamma oscillations (Cardin *et al.,* 2009; Sohal *et al.,* 2009; Takada *et al.,* 2014), which are important for the maintenance of attention, working memory and for the refinement of executive functions in humans and rodents (Fries *et al.,* 2001; Howard *et al.,* 2003; Cho *et al.,* 2006). Importantly, PV cells have also been involved in experience-dependent development of cortical circuits. Indeed, many studies on the visual cortex have proposed that the timing of the critical period of heightened plasticity is set by PV cell maturation (Fagiolini *et al.,*2004; Fagiolini and Hensch, 2000; Di Cristo *et al.,*2007; Sugiyama *et al.,* 2008; Morishita *et al.,* 2015). Cortical PV cell connectivity develops largely in the first 4 postnatal weeks in rodents. In fact, at the individual cell level, PV cell axonal arbors become significantly more complex and the density of perisomatic synapses around targeted cells increases during this time period. The molecular players involved in this process are still not completely understood.

Mechanistic target of rapamcyin (mTORC1) is a central player in cell growth throughout the organism. In the developing brain, mTORC1 dictates the overall growth of differentiating neuronal stem cells (Magri *et al.,* 2011) and post-mitotic neurons (Kwon *et al.,* 2003); further it is critical in defining neuronal polarity (Li *et al.,* 2008), axon guidance (Jaworski and Sheng, 2006), dendritic arborization (Urbanska *et al.,* 2012) and glutamatergic synapse formation (Tavazoie *et al.,* 2005; Bateup *et al.,* 2011). In addition, in mature neuron,

mTORC1 regulates protein synthesis-dependent, synaptic changes underlying learning and memory (Lipton and Sahin, 2014). Monogenic mutations in critical molecular regulators of mTORC1 are underlying causes of several diseases (Costa-Mattioli and Monteggia, 2013). In particular, mutations in the mTORC1-negative regulators *TSC1* or *TSC2 causes* Tuberous Sclerosis Complex, which is associated with neurological problems, including epilepsy, intellectual disabilities and autism (de Vries , 2010).

Several studies have shown that TSC-mTORC1 signaling pathway in cortical excitatory neurons regulates their connectivity (Bateup *et al.,* 2013; Bateup *et al.,* 2011; Tavazoie *et al.,* 2005), however whether and how it modulates cortical PV cell connectivity is unknown.

Here, we used a combination of single-cell genetic in cortical organotypic cultures, conditional knockout mice and high-resolution imaging to investigate the effects of Tsc1-mTORC1 pathway on the development of PV cell connectivity. We found that PV cells lacking Tsc1 show a premature increase of their axonal arbor complexity and bouton density in the first three postnatal weeks, followed by a striking loss of connectivity by adulthood. Further, conditional KO mice lacking Tsc1 in PV cells show anxiety and social recognition deficits, which are more severe when mTOR hperactivation starts postnatally.

4.3 Materials and Methods

Animals

Mice with *loxP* sites flanking exon 17 and 18 of *Tsc1*gene ($Tsc1^{flox/flox}$) were purchased from Jackson Laboratories. The $Tsc1^{flox/flox}$ mice were bred with wild type mice of Sv129 background to generate $Tsc1^{flox/wt}$ mice. Both $Tsc1^{flox/flox}$ and $Tsc1^{flox/wt}$ mice have been used for organotypic cultures to study the role of Tsc1 knockout in single PV cells. Two separate transgenic mouse lines expressing Cre recombinase, (1) Tg(*Nkx2.1*-Cre)[27] and (2)Tg(*PV*-Cre) (Runyan *et al.,* 2010) purchased from Jackson laboratories, were maintained as pure colonies.

Backcross between Tsc1$^{flox/flox}$ mice and Tg(*Nkx2.1*-Cre) produced Tsc1$^{flox/flox}$ or Tsc1$^{flox/+}$ (referred as Tsc1^{Ctrl}), Tg(*Nkx2.1*-Cre);Tsc1$^{flox/+}$ and Tg(*Nkx2.1*-Cre);Tsc1$^{flox/flox}$ mice. A similar breeding strategy was used to breed Tsc1$^{flox/flox}$ and Tg(*PV*-Cre) mice. All mice were housed under standard pathogen-free conditions in a 12h light/dark cycle with *ad libitum* access to sterilized laboratory chow diet. Animals were treated in accordance with Canadian Council for Animal Care and protocols were approved by the Animal Care Committee of CHU Ste-Justine Research Center.

Mice Genotyping

DNA was extracted from mouse tails and genotyped to detect the presence of Cre alleles and Tsc1 conditional and wild-type alleles. Polymerase chain reaction (PCR) was performed using primers F4536 (5'AGGAGGCCTCTTCTGCTACC-3'), R4830 (5'-CAGCTCCGACCATGA AGTG -3') and R6548 (5′-TGGGTCCTGACCTATCTCCTA-3′) with band sizes of 295 bp for the wild-type and 480 bp for the floxed allele. Primers for characterizing Cre in Tg(*Nkx2.1*-Cre) breeding were F1 (5'-AAGGCGGACTCGGTCCA CTCCG-3'), F2(5'-AAGGCGGACTCGG TCCACTCCG-3') and R1 (5'-TCGGATC CGCCGCATAACCAG-3') which generated 550bp and 220bp mutant and wild-type bands. Primers for detecting Cre in Tg(*PV*-Cre) breeding were F1 (5'-CAGCCTCTGTTCCACATACACTCC-3'), F2(5'- GCTCAGAGCCTCCATTCCCT-3') and R1 (5'-TCACTCGAGAGTACCAAGCAGGCAGGA GATATC-3') which generated 400bp and 526bp mutant and wild-type bands.

Slice culture and biolistic transfection

Slice culture preparation was done as described by Chattopadhyaya and coworkers (Chattopadhyaya *et al.,* 2013). Postnatal day 4 or 5 (P4 or P5) mouse pups were decapitated, and brains were rapidly removed and immersed in ice-cold culture medium (containing

DMEM, 20% horse serum, 1 mM glutamine, 13 mM glucose, 1 mM $CaCl_2$, 2 mM $MgSO_4$, 0.5 μm/ml insulin, 30 mM HEPES, 5 mM $NaHCO_3$, and 0.001% ascorbic acid). Coronal brain slices of the occipital cortex, 400 μm thick, were cut with a Chopper (Stoelting, Wood Dale, IL). Slices were then placed on transparent Millicell membrane inserts (Millipore, Bedford, MA), usually three slices/insert, in 30 mm Petri dishes containing 0.75 ml of culture medium. Finally, the slices were incubated in a humidified incubator at 34°C with a 5% CO_2-enriched atmosphere and the medium was changed three times per week. All procedures were performed under sterile conditions. Constructs to be transfected were incorporated into "bullets" that were made using 1.6 μm gold particles coated with a total of ~60 μg of the DNA(s) of interest. These bullets were used to biolistically transfect slices by Gene gun (Bio-Rad, Hercules, CA) at high pressure (180 ψ), and the transfected slices were incubated for 8 days *in vitro* under the same conditions as described above, before imaging. For each experimental group, cortical slices were prepared from at least three mice. On average 6-7 neurons were transfected per cortical organotypic slice. The majority of neurons labeled by this promoter were parvalbumin-positive (PV) basket cells (Chattopadhyaya *et al.,* 2004; Chattopadhyaya *et al.,* 2007*)*; while a minority (~10%) were pyramidal cells. Pyramidal cells were recognized by the complexity of their dendritic arbor, including an apical dendrite, and the presence of numerous dendritic spines.

Immunohistochemistry and confocal imaging

Mice were perfused transcardially with 1X PBS AND 4% PFA. Brains were postfixed with 4% PFA overnight followed by 30% sucrose solution in PBS. The brains were frozen with OCT and sagittal sections of 40 μm were produced using a cryostat (Leica). The following primary antibodies were used for immunohistochemistry on mouse cryosections or organotypic cultures: rabbit anti-phospho-S6 (1:1000, Cell Signaling), mouse anti-NeuN (1:400, Millipore), mouse PV (1:1000, Millipore), rabbit anti-PV (1:8000, Swant), guinea pig

anti-PV (1:1000,Synaptic Systems), rabbit anti-vGAT (1:1000, Synaptic Systems), mouse anti-gephyrin (1:500, Synaptic Systems). Secondary antibodies to visualize primary antibodies were Alexa-fluor conjugated 488, 555,594,633, and 647 (Life technologies). Images were taken using a Leica confocal microscope (SPE and SP8) and water immersion 20x (NA0.7) or glycerol immersion 63x (NA1.3) objective.

Image quantification in organotypic cultures and in vivo

For organotypic cultures, at least two confocal stacks of each BC axon arbor in the first 150μm from the basket cell soma using a 63X glycerol objective (NA1.3, Leica) and a Leica TCS SPE confocal microscope. PV cells were analysed as discussed in[28]. For *in vivo* analysis, images were acquired on the same day using identical confocal parameters and either using 20x water immersion objective (for analysis of % of PV cells colocalizing with pS6+ cells) or 63x glycerol objective (for analysis of PV, vGAT, pS6, gephyrin intensity and/or puncta counting). Three confocal stacks from 3 different brain sections were acquired in layer V of somatosensory cortex with z-step size 1μm. Images were exported in TIFF format. Cell soma of PV cells was quantified using Neurolucida (MBF Softwares). Fluorescence intensity of pS6 signal in PV cells was calculated using ImageJ. Intensity of PV and vGAT perisomatic staining was calculated on a traced cross-sectional area around NeuN somata using ImageJ. PV+, vGAT+, gephyrin+, PV+/vGAT+ and PV+/gephyrin+ punctas were counted around NeuN positive somata after selecting the confocal plane with the highest soma circumference using Neurolucida software. At least 10 NeuN positive somata were selected in each confocal stack. User was blind to genotype during all the analysis.

Western Blot

Western blots were performed on samples from four mice per group and from two separate experiments. Protein lysates were prepared by homogenizing tissue from rat hippocampus in

50 mM Tris–HCl (pH 7.6), 2 mM EDTA, 1% Igepal CA-630 (Sigma-Aldrich), and one tablet of protease inhibitor cocktail (Roche, Mississauga, ON, Canada). Tissues were disrupted using needles and a syringe, and centrifuged at 10000 g for 10 min at 4°C; the supernatant was then collected. Protein levels were quantified by Bradford Protein Assay (Bio-Rad, Mississauga, Ontario, Canada), and their concentrations were adjusted with deionized water. Samples were mixed with an equal volume of 2x Laemmli buffer, boiled for 5 min, and used immediately or stored at 80°C. Proteins were separated using 6.5% polyacrylamide separation gels and 5% stacking gels (Bio-Rad); equal amounts were loaded in each lane, and then transferred onto Immobilon-P Transfer Membrane, a poly(vinylidene difluoride) microporous membrane (Millipore, Temecula, California, USA). These membranes were then blocked by incubation in Tris-buffered saline blocking buffer with 5% dried milk and 0.1% Tween-20 solution. Membranes were probed with the following primary antibodies: anti-pS6 (Ser 240/244)1:10000, Cell Signaling) and anti-β actin (1:3000, Novus Biologicals). Rabbit or mouse HRP-conjugated secondary antibody used for detection of primary antibodies was purchased from Sigma-Aldrich. Immunoreactive bands were detected with Western Lightning Chemiluminescence Reagent Plus (PerkinElmer), and the signal was visualized by exposing the membrane to BioFlex MSI film for autoradiography, maximum sensitivity (InterScience). Bands for every sample were used for quantification, using imageJ software.

Mouse behavior tests

Investigators were blind to genotype during both testing and analysis.

Open Field

A mouse was placed at the centre of the open-field arena and the movement of the mouse was recorded by a video camera for 10 min. The recorded video file was later analyzed with

Smart video tracking system (v3.0, Harvard Apparatus). To measure exploratory behavior, total distance travelled during the 10 minute period was calculated. The open field arena was cleaned with 70% ethanol and wiped with paper towels between each trial.

Elevated plus maze

A mouse was placed at the junction of the two open and closed arms. Apparatus consisted of two open arms without walls across from each other and perpendicular to two closed arms with walls with a centre platform. Experiment was performed as described in Vogt et al, 2015[29]. Exploration time in this apparatus was recorded for 5 min with a video camera. Recorded video was scored to measure time spent in open arms, closed arms and center regions respectively.

T-maze

The T-maze apparatus consisted of a T-shaped walled chamber where mice (aged P43-45) were tested for two trials in order to assess working memory. An individual mouse was placed at the middle arm of the T-maze and was allowed to make a free choice to enter an arm at the T-junction. Once the mouse made a decision to go in left/right direction, it was blocked in that chamber for 10 seconds and was then taken out from the apparatus. The mouse was allowed to rest in an empty cage for a period of 50 seconds, then put back again in the middle arm and allowed to choose which arm to explore. This test was repeated for three consecutive days.

Three chamber social novelty test

A three-chamber arena was used to assess the social recognition performance of the mice (Silverman *et al.,* 2010). The tested animal (P38-P42) was placed in the middle of the central chamber and allowed to explore all the chambers for 10 min fir habituation. After

habituation, a wire cage containing an unfamiliar conspecific of the same sex and age (Stranger 1) was placed inside in chamber 1 while an empty wire cage was placed in chamber 2. The tested animal was allowed to freely explore the three chambers of the apparatus for 10 min. Social approach was evaluated by quantifying the time spent by the tested mice in each chamber during the 10 min session. At the end of this 10min, a new unfamiliar mouse of the same sex and the same age (Stranger 2) was placed in the previously unoccupied wire cage and the tested mouse was examined for an additional 10 min to assess preference for social novelty. Stanger 1 and stranger 2 animals originated from different home cages and had never been in physical contact with the tested mice or between each other. Social novelty was evaluated by quantifying the time spent by the tested mice in each chamber during the third 10 min session.

4.4 Results

mTORC1 activation in PV cells significantly increased during their synapse proliferation phase

The maturation of PV cell innervation is a prolonged process that reaches plateau only after 4 postnatal weeks in mouse cortex (Chattopadhyaya *et al.,* 2004). To investigate whether mTORC1 activation plays a role in this process, we first analyzed the time course of pS6 expression, one of the direct downstream effectors of mTORC1, in PV cells identified by PV immunolabeling (Fig.*1A*). We found that both the proportion of PV cells expressing pS6 and the mean intensity of pS6 signal significantly increased between P18 and P26 in somatosensory cortex (Fig.*1A-C;* Student t-test, $p<0.05$). Similar results were obtained in visual cortex (data not shown), indicating that this process is not specific to a particular cortical region. To investigate whether increase of pS6 expression levels was a generalized phenomenon during this developmental window, we quantified pS6 levels in NeuN+ neurons

that represent for the most part pyramidal cells (Fig.*1D*). We found no significant difference in the number of NeuN+ cells expressing pS6 between P18 and P26 (Fig.1E; Student t-test, $p>0.05$). Further, western blot analysis of pS6 levels also failed to detect differences between P18 and P26 (Fig.*S1*; Student t-test, $p>0.05$), which is consistent with the notion that the increase of pS6 expression levels is cell-type specific during this developmental time window, as PV cells represent ~10% of all cortical neurons. Since between P18-26 the density of perisomatic GABAergic synapses formed by PV cells increased significantly (Chattopadhyaya *et al.,* 2004), we hypothesized that mTORC1 activation plays a role in this process.

Tsc1, in a protein complex with Tsc2, inhibits mTORC1 activation. Perturbations of TSC1, and thus mTORC1, clearly alter several aspects of neuronal function (Lipton and Sahin, 2014); however, due to the many homeostatic feedback mechanisms that influence neural circuit development, it is unclear which perturbations are directly caused by Tsc1-mTORC1 signaling dysregulation and which are induced as a consequence of altered neuronal activity. Next, we used *in vitro* and *in vivo* approaches to determine the cell-autonomous and network phenotypes resulting from genetic deletion of *Tsc1* in cortical PV cells.

mTORC1 hyperactivation in single PV cells induced a premature increase in bouton density and axon branching

To examine the role of Tsc1 in the postnatal maturation of cortical PV cell connectivity, we used a transgenic mouse carrying a conditional allele of Tsc1 (Kwaitkowski *et al.,* 2002), which allows cell type and developmental stage restricted knockout of Tsc1. To reduce Tsc1 expression in PV cells and simultaneously label their axons and synapses, we used a previously characterized promoter region P_{G67} (Chattopadhyaya *et al.,* 2004); to express either Cre recombinase together with GFP (P_{G67}-GFP/Cre) or GFP alone (control) in PV cells

in cortical organotypic cultures from $Tsc1^{flox/flox}$ and $Tsc1^{flox/wt}$ mice. This approach allowed us to generate $Tsc1^{-/-}$ and $Tsc1^{+/-}$ PV cells in an otherwise wild-type background, respectively. Deletions of either one or both *Tsc1* alleles significantly increased pS6 expression levels in transfected PV cells (Fig.*S2*; one-way ANOVA with Holm-Sidak post hoc analysis, $p<0.05$), suggesting mTORC1 hyperactivation. Conversely, cell soma size was significantly increased only in $Tsc1^{-/-}$ PV cells (Fig. *2F*; one-way ANOVA with Holm-Sidak post hoc analysis $p<0.05$).

Previous studies have shown that the basic features of maturation of perisomatic innervation formed by PV cells onto pyramidal cells are recapitulated in cortical organotypic cultures (Di Cristo *et al.,* 2004; Chattopadhyaya *et al.,* 2004). PV cells start out with simple axons, which develop into complex, highly branched arbors in the subsequent 4 weeks with a time course similar to that observed *in vivo* (Chattopadhyaya *et al.,* 2004). In particular, PV cell axonal arborization and bouton density increase significantly between EP18 (EP=P5+13 days *in vitro*) and EP24. To investigate the effect of premature mTORC1 activation on PV cell innervations, we biolistically tranfected PV cells at EP10 and analyzed them at EP18 (Fig.*S2A*). Following Tsc1 deletion, we quantified two aspects of individual PV cell connectivity – 1) the extent of perisomatic innervation around single targeted somata (terminal branching and perisomatic bouton density) and 2) the fraction of potentially innervated somata (percentage of innervation). We have previously shown that the vast majority of GFP-labeled boutons in our experimental conditions most likely represent presynaptic terminals (Chattopadhyaya *et al.,* 2004; Chattopadhyaya *et al.,* 2007; Wu *et al.,* 2012). We found that both $Tsc1^{-/-}$ and $Tsc1^{+/-}$ PV cells formed premature perisomatic innervations, characterized by increased bouton density (Fig.*2A-C, D*; boutons/soma in $Tsc1^{+/+}$ 6.2 ± 0.2, $Tsc1^{+/-}$ 12.4 ± 0.8, $Tsc1^{-/-}$ 10.5 ± 0.6, one-way ANOVA with Holm-Sidak post hoc analysis, $p<0.05$) and terminal axonal branching around NeuN+ contacted somata

(Fig.2*E;* one-way ANOVA with Holm-Sidak post hoc analysis, $p<0.05$). To determine whether the effects of Tsc1 deletion were due to mTORC1 hyperactivation, we treated cortical organotypic cultures with the mTORC1 inhibitor Rapamycin. Rapamycin treatment reversed the increase in bouton density in $Tsc1^{-/-}$ PV cells (Fig.*S3E* boutons/soma, $Tsc1^{+/+}$+Rapamycin, 7.8 ± 0.2 vs $Tsc1^{-/-}$+Rapamycin 7.3 ± 0.4, one-way ANOVA, $p>0.05$) as well as terminal branching (Fig. *S3H;* one-way ANOVA, $p>0.05$*)*. All together, these data suggest that mTORC1 hyperactivation lead to the premature formation of PV cell innervations in a cell autonomous manner.

mTORC1 hyperactivation in single PV cells impaired the maintenance of PV cell connectivity

Next, we asked whether the premature development of PV cell innervation was long-lasting. As described above, PV cells were transfected at EP10 and then analyzed either at EP24 (during the peak of the proliferation of PV cell innervations) or at EP34 (after PV cell innervation have reached stability). At EP24, $Tsc1^{-/-}$ PV cells were indistinguishable from age-matched wild-type cells (Fig.3E-H; boutons/soma in $Tsc1^{+/+}$ 9.15 ± 0.6, $Tsc1^{-/-}$ 8.9 ± 0.6, t-test, $p>0.05$). Conversely, at EP34, $Tsc1^{-/-}$ PV cells showed significantly poorer innervations than age-matched $Tsc1^{+/+}$ PV cells (Fig.3E-G; bouton/soma $Tsc1^{+/+}$ 10.9 ± 1.0, $Tsc1^{-/-}$ 5.9 ± 1.0; t-test, $p<0.01$). All together, these data show that dysregulated Tsc1-mTORC1 signaling in individual PV cells alters the development of their innervations, inducing first a premature increase in axonal branching and bouton density followed by excessive pruning (Fig. 3I).

Tsc1-mTOR signaling dysregulation in MGE-derived GABAergic neurons alters PV cell perisomatic synapse density in an age-dependent manner *in vivo*.

To investigate whether and how Tsc1 deletion affected PV cell innervations *in vivo*, we generated Tg(*Nkx2.1-Cre*);Tsc1$^{flox/flox}$ and Tg(*Nkx2.1-Cre*);Tsc1$^{flox/+}$ mice. Nkx2.1 is a transcription factor expressed starting at E10.5 by GABAergic cell precursors in the medial ganglionic eminence (MGE), which will give rise to cortical PV cells and somatostatin (SOM)+ GABAergic cells (Xu *et al.,* 2008)[27]. At P18, significantly more PV cells expressed pS6 at higher levels in Tg(*Nkx2.1-Cre*);Tsc1$^{flox/flox}$ compared to Tg(*Nkx2.1-Cre*);Tsc1$^{flox/+}$ and Tsc1^{Ctrl} mice, in somatosensory cortex (Fig.S4A,D; pS6 intensity values normalized to Tsc1^{Ctrl}). Conversely, Cre transfection in single PV cells in organotypic cultures increased mTORC1 activation independently of the number of floxed alleles (compare with Fig.2). On the other hand, consistent with what we observed following single-cell Tsc1 deletion, PV cell somata were significantly larger only in Tg(*Nkx2.1-Cre*);Tsc1$^{flox/flox}$ mice (Fig.S*4 B, E*; Konglomerov-Smirnov test, $p<0.01$). Interestingly, by P45 PV cells showed a four and two-fold increase in pS6 intensity in Tg(*Nkx2.1-Cre*);Tsc1$^{flox/flox}$ and Tg(*Nkx2.1-Cre*);Tsc1$^{flox/+}$ mice compared to control mice, respectively (Fig. S*4D*). PV cell somata were slightly larger in Tg(*Nkx2.1-Cre*);Tsc1$^{+/flox}$ compared to Tsc1^{Ctrl} mice, even if not as large as those in Tg(*Nkx2.1-Cre*);Tsc1$^{flox/flox}$ mice (Fig.*4E,F*), suggesting that deletion of one Tsc1 allele may have slow, cumulative effects *in vivo*, consistently to what previously reported in Purkinje cell-specific Tsc1 mutant mice (Tsai *et al.,* 2012).

It has been reported that Tsc1 deletion in cortical GABAergic neurons (Fu *et al.,* 2012a) or Purkinje cells (Tsai *et al.,* 2012) lead to neuronal loss in the targeted population. On the other hand, we did not observe any difference in PV cell density in conditional knockouts vs control littermates (data not shown). To investigate whether Tsc1 deletion, and consequent mTORC1 hyperactivation, affected perisomatic GABAergic synapses by PV cells, we immune-labeled brain sections with PV (which labels all PV cells), vGAT (presynaptic GABAergic marker) and gephrin (post-synaptic GABAergic marker). At P18, both

perisomatic PV signal intensity and PV+ puncta density were significantly increased in Tg(*Nkx2.1-Cre*);Tsc1$^{flox/flox}$ compared to Tg(*Nkx2.1-Cre*);Tsc1$^{flox/+}$ and Tsc1^{Ctrl} mice (Fig.*4 D-E*; one-way ANOVA with Holm-Sidak post hoc analysis, $p<0.05$). On the other hand, the densities of perisomatic vGAT puncta, PV+/vGAT+ puncta, gephyrin+ and PV+/gephyrin+ puncta were not significantly different between the genotypes (Fig.5 F, G; one-way ANOVA, $p>0.05$), suggesting that increased PV boutons surrounding pyramidal neurons many not be mature synapses.

Interestingly, at P45, PV puncta intensity and density were significantly reduced in Tg(*Nkx2.1-Cre*);Tsc1$^{flox/flox}$ compared to Tg(*Nkx2.1-Cre*);Tsc1$^{flox/+}$ and Tsc1^{Ctrl} mice (Fig.5; one-way ANOVA with Holm-Sidak post hoc analysis, $p<0.05$). Further, the density of perisomatic PV+/gephrin+ puncta was also significantly reduced (Fig.*6 G*; one-way ANOVA with Holm-Sidak post hoc analysis, $p<0.05$), suggesting that PV cells formed less synapses onto pyramidal cells. An alternative possibility is that overall PV expression levels were reduced, therefore reducing our ability to detect perisomatic boutons formed by PV+ cells. We think this was unlikely, as the levels of somatic PV expression were not affected (data not shown).

Tsc1-mTOR signaling dysregulation in MGE-derived GABAergic neurons alters the developmental time course and stability of PV cell axonal arbor and bouton density.

Interestingly, we found that PV cell innervations were only affected in Tg(*Nkx2.1-Cre*);Tsc1$^{flox/flox}$ but not Tg(*Nkx2.1-Cre*);Tsc1$^{flox/+}$ mice. On the other hand, Tsc1 deletion in single PV cells in cortical organotypic cultures affected PV cell axonal arbor and bouton density independent of the gene dosage (Fig.2). One possibility is that network single-allele deletion of Tsc1 may recruit compensatory signaling pathways *in vivo*, which are not activated when Tsc1 is deleted only in sparse PV cells or/and *in vitro*. To address this

question, we analyzed single PV cell axonal morphology at high resolution in organotypic cultures from Tg(*Nkx2.1-Cre*);Tsc1$^{flox/flox}$, Tg(*Nkx2.1-Cre*);Tsc1$^{flox/+}$ and Tsc1^{Ctrl} mice transfected with P_{G67}-GFP at different developmental stages (Fig. *6* and *7*). At EP18, before the peak of PV cell synapse proliferation, PV cells from both Tg(*Nkx2.1-Cre*);Tsc1$^{flox/flox}$ and Tg(*Nkx2.1-Cre*);Tsc1$^{flox/+}$ mice formed more complex perisomatic innervations, characterized by increased perisomatic bouton density (Fig.6A-*C, D*; one-way ANOVA with Holm-Sidak post hoc analysis, $p<0.01$) and terminal branching (Fig.*6E;* one-way ANOVA with Holm-Sidak post hoc analysis, $p<0.01$) compared to age-matched control PV cells. On the other hand, at EP34, after PV cells axonal arbors had reached stability, PV cells from both genotypes showed significantly reduced perisomatic bouton density (Fig.*7A-C, D*; one-way ANOVA with Holm-Sidak post hoc analysis, $p<0.05$), terminal branching (Fig.*8E;* one-way ANOVA with Holm-Sidak post hoc analysis, $p<0.05$) and percentage of innervated pyramidal neurons (Fig.*7F*; one-way ANOVA with Holm-Sidak post hoc analysis, $p<0.05$). Overall, these results confirm that embryonic deletion of *Tsc1* had a biphasic effect on PV cell innervation development and maintenance, by first accelerating the formation of PV cell innervations and then impairing their maintenance. Further, both one and two Tsc1 allele deletion in PV cells at the single and network level showed similar effects on PV cell innervations in organotypic cultures, suggesting that compensatory mechanisms may be recruited in Tg(*Nkx2.1-Cre*);Tsc1$^{+/flox}$ mice *in vivo,* but not *in vitro.*

Tsc1-mTOR signaling dysregulation in postnatal PV cells lead to reduced PV perisomatic synapses in adulthood.

Nkx2.1-Cre transgene is activated in cortical PV and SOM GABAergic neurons from a very early point during embryonic development. Next, we asked to what extent postnatal deletion of Tsc1 in PV cells recapitulated the effects observed in Tg(*Nkx2.1-Cre*);Tsc1^{flox} mice. To answer this question, we generated Tg(*PV-Cre*);Tsc1$^{flox/flox}$ and Tg(*PV-Cre*);Tsc1$^{flox/+}$ mice.

PV expression peaks after the third postnatal week in cortex. By using the RCE GFP reporter mouse, we confirmed that about 50% of all PV cells expressed GFP by P18, while this proportion rose to more than 75% (77±5%; n=3 mice) in P45 mice. The late CRE expression precluded the analysis of perisomatic GABAergic innervation at P18. At P45, we observed a higher proportion of PV cells co-localizing with pS6 immunoreactivity in Tg(*PV-Cre*);Tsc1$^{flox/flox}$ mice (Fig.*S5A,B*; one-way ANOVA with Holm-Sidak post hoc analysis, $p<0.05$). Further, we found a 2.5-fold increase in pS6 intensity in PV cells from Tg(*PV-Cre*);Tsc1$^{flox/flox}$ mice (Fig. S5C). Soma size was significantly increased in both genotypes, but significantly more in Tg(*PV-Cre*);Tsc1$^{flox/flox}$ mice (Fig.*S5D*; K-S test, $p<0.001$). Interestingly, both perisomatic PV intensity and puncta density around excitatory cells was significantly decreased in somatosensory cortex in both mutant mice (Fig. *8A-C, D-E*; one-way ANOVA with Holm-Sidak post hoc analysis, $p<0.05$). Moreover, the density of perisomatic PV+/gephrin+ punctas was also significantly decreased in both genotypes (Fig.*8G*; one-way ANOVA with Holm-Sidak post hoc analysis, $p<0.05$), suggesting that postnatal Tsc1 deletion, and consequent mTORC1 hyperactivation, lead to PV cell hypo-connectivity independent of gene dosage.

Tsc1-mTORC1 dysregulation in prenatal Nkx2.1-derived GABAergic cells or postnatal PV cells altered anxiety and social recognition.

Deletion of Tsc1 in specific neuron types affects different behaviors, depending on the cell type and age of recombination[33]. Here, we found that deletion of both *Tsc1* alleles in MGE-derived GABAergic neurons caused increased exploratory behavior in the open field (Fig.*9A*, one-way ANOVA with Holm-Sidak post hoc analysis, $p<0.05$) and anxiety in the elevated plus maze test (Fig.*9B*, one-way ANOVA with Holm-Sidak post hoc analysis, $p<0.05$). Interestingly, no behavior alterations could be detected before P30 in the two

above-mentioned behavioral paradigms (data not shown). Further, Tg(*Nkx2.1-Cre*);Tsc1$^{flox/flox}$ but not Tg(*Nkx2.1-Cre*);Tsc1$^{flox/+}$ mice, failed to alternate in the T-maze test (Fig.*9C*, one-way ANOVA with Holm-Sidak post hoc analysis, $p<0.05$), indicating the presence of working memory deficits.

Conversely, postnatal deletion of both *Tsc1* alleles in PV cells did not affect exploratory drive (Fig.9D; one-way ANOVA, $p>0.01$). In addition, Tg(*PV-Cre*);Tsc1$^{flox/flox}$ mice exhibit anti-anxiety like behavior in the elevated plus maze paradigm (Fig.9E; one-way ANOVA with Holm-Sidak post hoc analysis, $p<0.05$).

Interestingly, we found deficits in social behavior in both mutant lines, which were however more severe in Tg(*PV-Cre*);Tsc1^{flox} mice. Tg(*Nkx2.1-Cre*);Tsc1$^{lox/lox}$ and Tg(*Nkx2.1-Cre*);Tsc1$^{lox/+}$ mice showed a normal preference toward a mouse compared to an object (social approach; Fig.F1; two-way ANOVA, $p>0.05$), while they showed reduced interested towards a novel mouse compared to a known one (Fig.*9D*, two-way ANOVA with Bonferroni's post hoc analysis, $p<0.05$), suggesting that social novelty recognition behavior may be more sensitive to mTORC1 hyper-activation in MGE-derived GABAergic neurons. Interestingly, both Tg(*PV-Cre*);Tsc1$^{flox/flox}$ and Tg(*PV-Cre*);Tsc1$^{flox/+}$ mice showed deficits in social approach and social novelty paradigms (Fig.*9G1-G2*, two-way ANOVA with Bonferroni's post hoc analysis, $p<0.05$). In summary, Tsc1 deletion in PV cells lead to specific cognitive alterations, in particular in the social behavior domain.

4.5 Discussion

Neocortical PV cells are characterized by striking specificity in target innervation and plasticity of synaptic connections (Le Magueresse *et al.,* 2011). Development of the mature PV cell innervation fields is achieved through the ordered progression of a series of morphogenic events that include axon growth and branching, synapse formation and

refinement. mTORC1 pathway regulation by both genetic programs and neural activity is probably central to the establishment and plasticity of PV cell innervation patterns. In young neurons, mTORC1 pathway components are enriched in developing axons and contribute to local protein synthesis, which plays a role in axon interaction with their environment (Yoon *et al.,* 2009; Choi *et al.,* 2008; Nie *et al.,* 2010). In fact, it has been proposed that extracellular cues guiding axon growth may converge onto mTORC1-dependent pathways (Yoon *et al.,* 2009; Nie *et al.,* 2010). Here, we showed that mTORC1 activation increases during the phase of PV cell synapse proliferation and that Tsc1 loss-induced mTORC1 hyperactivation lead to prematurely increased PV cell innervations by P18, both in organotypic cultures and *in vivo*. As a widespread and general modulator of metabolism and local protein translation, mTORC1 in itself is unlikely to provide a specific signal for axon-target interactions. For example, mTORC1 may regulate, either directly or indirectly, the synthesis of transcription factors (Kobayashi *et al.,* 2015), adhesion molecules (Chattopadhyaya *et al.,* 2013; Brennaman *et al.,* 2013; Zhang *et al.,* 2015) or components of GABAergic signaling (Chattopadhyaya *et al.,* 2007; Baho and Di Cristo., 2012; Wu *et al.,* 2012; Fu *et al.,* 2012b), which have been shown to regulate PV cell innervation, but that are not exclusively expressed by PV cells. On the other hand, the possibility that mTORC1 activation may lead to the synthesis of specific molecular signals for the formation of distinct synaptic types, for example, glutamatergic vs GABAergic synapses, or soma-targeting, vs dendrite-targeting, GABAergic synapses, cannot be excluded. Identification of the RNAs regulated by mTORC1 in defined cell types during specific developmental phases will provide insights into the mechanisms regulating PV cell synapse formation.

One interesting finding is that dysregulation of Tsc1-mTORC1 signaling in MGE-derived precursors caused, after an initial acceleration of the formation of PV cell perisomatic boutons, a loss of PV cell innervations in adult mice. Loss of GABAergic inputs following

Tsc1 deletion has been reported in other adult mouse models. For example, Tg(*Dlx5/6*-Cre);Tsc1$^{flox/flox}$ mice, where Tsc1 was knockout embryonically in all GABAergic interneurons, showed reduced density of both cortical and hippocampal interneurons in adults (Fu *et al.,* 2012a). Further, deletion of Tsc1 specifically in postnatal pyramidal neurons induced cell-autonomous reduction of inhibitory inputs onto pyramidal cells (Bateup *et al.,* 2013). On the other hand, to our knowledge this is the first report showing that a phase of hyperinnervation may precede GABAergic connectivity loss. One interesting possibility is that mTORC1 hyperactivation may lead to the premature formation of more, but less efficient synapses. Our observation that, while the number and intensity of perisomatic PV+ puncta were increased in Tg(*Nkx2.1*-Cre);Tsc1$^{flox/flox}$ compared to Tsc1^{Ctrl} mice, the density of perisomatic PV+/VGAT+ puncta was not, supports this hypothesis. Another, not exclusive, possibility is that mTORC1 may play different roles during distinct phases of PV cell development. For example, during the peak of PV cell synapse proliferation mTORC1 activation may help to stabilize nascent synapses most likely in response to the suitability of the postsynaptic target or to the relative synaptic strength compared to neighboring synapses. In this scenario, indiscriminate activation of mTORC1 following Tsc1 deletion may then induce the stabilization of too many synapses, which would results in increased PV cell innervations. On the other hand, after PV cell innervation fields have reached maturity, mTORC1 activation may actually facilitate synaptic plasticity and destabilization. In this case, mTORC1 hyperactivation would indeed lead to the shrinkage of PV innervation fields. Similarly, it has been reported that blocking neural transmission has opposing effects on PV cell innervation fields depending on the developmental stage of the PV cells (Baho and Di Cristo, 2012; Wu *et al.,* 2012). The molecular mechanisms underlying this response switch may likely involve changes in the transcriptional profile of PV cells, which occur between the second and fourth postnatal week (Okaty *et al.,* 2009).

In this study, we consistently found that deletion of both *Tsc1* alleles lead to initial increase, followed later on by a massive loss, of PV cell innervations, both *in vivo* and in organotypic cultures from Tg(*Nkx2.1*-Cre);Tsc1$^{flox/flox}$ mice. However, Tsc1 haploinsufficient PV cells showed altered innervation fields *in vitro* but not *in vivo*. Similarly, PV cell soma size and pS6 intensity expression levels were increased only in Tg(*Nkx2.1*-Cre);Tsc1$^{flox/flox}$ mice *in vivo*. One possibility is that limited access to nutrients *in vivo* compared to the abundance of nutrients and growth factors present in the culture medium or/and the occurrence of different neuronal activity patters may recruit alternative pathways regulating mTORC1 downstream effectors *in vivo*. In addition, we cannot exclude that Tg(*Nkx2.1*-Cre);Tsc1$^{flox/+}$ mice may show altered evoked cortical GABAergic responses even in absence of detectable morphological alterations.

Mutations in several genes, whose protein products regulate mTORC1 activity, have been associated with neurodevelopmental disorders (Lipton and Sahin, 2014). A major question concerning neurodevelopmental disorders is how mutations in the different molecules genetically associated with these diseases converge to produce a common set of behavioral deficits. An influential hypothesis is that disrupted excitatory/inhibitory (E/I) balance is an initiating factor leading to perturbed circuit function. Altogether our data suggest that Tsc1 deletion in PV cells alter their developmental trajectory, resulting in a progressive loss of PV cell connectivity in adulthood. Importantly, we found that alterations of PV cell connectivity following Tsc1 deletion were cell autonomous (refer to Fig.2); therefore they could be an important contributing mechanisms to cognitive alterations in Tuberous Sclerosis (TSC) patients. Interestingly, many TSC patients respond positively to the drug Vigabatrin, which is an irreversible inhibitor of the GABA degrading enzyme, GABA transaminase (Curatolo *et al.,* 2001) suggesting deficits in GABAergic signaling. Further, loss of the phosphatase PTEN, an upstream modulator of mTORC1 whose mutations have been associated with

autisms spectrum disorders, led to altered distribution of MGE-derived cells and overall loss in cortical GABAergic neurons (Vogt *et al.,* 2015).

Here, we report that early embryonic deletion of Tsc1 in MGE-derived precursors, which generate cortical PV cells and SOM+ interneurons, lead to hyperactivity, increased anxiety and social novelty recognition deficits in young adults. Interestingly, postnatal Tsc1 deletion exclusively in PV cells induced similar, if not more severe, deficits in social novelty recognition, but did not increased anxiety or activity levels. Since Tg(*PV*-Cre);$Tsc1^{flox/flox}$ mice showed loss of cortical PV cell perisomatic boutons comparable, if not more pronounced, to what we observed in Tg(*Nkx2.1*-Cre);$Tsc1^{flox/flox}$ mice, the difference in anxiety-related behavior is most likely due the involvement of different subcortical circuits, as both Nkx2.1 and PV are expressed by different and only partially overlapping subcortical neurons.

In summary, our results show that regulated mTORC1 activation is critically involved in the establishment and maintenance of PV cell innervation in the cortex. Alterations of mTORC1 activation, either by genetic or environmental causes, may therefore permanently alter PV cell circuits, thus affecting specific behaviors, depending on the extent and time course of mTORC1 signaling modifications.

4.6 Acknowledgments

This work was supported by the Canadian Institutes of Health Research (G.D.C), Canada Foundation for Innovation (G.D.C), Savoy Foundation (G.D.C). We thank Dr. Devendra Amre (Université de Montréal) for his help with statistical analysis. We would like to thank Catherine Dubois for her technical assistance as well as the Comité Institutionnel de Bonne Pratiques Animales en Recherche (CIBPAR) and all the personnel of the animal facility of the Research Center of CHU Sainte-Justine (Université de Montreal) for their instrumental

technical support.

4.7 Figures

Figure 4.1

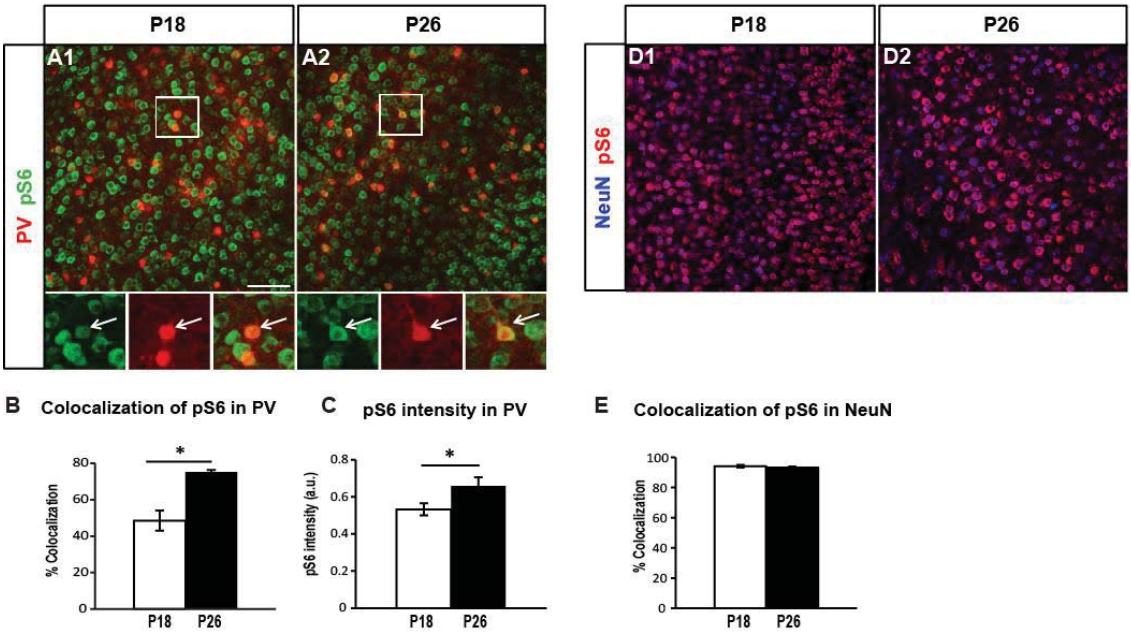

Figure 4.2

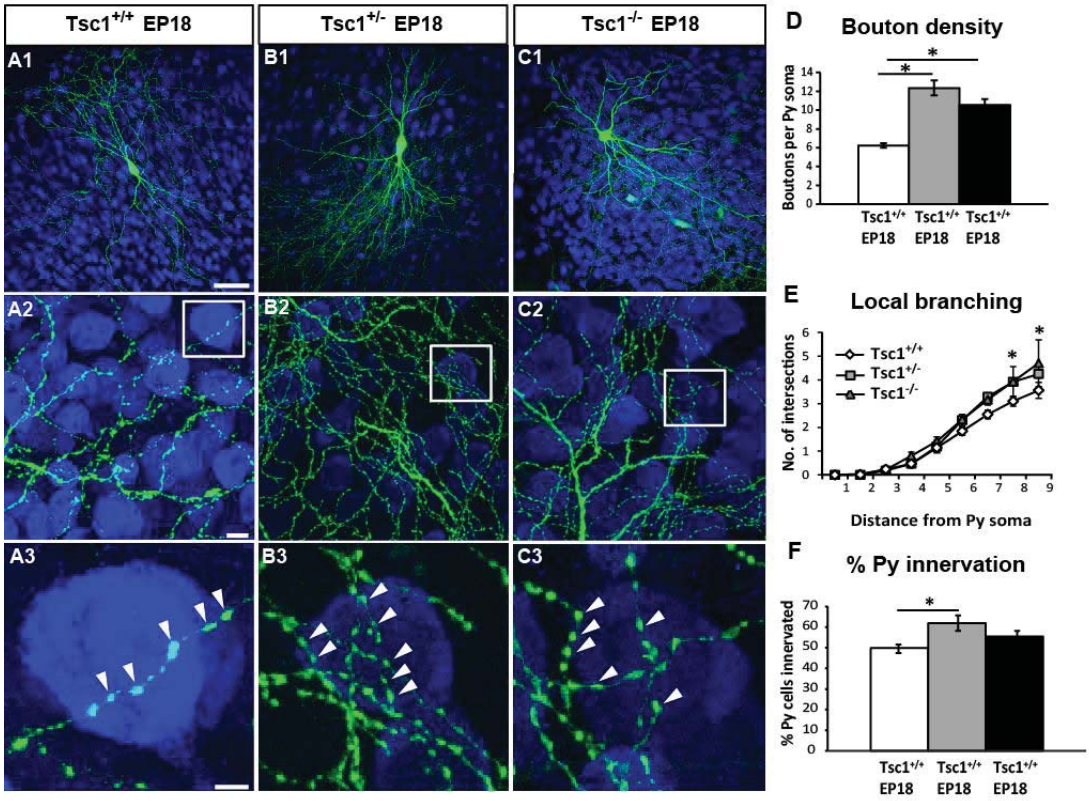
Tsc1+/+ EP18
Tsc1+/- EP18
Tsc1-/- EP18
A1
B1
C1
A2
B2
C2
A3
B3
C3
D
Bouton density
Boutons per Py soma
Tsc1+/+ EP18
Tsc1+/+ EP18
Tsc1+/+ EP18
E
Local branching
No. of intersections
Tsc1+/+
Tsc1+/-
Tsc1-/-
Distance from Py soma
F
% Py innervation
% Py cells innervated

Figure 4.3

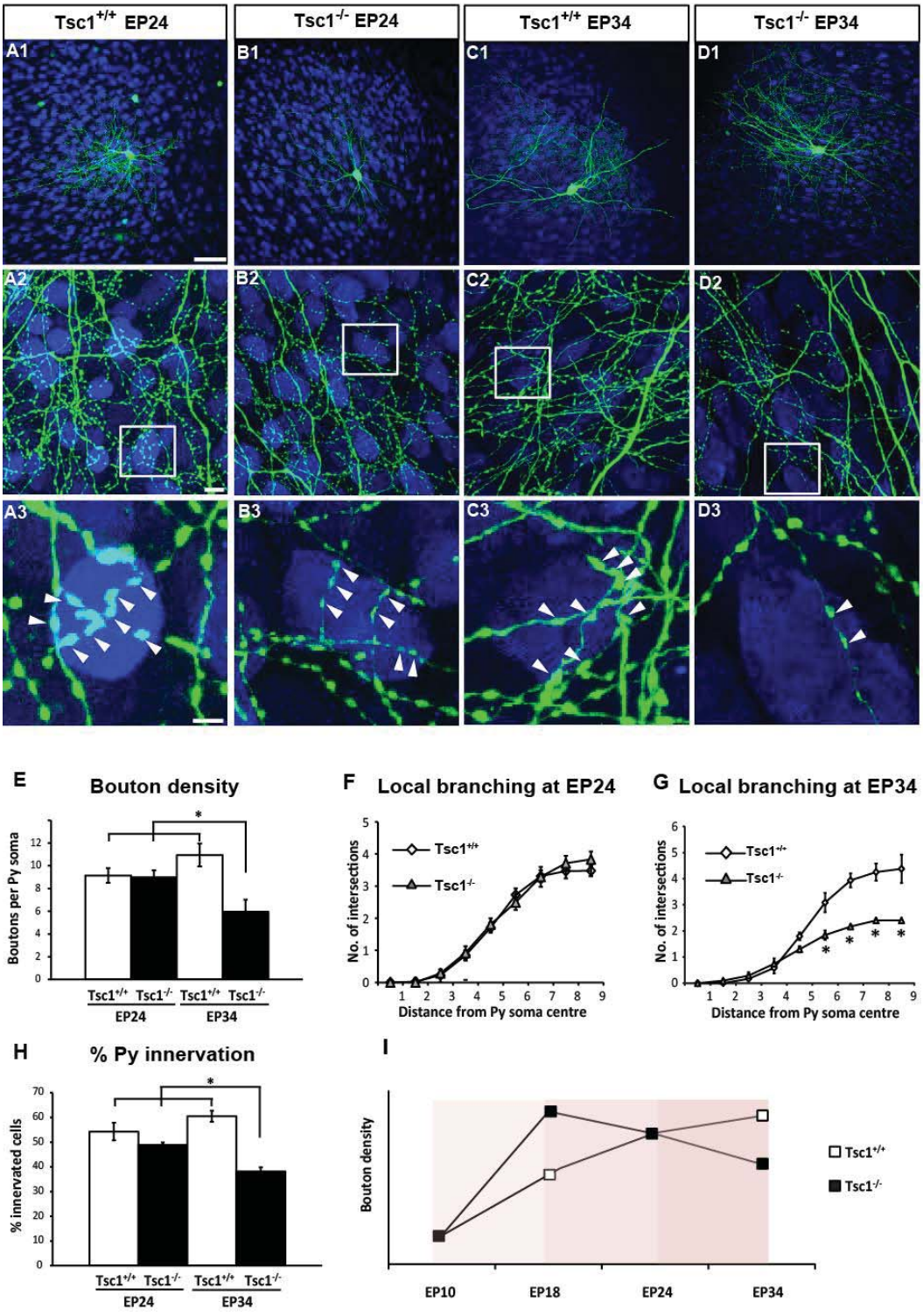
Tsc1+/+ EP24
Tsc1-/- EP24
Tsc1+/+ EP34
Tsc1-/- EP34
A1
B1
C1
D1
A2
B2
C2
D2
A3
B3
C3
D3
E
Bouton density
Boutons per Py soma
Tsc1+/+ Tsc1-/- Tsc1+/+ Tsc1-/-
EP24
EP34
F
Local branching at EP24
No. of intersections
Tsc1+/+
Tsc1-/-
Distance from Py soma centre
G
Local branching at EP34
No. of intersections
Tsc1+/+
Tsc1-/-
Distance from Py soma centre
H
% Py innervation
% innervated cells
Tsc1+/+ Tsc1-/- Tsc1+/+ Tsc1-/-
EP24
EP34
I
Bouton density
Tsc1+/+
Tsc1-/-
EP10
EP18
EP24
EP34

Figure 4.4

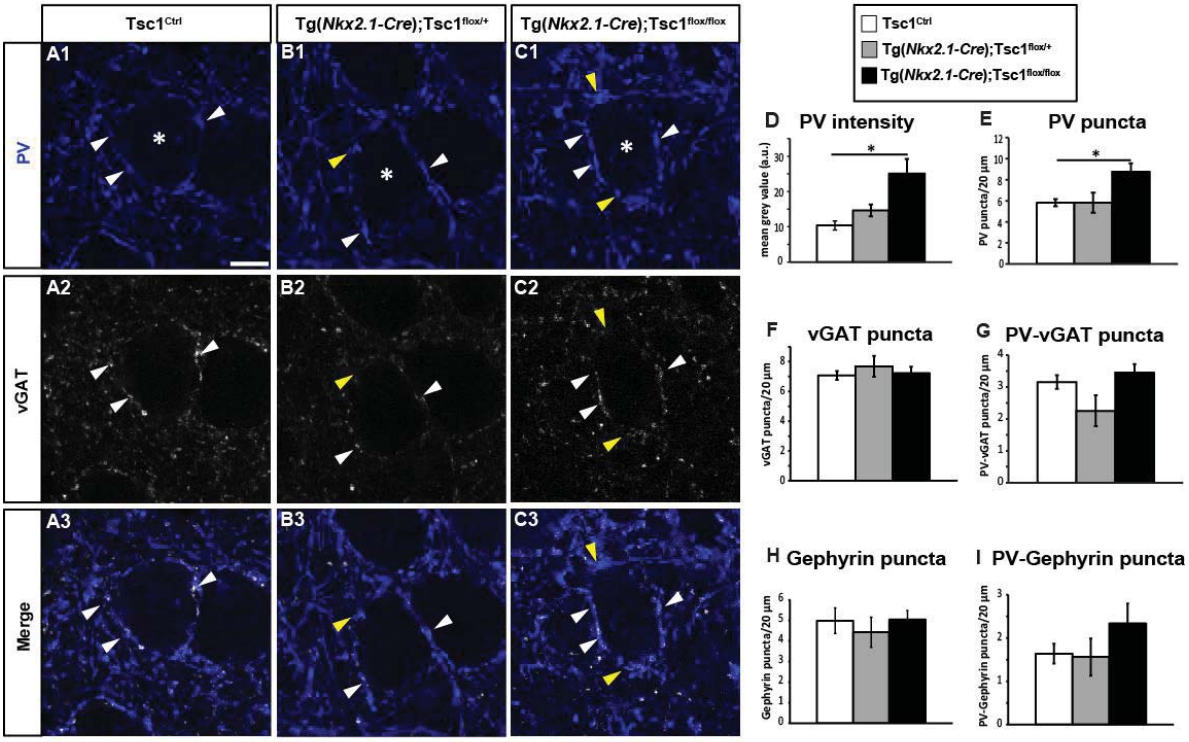
Tsc1Ctrl
Tg(Nkx2.1-Cre);Tsc1flox/+
Tg(Nkx2.1-Cre);Tsc1flox/flox
PV
vGAT
Merge
A1
B1
C1
A2
B2
C2
A3
B3
C3
D PV intensity
E PV puncta
F vGAT puncta
G PV-vGAT puncta
H Gephyrin puncta
I PV-Gephyrin puncta
mean grey value (a.u.)
PV puncta/20 µm
vGAT puncta/20 µm
PV-vGAT puncta/20 µm
Gephyrin puncta/20 µm
PV-Gephyrin puncta/20 µm

Figure 4.5

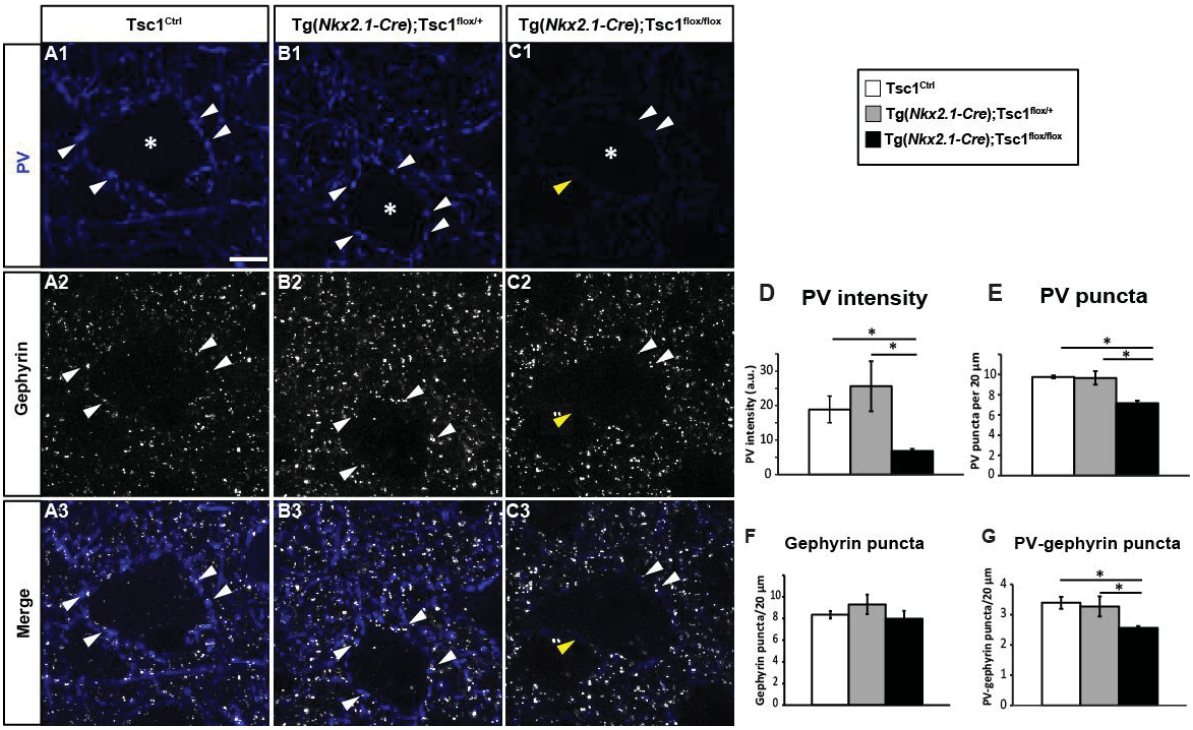
Tsc1Ctrl
Tg(Nkx2.1-Cre);Tsc1flox/+
Tg(Nkx2.1-Cre);Tsc1flox/flox
A1
B1
C1
PV
A2
B2
C2
Gephyrin
A3
B3
C3
Merge
D
PV intensity
PV intensity (a.u.)
E
PV puncta
PV puncta per 20 µm
F
Gephyrin puncta
Gephyrin puncta/20 µm
G
PV-gephyrin puncta
PV-gephyrin puncta/20 µm

Figure 4.6

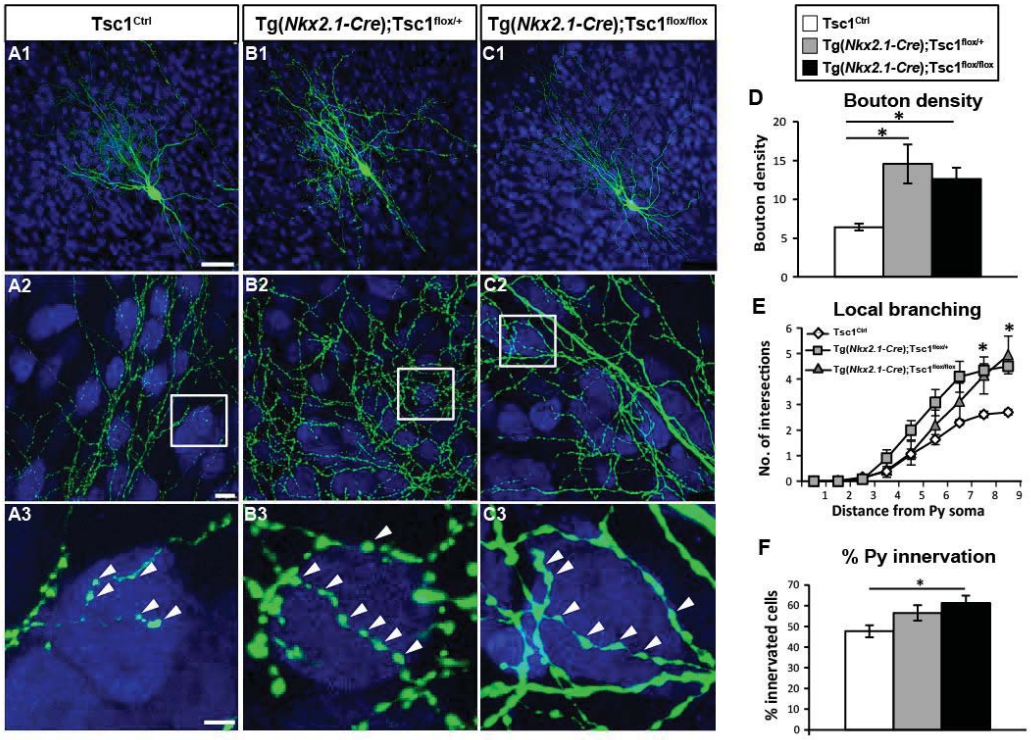
Tsc1Ctrl
Tg(Nkx2.1-Cre);Tsc1flox/+
Tg(Nkx2.1-Cre);Tsc1flox/flox
A1
B1
C1
A2
B2
C2
A3
B3
C3
D
Bouton density
Bouton density
E
Local branching
No. of intersections
Distance from Py soma
F
% Py innervation
% innervated cells

Figure 4.7

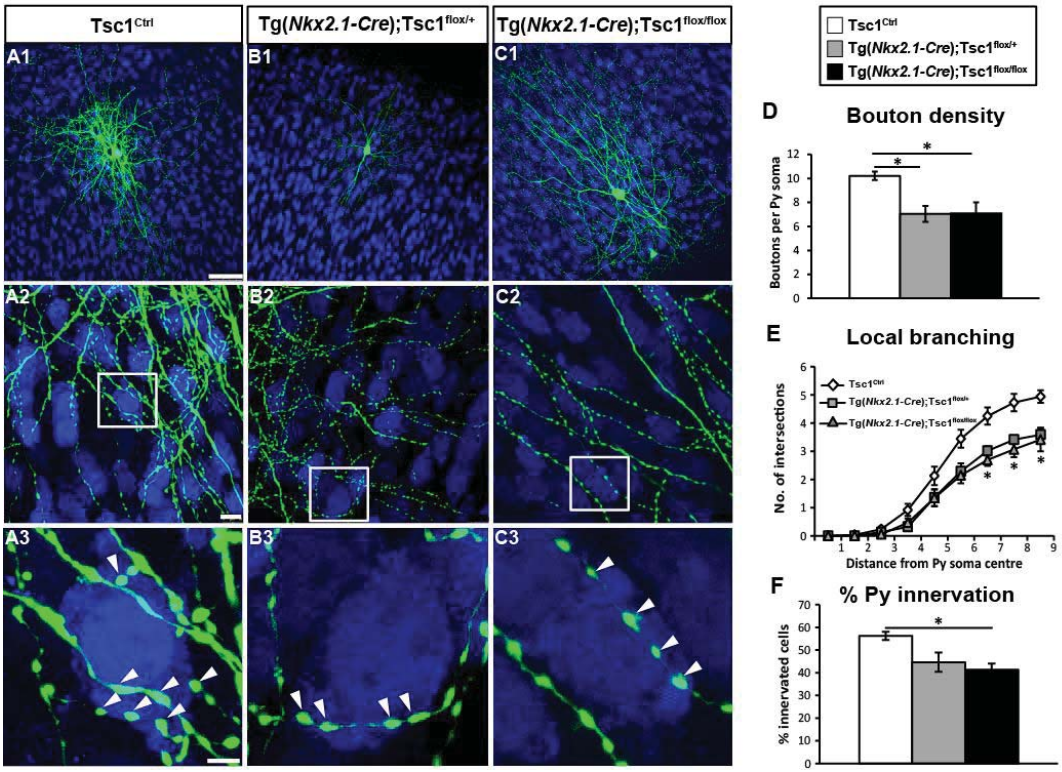

Figure 4.8

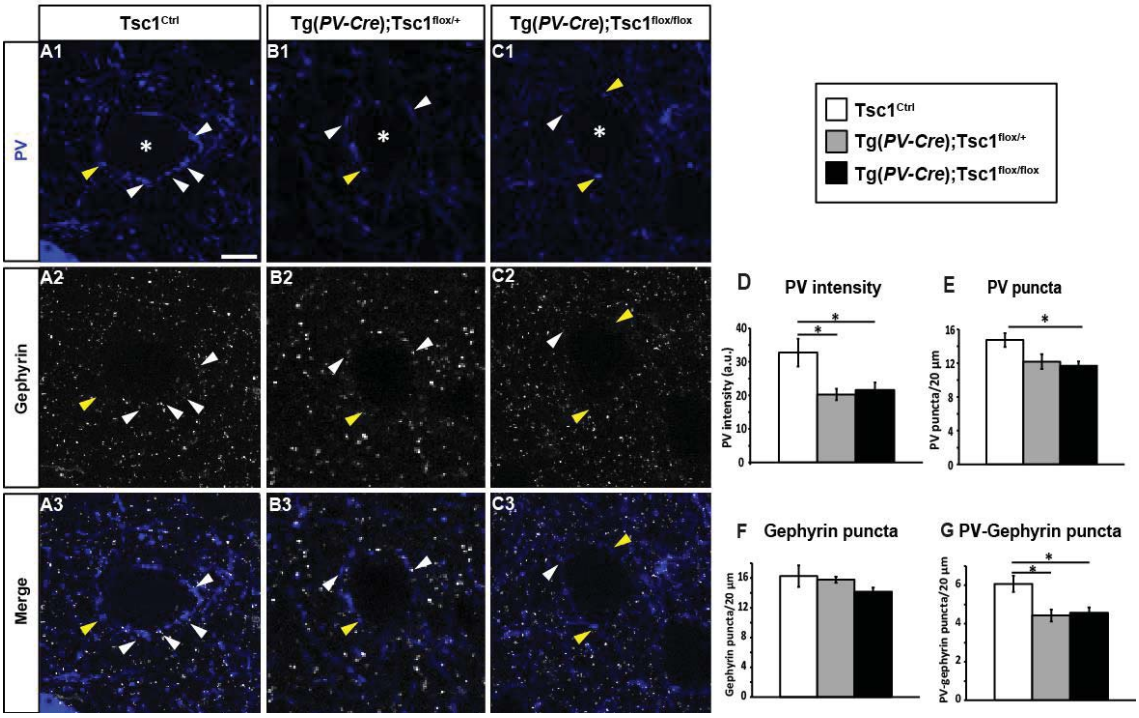

Figure 4.9

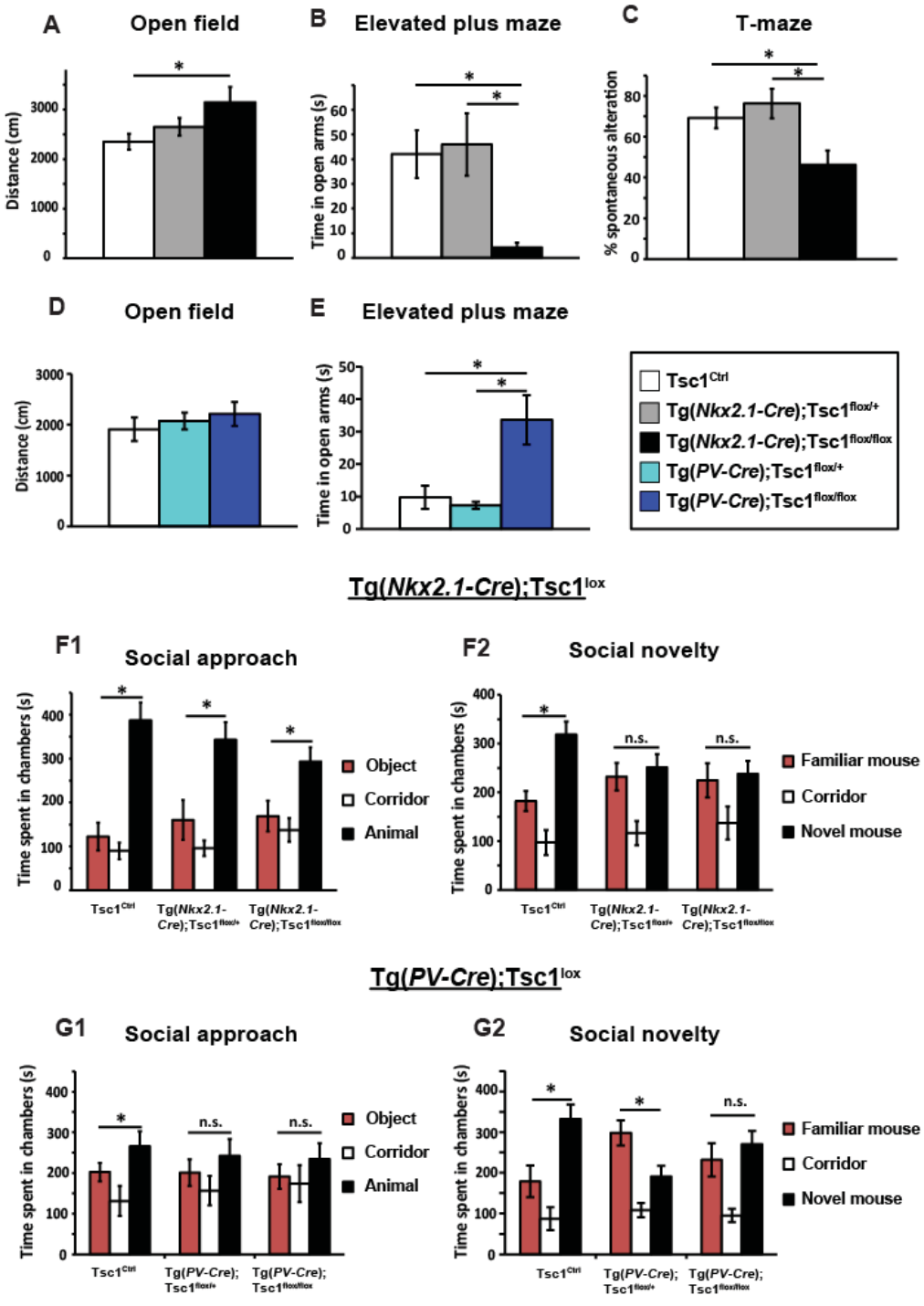
A
Open field
Distance (cm)
B
Elevated plus maze
Time in open arms (s)
C
T-maze
% spontaneous alteration
D
Open field
Distance (cm)
E
Elevated plus maze
Time in open arms (s)
Tsc1Ctrl
Tg(Nkx2.1-Cre);Tsc1flox/+
Tg(Nkx2.1-Cre);Tsc1flox/flox
Tg(PV-Cre);Tsc1flox/+
Tg(PV-Cre);Tsc1flox/flox
Tg(Nkx2.1-Cre);Tsc1lox
F1
Social approach
Time spent in chambers (s)
Object
Corridor
Animal
F2
Social novelty
n.s.
Familiar mouse
Corridor
Novel mouse
Tg(PV-Cre);Tsc1lox
G1
Social approach
G2
Social novelty

Figure 4.S1

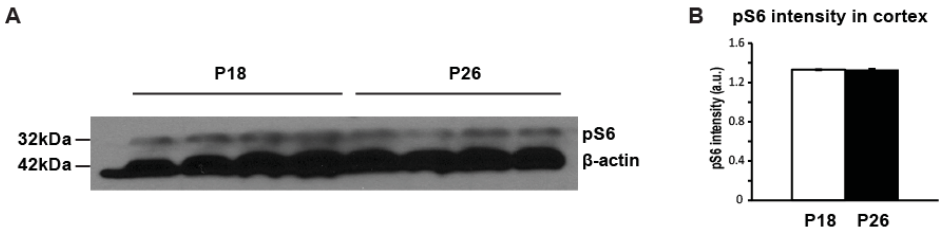

Figure 4.S2

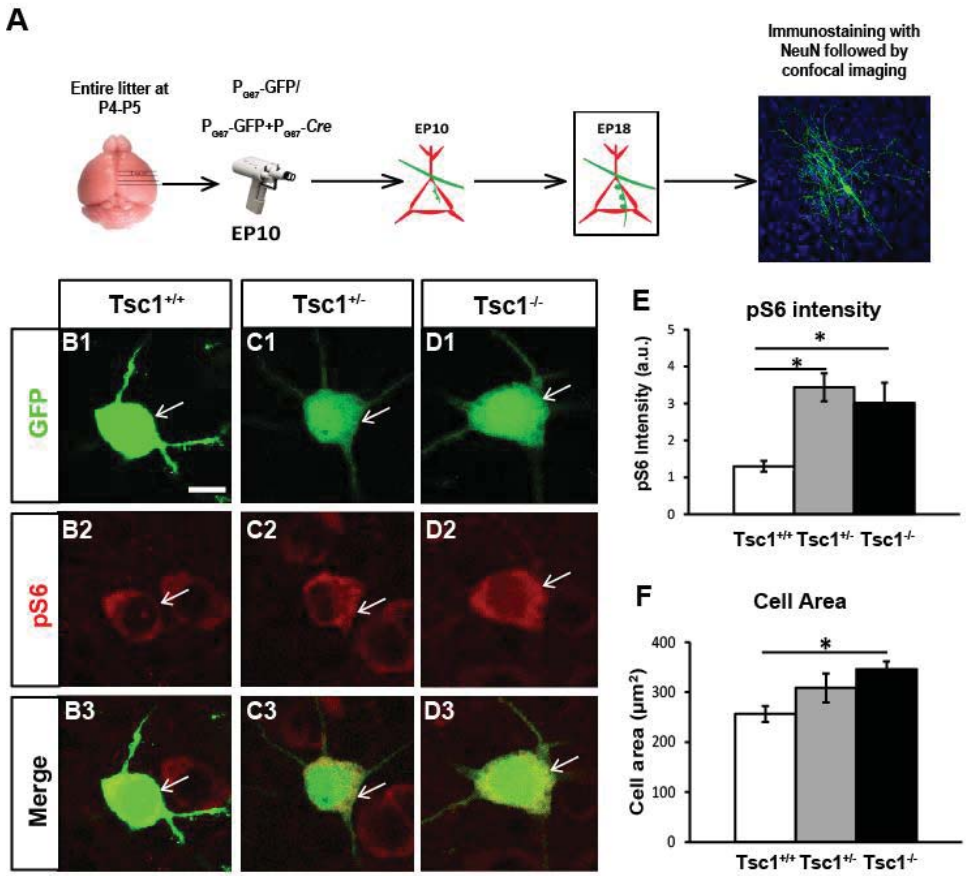

Figure 4.S3

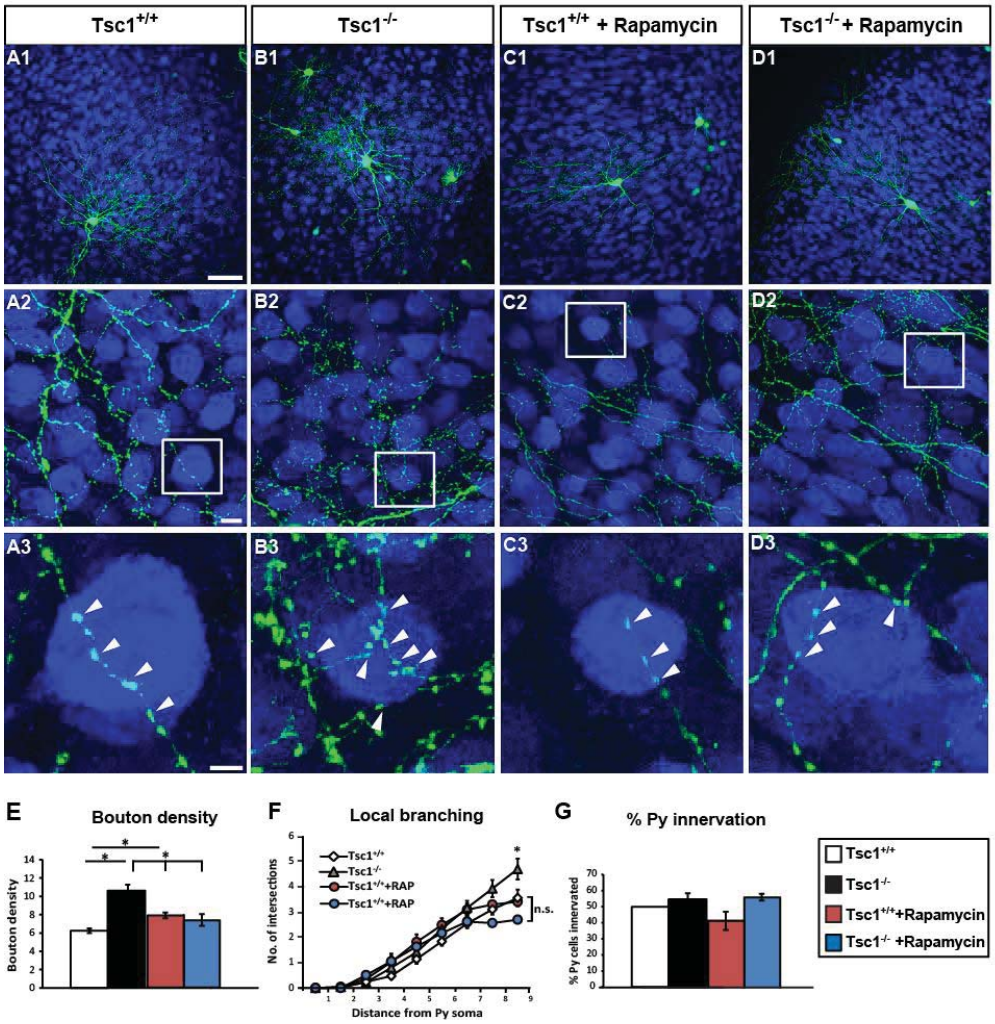
Tsc1+/+
Tsc1-/-
Tsc1+/+ + Rapamycin
Tsc1-/- + Rapamycin
A1
B1
C1
D1
A2
B2
C2
D2
A3
B3
C3
D3
E
Bouton density
Bouton density
F
Local branching
No. of intersections
Tsc1+/+
Tsc1-/-
Tsc1+/+RAP
Tsc1-/-+RAP
n.s.
Distance from Py soma
G
% Py innervation
% Py cells innervated
Tsc1+/+
Tsc1-/-
Tsc1+/+Rapamycin
Tsc1-/- +Rapamycin

Figure 4.S4

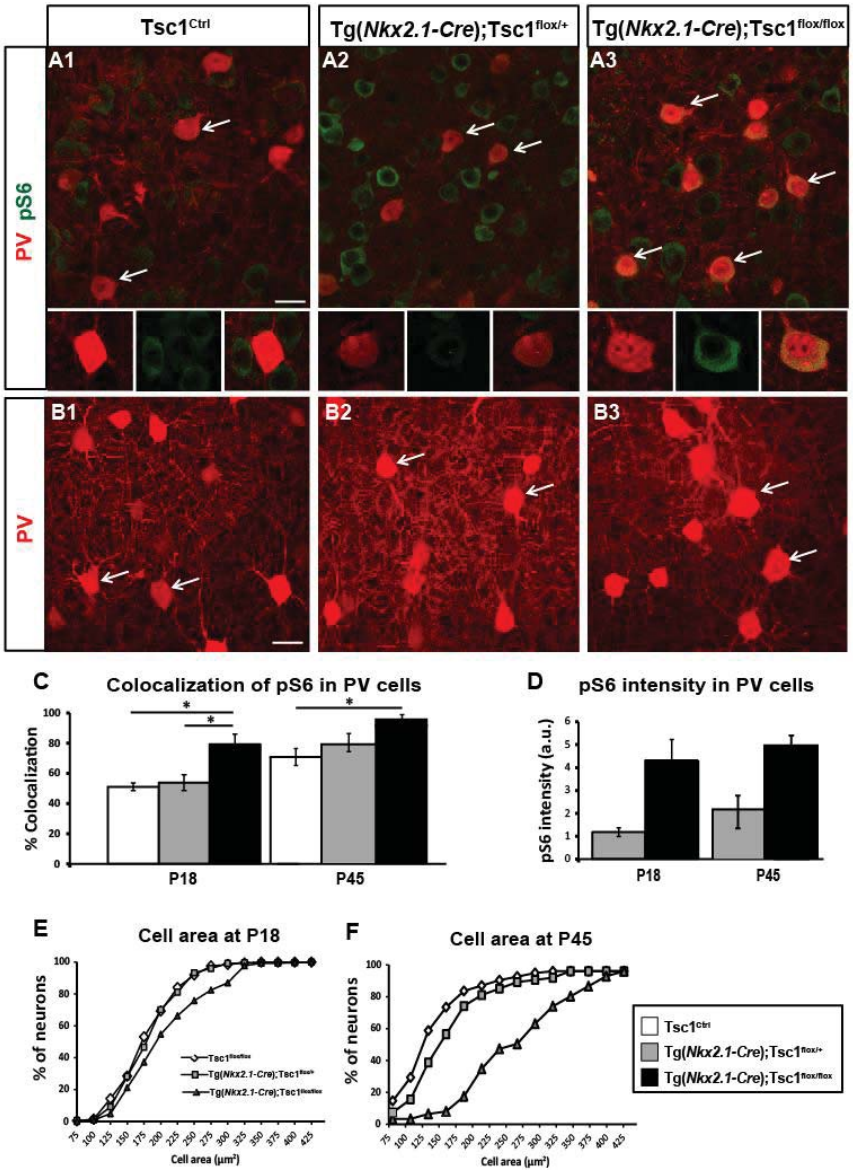
Tsc1Ctrl
Tg(Nkx2.1-Cre);Tsc1flox/+
Tg(Nkx2.1-Cre);Tsc1flox/flox
A1
A2
A3
PV pS6
B1
B2
B3
PV
C
Colocalization of pS6 in PV cells
% Colocalization
P18
P45
D
pS6 intensity in PV cells
pS6 intensity (a.u.)
E
Cell area at P18
% of neurons
Cell area (µm²)
F
Cell area at P45
Tsc1Ctrl
Tg(Nkx2.1-Cre);Tsc1flox/+
Tg(Nkx2.1-Cre);Tsc1flox/flox

Figure 4.S5

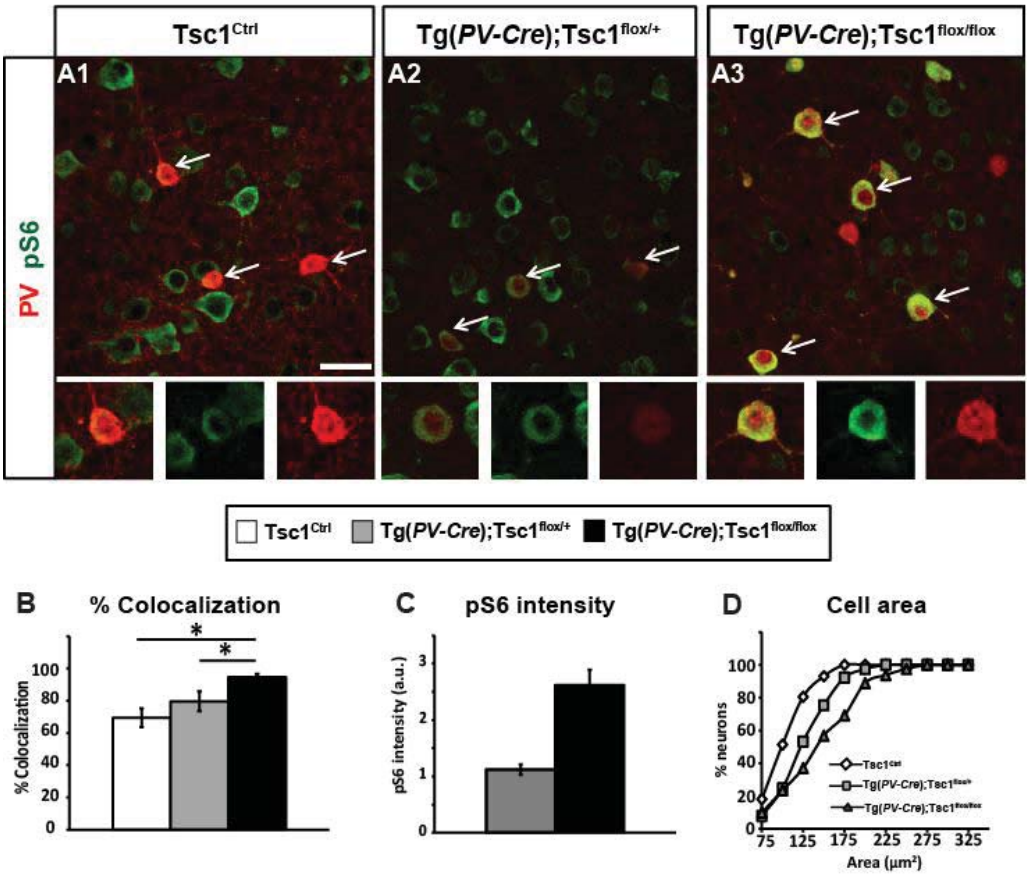
Tsc1Ctrl
Tg(PV-Cre);Tsc1flox/+
Tg(PV-Cre);Tsc1flox/flox
A1
A2
A3
PV pS6
Tsc1Ctrl
Tg(PV-Cre);Tsc1flox/+
Tg(PV-Cre);Tsc1flox/flox
B
% Colocalization
% Colocalization
C
pS6 intensity
pS6 intensity (a.u.)
D
Cell area
% neurons
Area (µm²)

Figure 4.1. mTOR activity increases specifically in PV cells between P18 and P26 . ***A***, Coronal sections of mouse somatosensory cortex immunostained for pS6 (green) and PV (red) at P18 (***A1***) and P26 (***A2***). ***B***, Significantly more PV cells express detectable levels of pS6 at P26 compared to P18 (t-test, *p<0.05). ***C***, Mean pS6 intensity in individual PV cells is also significanly higher at P26 (t-test, *p<0.05), n= 4 animals at P18; n=3 animals at P26. ***D***, Coronal sections of mouse somatosensory cortex immunostained for pS6 (red) and NeuN (blue) at P18 (***D1***) and P26 (***D2***). ***E***, Percentage of colocalization of pS6 and NeuN is not significanlty different between the two developmental ages. n=5 mice for both goups. Scale bars in ***A1-A2***, ***D1-D2***, 75µm. Bar graphs in ***B, C*** and ***E*** represent mean ± SEM.

Figure 4.2. Tsc1 knockout in single PV cells causes a premature increase of their axonal terminal branches and boutons density at EP18. ***A1***, EP18 $Tsc1^{+/+}$ PV cell showing characteristic branching (***A2***) and boutons (***A3***, arrowheads) on the postsynaptic somata indetified by NeuN immunostaining (blue). ***B, C***, PV cells lacking one copy (***B1-B3***) or both copies (***C1-C3***) of Tsc1 show increase in bouton density (***D***) (one-way ANOVA with Holm-Sidak post hoc analysis, *p<0.001) and local branching (***E***) (one-way ANOVA with Holm-Sidak post hoc analysis, *p<0.05). ***F***, Percentage of innervated cells for the 3 experimental groups (one-way ANOVA with Holm-Sidak post hoc analysis, *p<0.05). PV cells: n = 14 $Tsc1^{+/+}$, n= 7 $Tsc1^{+/-}$, n= 9 $Tsc1^{-/-}$. Scale bars: ***A1-C1***, 20 µm; ***A2-C2*** 10 µm, ***A3-C3***, 3 µm. Data in ***D, E*** and ***F*** represent mean ± SEM.

Figure 4.3. Tsc1 knockout in single PV cells impairs the long-term maintenance of their perisomatic innervations. ***A1***, EP24 $Tsc1^{+/+}$ and ***B1***, $Tsc1^{-/-}$ PV cells show similar axonal branching (***A2, B2***) and perisomatic bouton density (***A3, B3,*** arrowheads). ***C***, EP34 $Tsc1^{+/+}$ PV cell. ***D1, EP34*** $Tsc1^{-/-}$ PV cell showing significantly decreased axonal branching (compare **C2** and **D2**) and perisomatic boutons (compared **C3** and **D3**). (***E***) Bouton density (one-way ANOVA with Holm-Sidak post hoc analysis, *p<0.05), (***F, G***) local branching (test, *p<0.05) and ***H***, percentage of innervation are significantly reduced in EP34 $Tsc1^{-/-}$ PV cells (one-way ANOVA with Holm-Sidak post hoc analysis, *p<0.001). ***I,*** Schematic representation of bouton density development during the post-natal maturation of $Tsc1^{+/+}$ and $Tsc1^{-/-}$ PV cells. PV cells at EP24: n = 9 $Tsc1^{+/+}$, n= 6 $Tsc^{-/-}$ PV cells. PV cells at EP34: n= 5 $Tsc1^{+/+}$, n= 5 $Tsc1^{-/-}$. Scale bars: ***A1-C1***, 20 µm; ***A2-C2*** 10 µm, ***A3-C3***, 5 µm.

Figure 4.4. PV intensity and puncta density are increased in P18 Tg(*Nkx2.1-Cre*);$Tsc1^{flox/flox}$ mice. ***A-C***, Coronal sections of somatosensory cortex immunostained for PV (blue) and vGAT (grey) in $Tsc1^{Ctrl}$ mice (***A1-A3***), Tg(*Nkx2.1-Cre*);$Tsc1^{flox/+}$ mice (***B1-B3***) and Tg(*Nkx2.1-Cre*);$Tsc1^{flox/flox}$ mice (***C1-C3***). Asterisk indicates the likely location of neuronal cell bodies. White arrowheads denote PV/vGAT-colocalized puncta while yellow arrowheads denote PV puncta that do not colocalize with vGAT puncta (***D***)(***A1-C3***). ***D***, ***E*** Tg(*Nkx2.1-Cre*);$Tsc1^{flox/flox}$ mice show increased PV immunostaining intensity (one-way ANOVA with Holm-Sidak post hoc analysis, *p<0.05) and puncta density (***E***) (one-way ANOVA with Holm-Sidak post hoc analysis, *p<0.05). ***F-I.*** Quantification show no

significant differences in the density of vGAT puncta (**F),** PV/vGAT puncta (***G)***, gephyrin puncta (***H***) and PV/gephyrin puncta (***I***) between the 3 genotypes (one-way ANOVA, p>0.05). n = 5 $Tsc1^{Ctrl}$ mice, n= 5 Tg(*Nkx2.1-Cre*);$Tsc1^{flox/+}$ mice, n= 4 Tg(*Nkx2.1-Cre*);$Tsc1^{flox/flox}$ mice. Scale bar: 10 μm.

Figure 4.5. Tg(*Nkx2.1-Cre*);$Tsc1^{flox/flox}$ mice show reduced putative PV+ perisomatic synapses at P45. ***A-C***, Coronal sections of somatosensory cortex immunostained for PV (blue) and gephyrin (grey) in $Tsc1^{Ctrl}$ (***A1-A3***), Tg(*Nkx2.1-Cre*);$Tsc1^{flox/+}$ (***B1-B3***) and Tg(*Nkx2.1-Cre*);$Tsc1^{flox/flox}$ mice (***C1-C3***). Asterisks indicate the likely location of neuronal cell bodies. White arrowheads denote PV-gephyrin colocalized puncta while yellow arrowheads denote PV boutons that do not colocalize with gephyrin puncta (***A1-C3***). ***D***, ***E,*** Tg(*Nkx2.1-Cre*);$Tsc1^{flox/flox}$ mice show decreased PV immunostaining intensity (**D),** one-way ANOVA with Holm-Sidak post hoc analysis, *p<0.05) and PV puncta density (***E***) (one-way ANOVA with Holm-Sidak post hoc analysis, *p<0.001). ***F***, Gephyrin puncta density is not significantly different between the 3 genotypes (one-way ANOVA, p>0.05). ***G***, Tg(*Nkx2.1-Cre*);$Tsc1^{flox/flox}$ mice show reduced PV/gephyrin colocalized puncta density (one-way ANOVA with Holm-Sidak post hoc analysis, *p<0.05). n = 5 mice for all genotypes. Scale bar: 10 μm.

Figure 4.6. PV cells show prematurely rich perisomatic innervations in Tg(*Nkx2.1-Cre*);$Tsc1^{flox/flox}$ and Tg(*Nkx2.1-Cre*);$Tsc1^{flox/+}$ mice at EP18. ***A1***, A PV cell (green) among NeuN immunostained neurons (blue) in cortical organotypic cultures from a $Tsc1^{Ctrl}$ mouse at EP18. ***A2***, PV cells from $Tsc1^{Ctrl}$ animal show characteristic branching and boutons (arrowheads) on the postsynaptic somata (***A3***). PV cells from Tg(*Nkx2.1-Cre*);$Tsc1^{flox/+}$ mice (***B1-B3***) and Tg(*Nkx2.1-Cre*);$Tsc1^{flox/flox}$ mice (***C1-C3***) show increased bouton density (***D***) (one-way ANOVA with Holm-Sidak post hoc analysis, *p<0.05), and local branching (***E***) (one-way ANOVA with Holm-Sidak post hoc analysis, *p<0.05). ***F***, Percentage of innervation (one-way ANOVA with Holm-Sidak post hoc analysis, *p<0.05). PV cells: n = 7 from $Tsc1^{Ctrl}$ mice, n= 7 from Tg(*Nkx2.1-Cre*);$Tsc1^{flox/+}$ mice, n= 6 from Tg(*Nkx2.1-Cre*);$Tsc1^{flox/flox}$ mice. Scale bars: ***A1-C1***, 20 μm; ***A2-C2*** 10 μm, ***A3-C3***, 3 μm.

Figure 4.7. PV cells show significantly reduced perisomatic innervations in Tg(*Nkx2.1-Cre*);$Tsc1^{flox/flox}$ and Tg(*Nkx2.1-Cre*);$Tsc1^{flox/+}$ mice at EP34 . ***A,*** A PV cell (green) among NeuN immunostained neurons (blue) in cortical organotypic cultures from a $Tsc1^{Ctrl}$ mouse at EP34. ***B, C,*** PV cells from Tg(*Nkx2.1-Cre*);$Tsc1^{flox/+}$ mice (***B1-B3***) or Tg(*Nkx2.1-Cre*);$Tsc1^{flox/flox}$ mice (***C1-C3***) show decreased bouton density (***D***) (one-way ANOVA with Holm-Sidak post hoc analysis, *p<0.05), and local branching (***E***) (one-way ANOVA with Holm-Sidak post hoc analysis, *p<0.05). ***F***, Percentage of innervation is also significantly lower for PV cells from Tg(*Nkx2.1-Cre*);$Tsc1^{flox/flox}$ mice (one-way ANOVA with Holm-Sidak post hoc analysis, *p<0.05). Arrowheads indicate boutons. n = 6 PV cells for all genotypes. Scale bars: ***A1-C1***, 20 μm; ***A2-C2*** 10 μm, ***A3-C3***, 3 μm.

Figure 4.8. Postnatal knockout of Tsc1 in PV cells causes a significant reduction of putative PV perisomatic synapse at P45. ***A-C***, Coronal sections of somatosensory cortex immunostained for PV (blue) and gephyrin (grey) in $Tsc1^{Ctrl}$ mice (***A1-A3***), Tg(*PV-*

Cre);Tsc1$^{flox/+}$ mice (***B1-B3***) and Tg(*PV-Cre*);Tsc1$^{flox/flox}$ mice (***C1-C3***). Asterisks indicate the likely location of neuronal cell bodies. White arrowheads denote PV-gephyrin colocalized boutons, while yellow arrowheads denote PV boutons that do not colocalize with gephyrin puncta (***A1-C3***). ***D***, Perisomatic PV signal intensity (one-way ANOVA with Holm-Sidak post hoc analysis, *p<0.05). ***E,*** PV puncta density (one-way ANOVA with Holm-Sidak post hoc analysis, *p<0.05). ***F***, gephyrin puncta density (one-way ANOVA, p>0.05). ***G***, PV/gephyrin colocalized puncta (one-way ANOVA with Holm-Sidak post hoc analysis, *p<0.05). n = 5 mice for all genotypes. Scale bar: 10 μm.

Figure 4.9. Tsc1 knockout in GABAergic cells causes hyperactivity, anxiety behaviour and social behavioural deficits. ***A***, Open field test: Quantification of distance travelled during exploratory activity in an open field arena at P33 shows increased exploratory drive in Tg(*Nkx2.1-Cre*);Tsc1$^{flox/flox}$ mice (one-way ANOVA with Holm-Sidak post hoc analysis, *p<0.05). n = 14 Tsc1^{Ctrl} mice, n= 10 Tg(*Nkx2.1-Cre*);Tsc1$^{flox/+}$ mice, n= 10 Tg(*Nkx2.1-Cre*);Tsc1$^{flox/flox}$ mice. ***B***, Elevated plus maze : Quantification of time spent in the open arms of elevated plus maze arena at P35 shows increased anxiety like behaviour in Tg(*Nkx2.1-Cre*);Tsc1$^{flox/flox}$ mice (one-way ANOVA with Holm-Sidak post hoc analysis, *p<0.05). n = 14 Tsc1^{Ctrl} mice, n= 12 Tg(*Nkx2.1-Cre*);Tsc1$^{flox/+}$ mice, n= 10 Tg(*Nkx2.1-Cre*);Tsc1$^{flox/flox}$ mice. ***C***, T-maze : Tg(*Nkx2.1-Cre*);Tsc1$^{flox/flox}$ mice shows less spontaneous alterations in a T-maze paradigm for test of working memory (one-way ANOVA with Holm-Sidak post hoc analysis, *p<0.01). n = 23 Tsc1^{Ctrl} mice, n= 10 Tg(*Nkx2.1-Cre*);Tsc1$^{flox/+}$ mice, n= 20 Tg(*Nkx2.1-Cre*);Tsc1$^{flox/flox}$ mice.***D***, Open field test: Quantification of distance travelled during exploratory activity in an open field arena at P33 shows exploratory drive in Tg(*PV-Cre*);Tsc1$^{flox/flox}$ and Tg(*PV-Cre*);Tsc1$^{flox/+}$ mice are similar to Tsc1^{Ctrl} (one-way ANOVA with Holm-Sidak post hoc analysis, p>0.05).). n = 12 Tsc1^{Ctrl} mice, n= 10 Tg(*PV-Cre*);Tsc1$^{flox/+}$ mice, n= 10 Tg(*PV-Cre*);Tsc1$^{flox/flox}$ mice. ***E***, Elevated plus maze : Quantification of time spent in the open arms of elevated plus maze arena at P35 shows anti-anxiety like behaviour in Tg(*PV-Cre*);Tsc1$^{flox/flox}$ mice (one-way ANOVA with Holm-Sidak post hoc analysis, *p<0.05). n = 21 Tsc1^{Ctrl} mice, n= 13 Tg(*PV-Cre*);Tsc1$^{flox/+}$ mice, n= 13 Tg(*PV-Cre*);Tsc1$^{flox/flox}$ mice. ***F1***, In the social approach paradigm, both Tg(*Nkx2.1-Cre*);Tsc1$^{flox/+}$ and Tg(*Nkx2.1-Cre*);Tsc1$^{flox/flox}$ mice spend significantly more time with animal compared to object similar to Tsc1^{Ctrl} mice, (two-way ANOVA with Bonferroni's post hoc analysis, *p<0.05). ***F2***, Unlike Tsc1^{Ctrl} mice, both Tg(*Nkx2.1-Cre*);Tsc1$^{flox/+}$ and Tg(*Nkx2.1-Cre*);Tsc1$^{flox/flox}$ mice failed to show preference for social novelty (two-way ANOVA with Bonferroni's post hoc analysis, *p<0.05). n = 14 Tsc1^{Ctrl} mice, n= 15 Tg(*Nkx2.1-Cre*);Tsc1$^{flox/+}$ mice, n= 13 Tg(*Nkx2.1-Cre*);Tsc1$^{flox/flox}$ mice. Unlike Tsc1^{Ctrl} mice, both Tg(*PV-Cre*);Tsc1$^{flox/+}$ and Tg(*PV-Cre*);Tsc1$^{flox/flox}$ mice failed to show preference for social approach (***G1***) and social novelty (***G2***) (two-way ANOVA with Bonferroni's post hoc analysis, *p<0.05). n ≥10 for each group in all behavioural studies. n = 12 Tsc1^{Ctrl} mice, n= 15 Tg(*PV-Cre*);Tsc1$^{flox/+}$ mice, n= 12 Tg(*PV-Cre*);Tsc1$^{flox/flox}$ mice. Data in ***A-G*** represent mean ± SEM.

Figure 4.S1. pS6 expression levels are constant in the cortex between the 2nd and 4th post-natal week of development. ***A***, Western blot for pS6 on somatosensory cortex of P18

and P26 mice. n = 4 animals at P18 and P26. Each lane represents a different animal. ***B***, Quantification show no difference in pS6 expression levels (band at 32 KDa, Student t-test, p>0.05).Values in ***B*** represent mean ± SEM.

Figure 4.S2. Tsc1 knockout in single PV cells lead to increase in mTOR activity and somatic hypertrophy. ***A,*** Schematics of experimental procedure. ***B, C, D*** PV cells from cortical organotypic cultures transfected with P_{G67} ($Tsc1^{+/+}$ control cells) or P_{G67}-Cre ($Tsc1^{+/-}$ and $Tsc1^{-/-}$) immunostained for pS6 (red) at EP18. ***E***, Somatic pS6 intensity is increased in both $Tsc1^{+/-}$ (***C2***) and $Tsc1^{-/-}$ PV cells (***D2***) compared to $Tsc1^{+/+}$ PV cells (one-way ANOVA with Holm-Sidak post hoc analysis, *p<0.05). ***F***, $Tsc1^{-/-}$ cells have increased soma area (one-way ANOVA with Holm-Sidak post hoc analysis, *p<0.05). Scale bar: 10μm.

Figure 4.S3. Premature increase in perisomatic innervations formed by $Tsc1^{-/-}$ PV cells is mTORC1-dependent. ***A, B***, $Tsc1^{-/-}$ PV cell (green) shows more complex terminal axonal branching (**A2, B2)** and increased bouton density at EP18 (**A3, B3,** arrowheads) compared to control, age-matched PV cells. **C, D:** Rapamycin treatment from EP12-18 does not affect bouton density and local branching of $Tsc1^{+/+}$ PV cells (**C**), while it normalizes perisomatic innervations formed by $Tsc1^{-/-}$ PV cells (**D)**. $Tsc1^{-/-}$ PV cells show increased bouton density (***E***) (one-way ANOVA with Holm-Sidak post hoc analysis, *p<0.05) and local branching (***F***) (one-way ANOVA with Holm-Sidak post hoc analysis, *p<0.05) compared to the other groups. ***G***, Percentage of innervation. PV cells: n = 14 $Tsc1^{+/+}$ PV cells, n= 9 $Tsc1^{-/-}$ PV cells, n= 4 $Tsc1^{+/+}$ + Rapamycin PV cells, n= 4 $Tsc1^{-/-}$ + Rapamycin PV cells, Scale bars: ***A1-D1***, 100 μm; ***A2-D2*** and ***A3-D3***, 5 μm.

Figure 4.S4. Cortical PV cells of Tg(*Nkx2.1-Cre*);$Tsc1^{flox/flox}$ mice show increased mTOR activity and somatic hypertrophy. ***A***, Coronal sections of somatosensory cortex immunostained for PV (red) and pS6 (green) (**A**) or PV only (**B**) in $Tsc1^{Ctrl}$ mice (***A1, B1***), Tg(*Nkx2.1-Cre*);$Tsc1^{flox/+}$ mice (***A2, B2***) and Tg(*Nkx2.1-Cre*);$Tsc1^{flox/flox}$ red, mice (***A3, B3***) at P18. Lower panels show higher magnification of individual PV cells. ***C***, In Tg(*Nkx2.1-Cre*);$Tsc1^{flox/flox}$ mice, more PV cells colocalize with pS6 (one-way ANOVA with Holm-Sidak post hoc analysis, *p<0.05) compared to Tg(*Nkx2.1-Cre*);$Tsc1^{flox/+}$ and wild-type mice at P18 and P45. ***D***, pS6 expression intensity in PV cells normalized to wild-type controls at P18 and P45. ***E***, **F,** Quantification of PV cell area shows somatic hypertrophy in Tg(*Nkx2.1-Cre*);$Tsc1^{flox/flox}$ mice at both P18 and P45 (P18: K-S test, *p<0.01; P45: K-S test, *p<0.001), and in Tg(*Nkx2.1-Cre*);$Tsc1^{flox/+}$ mice at P45 (P18: K-S test, *p<0.05), n = 11 $Tsc1^{Ctrl}$ mice, , n= 5 Tg(*Nkx2.1-Cre*);$Tsc1^{flox/+}$ mice, n= 7 Tg(*Nkx2.1-Cre*);$Tsc1^{flox/flox}$ mice at P18. n = 6 mice for all genotypes at P45. Scale bar, 20 μm.

Figure 4.S5. Cortical PV cells show increased mTOR activity and somatic hypertrophy in Tg(*PV-Cre*);$Tsc1^{flox/flox}$ mice. ***A***, Coronal sections of somatosensory cortex immunostained for PV (red) and pS6 (green) in $Tsc1^{Ctrl}$ (***A1***), Tg(*PV-Cre*);$Tsc1^{flox/+}$ (***A2***) and Tg(*PV-Cre*);$Tsc1^{flox/flox}$ mice (***A3***) at P45. Lower panels show individual PV cells. ***B***, Both

Tg(*PV-Cre*);Tsc1$^{flox/+}$ and Tg(*PV-Cre*);Tsc1$^{flox/flox}$ mice show increased percentage of colocalization of pS6 in PV cells (one-way ANOVA with Holm-Sidak post hoc analysis, *p<0.05). ***C***, Quantification of pS6 expression intensity in PV cells normalized to wild-type controls show two-fold increase in Tg(*PV-Cre*); Tsc1$^{flox/flox}$ mice, but not in Tg(*PV-Cre*);Tsc1$^{flox/+}$ mice is similar to controls. ***D***, PV cells show somatic hypertrophy in mice mutant groups (K-S test, *p<0.001) at P45. n = 5 mice for all genotypes at P45. Scale bar, 20 μm.

4.8 References

Bateup, H.S., Johnson, C.A., Denefrio, C.L., Saulnier, J.L., Kornacker, K., and Sabatini, B.L. (2013). Excitatory/inhibitory synaptic imbalance leads to hippocampal hyperexcitability in mouse models of tuberous sclerosis. Neuron *78*, 510-522.

Bateup, H.S., Takasaki, K.T., Saulnier, J.L., Denefrio, C.L., and Sabatini, B.L. (2011). Loss of Tsc1 in vivo impairs hippocampal mGluR-LTD and increases excitatory synaptic function. The Journal of neuroscience : the official journal of the Society for Neuroscience *31*, 8862-8869.

Brennaman, L.H., Zhang, X., Guan, H., Triplett, J.W., Brown, A., Demyanenko, G.P., Manis, P.B., Landmesser, L., and Maness, P.F. (2013). Polysialylated NCAM and ephrinA/EphA regulate synaptic development of GABAergic interneurons in prefrontal cortex. Cereb Cortex *23*, 162-177.

Cardin, J.A., Carlen, M., Meletis, K., Knoblich, U., Zhang, F., Deisseroth, K., Tsai, L.H., and Moore, C.I. (2009). Driving fast-spiking cells induces gamma rhythm and controls sensory responses. Nature *459*, 663-667.

Chattopadhyaya, B., Baho, E., Huang, Z.J., Schachner, M., and Di Cristo, G. (2013). Neural cell adhesion molecule-mediated Fyn activation promotes GABAergic synapse maturation in postnatal mouse cortex. The Journal of neuroscience : the official journal of the Society for Neuroscience *33*, 5957-5968.

Chattopadhyaya, B., Di Cristo, G., Higashiyama, H., Knott, G.W., Kuhlman, S.J., Welker, E., and Huang, Z.J. (2004). Experience and activity-dependent maturation of perisomatic GABAergic innervation in primary visual cortex during a postnatal critical period. The Journal of neuroscience : the official journal of the Society for Neuroscience *24*, 9598-9611.

Chattopadhyaya, B., Di Cristo, G., Wu, C.Z., Knott, G., Kuhlman, S., Fu, Y., Palmiter, R.D., and Huang, Z.J. (2007). GAD67-mediated GABA synthesis and signaling regulate inhibitory synaptic innervation in the visual cortex. Neuron *54*, 889-903.

Cho, R.Y., Konecky, R.O., and Carter, C.S. (2006). Impairments in frontal cortical gamma synchrony and cognitive control in schizophrenia. Proc Natl Acad Sci U S A *103*, 19878-19883.

Choi, Y.J., Di Nardo, A., Kramvis, I., Meikle, L., Kwiatkowski, D.J., Sahin, M., and He, X. (2008). Tuberous sclerosis complex proteins control axon formation. Genes & development *22*, 2485-2495.

Costa-Mattioli, M., and Monteggia, L.M. (2013). mTOR complexes in neurodevelopmental and neuropsychiatric disorders. Nature neuroscience *16*, 1537-1543.

Curatolo, P., Verdecchia, M., and Bombardieri, R. (2001). Vigabatrin for tuberous sclerosis complex. Brain Dev *23*, 649-653.
de Vries, P.J. (2010). Targeted treatments for cognitive and neurodevelopmental disorders in tuberous sclerosis complex. Neurotherapeutics : the journal of the American Society for Experimental NeuroTherapeutics *7*, 275-282.

Di Cristo, G., Chattopadhyaya, B., Kuhlman, S.J., Fu, Y., Belanger, M.C., Wu, C.Z., Rutishauser, U., Maffei, L., and Huang, Z.J. (2007). Activity-dependent PSA expression regulates inhibitory maturation and onset of critical period plasticity. Nature neuroscience *10*, 1569-1577.

Di Cristo, G., Wu, C., Chattopadhyaya, B., Ango, F., Knott, G., Welker, E., Svoboda, K., and Huang, Z.J. (2004). Subcellular domain-restricted GABAergic innervation in primary visual cortex in the absence of sensory and thalamic inputs. Nature neuroscience *7*, 1184-1186.

Fagiolini, M., Fritschy, J.M., Low, K., Mohler, H., Rudolph, U., and Hensch, T.K. (2004). Specific GABAA circuits for visual cortical plasticity. Science *303*, 1681-1683.

Fagiolini, M., and Hensch, T.K. (2000). Inhibitory threshold for critical-period activation in primary visual cortex. Nature *404*, 183-186.

Fishell, G., and Rudy, B. (2011). Mechanisms of inhibition within the telencephalon: "where the wild things are". Annu Rev Neurosci *34*, 535-567.

Fries, P., Reynolds, J.H., Rorie, A.E., and Desimone, R. (2001). Modulation of oscillatory neuronal synchronization by selective visual attention. Science *291*, 1560-1563.

Fu, C., Cawthon, B., Clinkscales, W., Bruce, A., Winzenburger, P., and Ess, K.C. (2012a). GABAergic interneuron development and function is modulated by the Tsc1 gene. Cereb Cortex *22*, 2111-2119.

Fu, Y., Wu, X., Lu, J., and Huang, Z.J. (2012b). Presynaptic GABA(B) Receptor Regulates Activity-Dependent Maturation and Patterning of Inhibitory Synapses through Dynamic Allocation of Synaptic Vesicles. Front Cell Neurosci *6*, 57.

Howard, M.W., Rizzuto, D.S., Caplan, J.B., Madsen, J.R., Lisman, J., Aschenbrenner-Scheibe, R., Schulze-Bonhage, A., and Kahana, M.J. (2003). Gamma oscillations correlate with working memory load in humans. Cereb Cortex *13*, 1369-1374.

Jaworski, J., and Sheng, M. (2006). The growing role of mTOR in neuronal development and plasticity. Mol Neurobiol *34*, 205-219.

Kobayashi, Y., Ye, Z., and Hensch, T.K. (2015). Clock genes control cortical critical period timing. Neuron *86*, 264-275.

Kwiatkowski, D.J., Zhang, H., Bandura, J.L., Heiberger, K.M., Glogauer, M., el-Hashemite, N., and Onda, H. (2002). A mouse model of TSC1 reveals sex-dependent lethality from liver

hemangiomas, and up-regulation of p70S6 kinase activity in Tsc1 null cells. Hum Mol Genet *11*, 525-534.

Kwon, C.H., Zhu, X., Zhang, J., and Baker, S.J. (2003). mTor is required for hypertrophy of Pten-deficient neuronal soma in vivo. Proc Natl Acad Sci U S A *100*, 12923-12928.

Le Magueresse, C., Alfonso, J., Khodosevich, K., Arroyo Martin, A.A., Bark, C., and Monyer, H. (2011). "Small axonless neurons": postnatally generated neocortical interneurons with delayed functional maturation. The Journal of neuroscience : the official journal of the Society for Neuroscience *31*, 16731-16747.

Li, Y.H., Werner, H., and Puschel, A.W. (2008). Rheb and mTOR regulate neuronal polarity through Rap1B. The Journal of biological chemistry *283*, 33784-33792.

Lipton, J.O., and Sahin, M. (2014). The neurology of mTOR. Neuron *84*, 275-291.

Magri, L., Cambiaghi, M., Cominelli, M., Alfaro-Cervello, C., Cursi, M., Pala, M., Bulfone, A., Garcia-Verdugo, J.M., Leocani, L., Minicucci, F.*, et al.* (2011). Sustained activation of mTOR pathway in embryonic neural stem cells leads to development of tuberous sclerosis complex-associated lesions. Cell Stem Cell *9*, 447-462.

Morishita, H., Cabungcal, J.H., Chen, Y., Do, K.Q., and Hensch, T.K. (2015). Prolonged Period of Cortical Plasticity upon Redox Dysregulation in Fast-Spiking Interneurons. Biol Psychiatry *78*, 396-402.

Nie, D., Di Nardo, A., Han, J.M., Baharanyi, H., Kramvis, I., Huynh, T., Dabora, S., Codeluppi, S., Pandolfi, P.P., Pasquale, E.B.*, et al.* (2010). Tsc2-Rheb signaling regulates EphA-mediated axon guidance. Nature neuroscience *13*, 163-172.

Okaty, B.W., Miller, M.N., Sugino, K., Hempel, C.M., and Nelson, S.B. (2009). Transcriptional and electrophysiological maturation of neocortical fast-spiking GABAergic interneurons. The Journal of neuroscience : the official journal of the Society for Neuroscience *29*, 7040-7052.

Runyan, C.A., Schummers, J., Van Wart, A., Kuhlman, S.J., Wilson, N.R., Huang, Z.J., and Sur, M. (2010). Response features of parvalbumin-expressing interneurons suggest precise roles for subtypes of inhibition in visual cortex. Neuron *67*, 847-857.

Silverman, J.L., Yang, M., Lord, C., and Crawley, J.N. (2010). Behavioural phenotyping assays for mouse models of autism. Nat Rev Neurosci *11*, 490-502.

Sohal, V.S., Zhang, F., Yizhar, O., and Deisseroth, K. (2009). Parvalbumin neurons and gamma rhythms enhance cortical circuit performance. Nature *459*, 698-702.

Sugiyama, S., Di Nardo, A.A., Aizawa, S., Matsuo, I., Volovitch, M., Prochiantz, A., and Hensch, T.K. (2008). Experience-dependent transfer of Otx2 homeoprotein into the visual cortex activates postnatal plasticity. Cell *134*, 508-520.

Takada, N., Pi, H.J., Sousa, V.H., Waters, J., Fishell, G., Kepecs, A., and Osten, P. (2014). A developmental cell-type switch in cortical interneurons leads to a selective defect in cortical

oscillations. Nat Commun *5*, 5333.

Tavazoie, S.F., Alvarez, V.A., Ridenour, D.A., Kwiatkowski, D.J., and Sabatini, B.L. (2005). Regulation of neuronal morphology and function by the tumor suppressors Tsc1 and Tsc2. Nature neuroscience *8*, 1727-1734.

Tsai, P.T., Hull, C., Chu, Y., Greene-Colozzi, E., Sadowski, A.R., Leech, J.M., Steinberg, J., Crawley, J.N., Regehr, W.G., and Sahin, M. (2012). Autistic-like behaviour and cerebellar dysfunction in Purkinje cell Tsc1 mutant mice. Nature *488*, 647-651.

Urbanska, M., Gozdz, A., Swiech, L.J., and Jaworski, J. (2012). Mammalian target of rapamycin complex 1 (mTORC1) and 2 (mTORC2) control the dendritic arbor morphology of hippocampal neurons. The Journal of biological chemistry *287*, 30240-30256.

Vogt, D., Cho, K.K., Lee, A.T., Sohal, V.S., and Rubenstein, J.L. (2015). The parvalbumin/somatostatin ratio is increased in Pten mutant mice and by human PTEN ASD alleles. Cell Rep *11*, 944-956.

Wu, X., Fu, Y., Knott, G., Lu, J., Di Cristo, G., and Huang, Z.J. (2012). GABA signaling promotes synapse elimination and axon pruning in developing cortical inhibitory interneurons. The Journal of neuroscience: the official journal of the Society for Neuroscience *32*, 331-343.

Xu, Q., Tam, M., and Anderson, S.A. (2008). Fate mapping Nkx2.1-lineage cells in the mouse telencephalon. J Comp Neurol *506*, 16-29.

Yoon, B.C., Zivraj, K.H., and Holt, C.E. (2009). Local translation and mRNA trafficking in axon pathfinding. Results and problems in cell differentiation *48*, 269-288.

Zhang, B., Chen, L.Y., Liu, X., Maxeiner, S., Lee, S.J., Gokce, O., and Sudhof, T.C. (2015). Neuroligins Sculpt Cerebellar Purkinje-Cell Circuits by Differential Control of Distinct Classes of Synapses. Neuron *87*, 781-796.

Chapter 5. Discussion

About 50% of epilepsy patients suffer from genetic generalized epilepsy[100]. Progress in sequencing techniques in the past decades has lead to the identification of novel mutations in various ligand-gated ion channels (e.g. $GABA_A$ receptor) as a causative factor in epilepsy. While assessing mutaions in heterologous cell lines has been the norm to establish a loss-of-fuction model to each of these mutations, there have been controversies in the past as data from different laboratories sometimes failed to overlap. Typically, to address such a situation one has to develop knock-out mice in order to gain further insight. From a futuristic perspective, this approach of mutational screening runs the risk of being a resourse-consuming venture as the database of such mutations is non-exhaustive and will continue to grow owing to the progress in sequencing techniques. The work discussed in chapter 3, highlights a key advantage of using single-cell genetics technique as an alternative to heterologous cell line screening. The data further suggests that a simple loss of function model is a rather incomplete way of explaining a situation as different mutations in the same gene can lead to distinct consequences both at the cellular and synaptic levels.

In chapter 4, the role of the mTOR pathway in PV+ BC development has been studied in both *in vitro* and *in vivo* conditions. The data suggests Tsc1 loss in both single PV+ cells and PV+ cell network leads to reduced PV connectivity in adulthood. Further, two diferent Cre-expressing transgenic mouse lines have been used which differs in the temporal and spatial origin of Cre expression. Interestingly, post-natal loss of Tsc1 in PV cells has more severe effects in terms of PV connectivity and social behavior.

While chapter 3 highlights the key advantage of using single cell genetics as a powerful tool to identify how specific gene mutations lead to changes at cellular and synaptic levels,

chapter 4 extensively uses this technique to gain deeper insight on the nature of these changes over a developmental time window. In order to add multiple perspectives to the data discussed in chapter 3 and 4, this section attempts to answer the possible mechanisms involved, the limitations of this study, the clinical relevance as well the scope for future studies.

5.1 Spatial and temporal origin of Tsc1 knockout determine the extent of PV cell connectivity alterations and mouse behavioral deficits

As previous studies have highlighted that both the timing and spatial origin of Tsc1 loss contribute to diverse phenotypes, we used separate breeding strategies to address this aspect in GABAergic neurons. The Tg(*Nkx2.1*-Cre) line drives *Cre* expression in both SST- and PV-expressing cells of the cortex and hippocampus (apart from other brain areas) and starts early at E10.5 in the basal telencephalon (**Table5.1**). This allowed us to achieve loss of Tsc1 in MGE-based progenitor cells at an embryonic stage and hence determine the early role of Tsc1 in PV cells. The second *Cre*-driving line, Tg (*PV*-Cre), has a late post-natal expression (P14) and henceforth allowed us to determine the effect of Tsc1loss on structural connectivity of PV cells during post-natal development.

Primarily, we found that loss of Tsc1in Tg(*Nkx2.1*-Cre);$Tsc1^{flox/flox}$ mice causes an initial increase in axonal branching and boutons density of PV cells in juvenile mice (P18) followed by hypo-connectivity in young adults (P45). This phenomenon is also recapitulated in cortical organotypic cultures from these mice where individual PV-expressing cortical BCs show increased innervation at EP18 but strongly reduced axonal arbor and bouton density at EP32. One possible hypothesis is that bouton hyper-proliferation and excessive axon growth caused by mTOR hyperactivation in PV cells leads to consequent hypo-connectivity at later stages. In fact, even if more boutons are formed, they may not be correctly opposed to postsynaptic

specializations, therefore leading to less efficient synapses. Our data showing that while the number of PV perisomatic puncta is increased, the number of PV-gephyrin colocalizing puncta is not in P18 mice Tg(*Nkx2.1*-Cre);Tsc1$^{flox/flox}$ mice compared to control littermates support this speculation. Another possibility is that mTOR activation may play two distinct and opposing roles in different phases of PV cell connectivity development. For example, mTOR activation may promote axon growth and bouton formation in actively growing PV cells, while it may constrain synapse plasticity in adult PV cells. More experiments will be required to clarify this point.

Although Tg(*PV*-Cre);Tsc1$^{flox/flox}$ mice develop PV hypo-connectivity at later stages (P45), it is unknown if hyper-connectivity occurs at P18. In fact, while using the endogenous PV promoter to drive *Cre* expression confers PV-BC specificity, one limitation is that the *Cre* expression well after the first postnatal week. Whereas by P30 ~75% of PV cells show GFP expression when using a reporter line (RCE mouse, add reference), the proportion of GFP+ PV cells is more variable and closer to 50% in P18 mice (data not shown). It is therefore challenging to identify in which PV cell Tsc1 has already recombined by P18 and to selectively quantify their synaptic innervation. One possibility is to use a mouse where GFP is expressed upon *Cre* expression. As mentioned above, we indeed generated Tg(*PV*-Cre);Tsc1$^{flox/flox}$; RCE mice and used them to monitor and quantify Cre-mediated GFP expression at different ages; however GFP signal was too low, even following antibody-mediated amplification, to reliably quantify GFP+ puncta.

Nevertheless, single-cell Tsc1 deletion in cortical organotypic cultures shows that cell-autonomous loss of Tsc1 (heterozygous and homozygous) in single PV-expressing cortical PV cells leads to hyper-connectivity at EP18. However, it still needs to be ascertained if the mutant BCs loses connectivity over time. Moreover, as discussed above, it remains to be investigated if the apparent state of hyper-connectivity at P18 *in vivo* (increase in perisomatic

PV intensity and puncta density, **Figure 4.4 D,E**) or at EP18 *in vitro* (increase in PV-BC bouton density and axonal branching, **Figure 4.6 D,E**) reflect a state of functional maturity. Additional studies involving electron microscopy will reveal the pre- and post-synaptic ultra-structures at these punctas or boutons to gain an understanding of their developmental state. Further, electrophysiological recording using dual patch technique is the most direct method to study the presence of functional synapses between a pair of cells. This technique consist in the stimulation of a PV cell with an electrode and subsequently recording of the inhibitory output of that cell on a nearby, connected pyramidal cell. Dual patch recordings will give further insight into the functional state of mutant PV cell synapses during different stages of development.

Interestingly, our data also suggest that the inactivation of Tsc1 floxed alleles by the Tg(*PV*-Cre) induces more severe phenotypes in terms of PV connectivity (reduced PV and PV-gephyrin co-localized puncta density) compared to what observed in Tg(*Nkx2.1*-Cre);Tsc1$^{flox/flox}$ mice (**Fig.4.8 *E,G***). In fact, Tsc1 gene dosage plays a crucial role when Tsc1 ablation occurs at an early stage as Tg(*Nkx2.1*-Cre);Tsc1$^{flox/+}$ mice show PV cell connectivity similar to age-matched controls. On the other hand, post-natal loss of Tsc1 in Tg(*PV*-Cre);Tsc1$^{flox/+}$ mice causes significant deficits. Altogether, these data indicate that the temporal window of Tsc1 knockout is crucial in determining both the effect of gene dosage and the severity of loss of connectivity.

Perhaps, the most intriguing observation made in this study is the dynamic shift in terms of PV cell connectivity during the developmental time course in the cortex. Loss of Tsc1 in glutamatergic pyramidal cells in hippocampus cultures lead to decrease in dendritic spine density[184]. However, *in vivo* loss of Tsc1 (in mice) has shown variable results in terms of spine density. While analysis of Tsc1 null-neuron pyramidal cells from a Tg(*SynI*-Cre);Tsc1$^{flox/flox}$ mice recapitulate the *in vitro* findings in terms of spine density[110], other

studies have contradicted them[179]. Therefore it remains controversial about the exact role of Tsc1 in excitatory synapse formation and maintenance in the context of spine density. However, electrophysiological recordings show increase in mEPSC frequency in Tsc1 deficient pyramidal cells. This indicates that loss of Tsc1 increases the number of synapses formed onto the postsynaptic neuron[179]. Contrary to the loss of spines in hippocampal pyramidal cells, loss of Tsc1in cerebellar Purkinje cells lead to increase in spine density[175]. Therefore, in context of our findings in cortical PV cells, it is pertinent to complement the data with patch clamp recordings at the different time points in cortical development.

Behavioral studies in both the conditional mouse models identify deficits in the social novelty paradigm. On the other hand, these mouse lines show opposite behavior in the elevated plus maze test, which suggest the presence of different anxiety responses. In fact, while the Tg(*Nkx2.1*-Cre);Tsc1$^{flox/flox}$ show strong anxiety-like behavior coupled with higher exploratory drive in the open field arena, Tg(*PV*-Cre);Tsc1$^{flox/flox}$ mice display a surprising lack of anxiety. There could be several possible explanations for this difference in anxiety response in the two conditional mouse models. The dual role of GABA in controlling anxiolytic or anxiogenic responses have been well acknowledged in studies involving Benzodiazepine mediated $GABA_A$ receptor modulations[97,207]. Further, the two mice models discussed above target different GABAergic cell populations with distinct spatial and temporal specificity (**Table 5.1**). Therefore differences arising due to modulation in GABAergic activity in different brain regions could contribute to the variability in anxiety responses in these animals.

Given that mTOR hyperactivaion enhances the translational capacity of cells, it will be interesting to study if alterations in the expression of proteins involved either in maintenance of intrinsic excitability or control of synaptic inputs onto GABAergic cells contribute to the underlying mechanisms for the observed phenotypes. Both these factors contribute in

determining the extent of GABAergic output on target cells. For example, GABA activity itself is a crucial factor in determining the extent of connectivity in interneurons[61], thus it will be interesting to explore whether the expression of proteins involved in the synthesis ($GAD_{65/67}$), packaging (vGAT) or release of GABA itself is affected. Indeed, Chattopadhyaya and co-workers report increased bouton density and branching at EP18 in GAD67 knockout BCs[58] which is recapitulated in our findings in $Tsc1^{+/-}$ and $Tsc1^{-/-}$ cells. Changes in intrinsic excitability could significantly impact GABA release. Previous studies have reported decrease in input resistance in Tsc1 deficient cells rendering them less excitable[175,179]. Raab-Graham and co-workers have shown $K_v1.1$ channel expression is modulated by mTOR activity[208]. If K_v channel expression is modulated in Tsc1 deficient PV cells remains a question at large. It also needs to be investigated if excitatory inputs onto PV cells may be altered because of possible deficits in glutamatergic synapse composition. A potential candidate protein is neuronal activity-regulated pentraxin (Narp), which is known to be prominently present in excitatory synapses of PV cells and play a role in AMPA receptor clustering[209]. Other possibilities include perturbation in ErbB4-Nrg1signalling, which is involved in development of cortical inhibitory circuits[210].

Promoter driving *Cre* expression	Time of *Cre* expression	Brain regions targeted	Cell types targeted	Citation
Nkx2.1	E10.5	Cortex, Hippocampus, Hypothalamus, Amygdala, Olfactory bulb, Striatum, Globus pallidus, Septum, and Nucleus basalis.	PV,SST	Xu et al, 2008[211].
PV	P14	Cortex, Hippocampus, Cerebellum and PV cells in other brain regions.	PV	Taniguchi et al, 2011[212].

Table 5.1. Cre expression under *Nkx2.1* and *PV* promoters has different spatio-temporal origins.

5.2 Limitations of the study

In this study, we have consistently found that knockout of both the Tsc1 alleles leads to an initial hyper-connectivity of PV cells both *in vivo* (Tg(*Nkx2.1*-Cre);$Tsc1^{flox/flox}$) and in organotypic cultures. These results are recapitulated in $Tsc1^{-/-}$ BCs in an otherwise wild-type background in organotypic cultures at EP18. However, the effect of gene dosage is stronger *in vivo* as we do not observe any changes in terms of connectivity at P18 in the Tg(*Nkx2.1*-Cre);$Tsc1^{flox/+}$ mice. Conversely, BCs in organotypic cultures from Tg(*Nkx2.1*-Cre);$Tsc1^{flox/+}$ mice as well as single cell knockouts ($Tsc1^{+/-}$) have unusually high connectivity at P18 **(Fig 4.2** and **4.6**). Therefore we found discrepancy in the degree of PV cell connectivity between *in vivo* and *in vitro* studies in the context of heterozygous loss of Tsc1. The answer might lay in differences in the external factors in the milieu while comparing an *in vivo* to an *in vitro* system. In a culture system, the medium has an abundance of nutrients and growth factors (e.g. insulin); whereas, nutrient availability *in vivo* is variable and probably more limited. As nutrient availability positively modulates mTOR pathway activity, a nutrient-rich environment might act as an additional cue to promote hyperactivity of the mTOR pathway. It would be interesting to see if the heterozygous loss of Tsc1 is still capable of exhibiting such pronounced hyper-connectivity when a depleted (reduced amount of insulin and other growth factors) medium is used.

Our study of PV cell connectivity *in vivo* is focused in the somatosensory cortex. Mammalian cortex is highly segmented and each region is specialized to control various sensory, motor and cognitive processes. We have performed a battery of behavioral experiments, which implicates many cortical regions along with hippocampus, amygdala, nucleus accumbens and cerebellum. We report deficits in working memory and social behavior, which are complex

cognitive process and involve synchronized activation of multiple brain areas. Further investigation of PV cell connectivity in other cortical areas like the pre-frontal cortex is needed to clarify the cellular basis of these behavioral deficits. Such studies will also enable us to compare the extent of perturbation in PV circuitry in different brain regions.

5.3 What drives the PV network from a state of hyper-connectivity to hypo-connectivity: Possible role of altered PV-PV disinhibition

PV-expressing cells not only contact hundreds of neighbouring excitatory cells but also target other PV cells. Since our findings clearly indicate loss of PV connectivity on excitatory cells at P45, it paves the road to hypothesize that PV-PV connectivity could be altered, too. There could be potentially two situations that can lead to PV-pyramidal cell hypo-connectivity, (1) PV cells can have hyper-connectivity on other PV cells at around P18 which will lead to a stronger disinhibition and eventually suppress the activity of PV cells, or (2) if the network of excitatory cells targeted by mutant PV cells impose a modulatory effect on the mutant PV cells causing to lose their connections. Interestingly, gephyrin immunostaining of PV cells in the Tg(*Nkx2.1*-Cre);Tsc1$^{flox/flox}$ show a sharp trend towards an increase of gephyrin punctas on PV cell somata at P45, which suggest that PV somata may be receiving more inhibition. On the other hand, at this same age, PV cell connectivity onto pyramidal cells is reduced. This preliminary observation needs to be validated by increasing the number of animals analyzed and by electrophysiological recordings from PV cells. It is reasonable to expect an increase in miniature inhibitory events on PV cells if the above-mentioned mechanism occurs. However, it is not possible to identify PV boutons on a PV cell with the immunostaining approach I used in my work. One alternative approach is to co-label for synaptotagmin 2 (SYT2), which is a vesicular protein present exclusively in PV cell terminals, gephyrin (postsynaptic GABAergic marker) and PV, and then quantify SYT2-gephyrin colocalized puncta around PV cell somata. Increase in SYT2-gephyrin colocalized

punctas around PV somas would support our hypothesis, however, why the PV cells do not lose these connections unlike pyramidal cells would remain an open question. What factors modulate inhibitory inputs on other inhibitory cell is still not well understood and future work will reveal the underlying mechanisms involved in this process.

5.4 Implication for human diseases

Although this work *per se* was not aimed at creating an animal model of TSC, some key findings in terms of neuronal connectivity and social behavior have strong clinical correlations. Anxiety related behavior is often associated with TSC and our mice models recapitulate similar phenotypes. Many TSC patients have responded positively to the drug Vigabartin, which is an irreversible inhibitor of the GABA degrading enzyme GABA transaminase[213] suggesting deficits in GABAergic signaling.

Epileptic seizure is one of the most common comorbidity associated with TSC patients and some TSC mouse models have reported spontaneous epileptic seizures. Although we did not observe any spontaneous seizures in our mice models, we predict that these mice might have lower threshold for seizure susceptibility similar to what was reported for the *Dlx5/6*-Cre-Tsc1$^{lox/lox}$ mice[173] (Fu et al, 2011). EEG recordings may also reveal deficits in specific brain oscillation frequencies, as PV cells have shown to strongly regulate the power of gamma oscillations (30-80Hz range).

The presence of giant interneurons has been reported from tissue biopsy of cortical tubers in TSC patients[163]. We observed somatic hypertrophy in PV cells in both Tg(*Nkx2.1*-Cre);Tsc1$^{flox/flox}$ and Tg(*PV*-Cre);Tsc1$^{flox/flox}$ mice in the absence of cortical tubers. Therefore, further investigation is needed to characterize the deficits in GABAergic network in TSC patients.

Altogether our data suggest that progressive loss of PV cell connectivity may lead to reduced inhibition in these mice. Importantly, an imbalance of excitation/inhibition (E/I) ratio has been suggested to be one of the underlying basis of specific behavioral deficits, in both autistic and epileptic patients and experimental animal models. Thus, PV cells hypoconnectivity caused by mTOR hyperactivation may contribute to altered cognition and social behavior in patients showing these phenotypes.

5.5 $GABA_A$ receptors and epilepsy

Although several reports have suggested that mutations in $GABA_A$ receptors are associated with epilepsy, how these $GABA_A$ mutations perturb cortical excitatory and inhibitory cell connectivity is poorly understood. Our findings suggest that pyramidal cell dendritic spines and BC axonal synapses are affected in a mutation-specific manner. It will be interesting to address if epilepsy in TSC patients shares a common mechanism of pathophysiology with epilepsy arising from $GABA_A$ receptor mutations, since in both cases there is an alteration in the excitation/inhibition (E/I) ratio.

Loss of dendritic spine density has been reported in pyramidal cells in epilepsy patients. But this is often thought to be a product of epileptic seizures that lead to excessive glutamate release and excitotoxicity[214]. As discussed earlier, Tsc1 knockout in hippocampal pyramidal cells also lead to decreased spine density. Interestingly, we found that although the mutation A322D caused increase in spine density, D21N mutants showed a reverse trend. What molecular mechanisms are at work and how they differ in a mutation-specific manner remains to be explored in future. Further, expression of these mutant $GABA_A$ receptors in cortical BCs could change the inhibitory inputs on these cells which in turn will influence the excitability of the BCs. Electrophysiological recordings in both pyramidal and GABAergic BCs expressing mutant $GABA_A$ receptors will confirm if the amplitude and frequency of post

synaptic inhibitory current in these cells change. Lack of adequate inhibition is a common feature in an epileptic brain; however, if changes in the inhibitory inputs on GABAergic cells lead to hyperexcitability remains an open question.

5.6 Concluding remarks

In my thesis work, I have tried to address the broader objectives regarding the role of the mTOR pathway and $GABA_A$ receptors in cortical BC development. However, these findings demand deeper analysis into underlying mechanisms for the observed phenotypes both *in vitro* and *in vivo*. This section points at the possible avenues to answer questions, which have been outside the scope of this thesis.

Epilepsy is perhaps the most common form of morbidity observed in TSC patients. Many of the conditional knockout models, where loss of Tsc genes occurs in excitatory, glial or inhibitory cells report seizure or a lower threshold for seizure susceptibility[168-170,173,176]. Although, both the GABAergic conditional mice models described in this work do not show spontaneous seizures, they must be screened for alteration in seizure threshold. Preconvulsants like fluorythyl or ketamine could be used for seizure induction in these models. Also, as discussed previously, PV cells control gamma oscillations in the brain. EEG recording of gamma oscillations from Tg(*Nkx2.1*-Cre);$PTEN^{flox/flox}$ mice show decrease in gamma oscillations during rest and increased gamma oscillations during social activity[198]. Since, PTEN is a negative regulator of mTOR pathway, similarly to Tsc1; it is very likely we will find similar deficits in terms of gamma oscillations in our mouse models.

Deficits in social behavior, communication and repetitive behavior are core features of autism in human patients[215]. While we just tested our mice for social novelty paradigm, it is essential to look at other paradigms like sociability, reciprocal social behavior in home cage and separate cage and sexual motivation while interacting with opposite sex. In addition, marble

burying task and assessment of self-grooming are two paradigms that can be used to investigate repetitive behaviors in our models. Recording of ultrasonic vocalizations to assess mother-pup interaction will point out deficits in social communication.

Finally, a complete transcriptional and proteomic profiling is necessary to identify candidate genes and proteins whose expression is dysregulated in PV cells in our mouse models. GFP tagging of PV cells will facilitate the sorting of PV cells from brain tissue using fluorescence assisted cell sorting (FACS) technique. Once sorted, these cells can be used for microarray analysis for quantifying expression profiles of mRNAs and proteins.

Chapter 6. Bibliography

1. Anderson, S.A., et al., *Interneuron migration from basal forebrain to neocortex: dependence on Dlx genes.* Science, 1997. **278**(5337): p. 474-6.
2. Sussel, L., et al., *Loss of Nkx2.1 homeobox gene function results in a ventral to dorsal molecular respecification within the basal telencephalon: evidence for a transformation of the pallidum into the striatum.* Development, 1999. **126**(15): p. 3359-70.
3. Wonders, C.P., et al., *A spatial bias for the origins of interneuron subgroups within the medial ganglionic eminence.* Dev Biol, 2008. **314**(1): p. 127-36.
4. Xu, Q., et al., *Origins of cortical interneuron subtypes.* J Neurosci, 2004. **24**(11): p. 2612-22.
5. Butt, S.J., et al., *The temporal and spatial origins of cortical interneurons predict their physiological subtype.* Neuron, 2005. **48**(4): p. 591-604.
6. Du, T., et al., *NKX2.1 specifies cortical interneuron fate by activating Lhx6.* Development, 2008. **135**(8): p. 1559-67.
7. Denaxa, M., et al., *Maturation-promoting activity of SATB1 in MGE-derived cortical interneurons.* Cell Rep, 2012. **2**(5): p. 1351-62.
8. Close, J., et al., *Satb1 is an activity-modulated transcription factor required for the terminal differentiation and connectivity of medial ganglionic eminence-derived cortical interneurons.* J Neurosci, 2012. **32**(49): p. 17690-705.
9. Flames, N., et al., *Delineation of multiple subpallial progenitor domains by the combinatorial expression of transcriptional codes.* J Neurosci, 2007. **27**(36): p. 9682-95.
10. Gelman, D.M. and O. Marin, *Generation of interneuron diversity in the mouse cerebral cortex.* Eur J Neurosci, 2010. **31**(12): p. 2136-41.
11. Kepecs, A. and G. Fishell, *Interneuron cell types are fit to function.* Nature, 2014. **505**(7483): p. 318-26.
12. Nery, S., G. Fishell, and J.G. Corbin, *The caudal ganglionic eminence is a source of distinct cortical and subcortical cell populations.* Nat Neurosci, 2002. **5**(12): p. 1279-87.
13. Xu, Q., et al., *Origins of cortical interneuron subtypes.* J Neurosci, 2004. **24**(11): p. 2612-22.
14. Tricoire, L., et al., *Common origins of hippocampal Ivy and nitric oxide synthase expressing neurogliaform cells.* J Neurosci, 2010. **30**(6): p. 2165-76.
15. Gelman, D.M., et al., *The embryonic preoptic area is a novel source of cortical GABAergic interneurons.* J Neurosci, 2009. **29**(29): p. 9380-9.
16. Guo, J. and E.S. Anton, *Decision making during interneuron migration in the developing cerebral cortex.* Trends Cell Biol, 2014. **24**(6): p. 342-51.
17. Polleux, F., et al., *Control of cortical interneuron migration by neurotrophins and PI3-kinase signaling.* Development, 2002. **129**(13): p. 3147-60.
18. Powell, E.M., W.M. Mars, and P. Levitt, *Hepatocyte growth factor/scatter factor is a motogen for interneurons migrating from the ventral to dorsal telencephalon.* Neuron, 2001. **30**(1): p. 79-89.

19. Pozas, E. and C.F. Ibanez, *GDNF and GFRalpha1 promote differentiation and tangential migration of cortical GABAergic neurons.* Neuron, 2005. **45**(5): p. 701-13.
20. Rudolph, J., et al., *Ephrins guide migrating cortical interneurons in the basal telencephalon.* Cell Adh Migr, 2010. **4**(3): p. 400-8.
21. Zhu, Y., et al., *Cellular and molecular guidance of GABAergic neuronal migration from an extracortical origin to the neocortex.* Neuron, 1999. **23**(3): p. 473-85.
22. Zimmer, G., et al., *Ephrin-A5 acts as a repulsive cue for migrating cortical interneurons.* Eur J Neurosci, 2008. **28**(1): p. 62-73.
23. Flames, N., et al., *Short- and long-range attraction of cortical GABAergic interneurons by neuregulin-1.* Neuron, 2004. **44**(2): p. 251-61.
24. Sanchez-Alcaniz, J.A., et al., *Cxcr7 controls neuronal migration by regulating chemokine responsiveness.* Neuron, 2011. **69**(1): p. 77-90.
25. Wonders, C.P. and S.A. Anderson, *The origin and specification of cortical interneurons.* Nat Rev Neurosci, 2006. **7**(9): p. 687-96.
26. DeFelipe, J., *Cortical interneurons: from Cajal to 2001.* Prog Brain Res, 2002. **136**: p. 215-38.
27. Markram, H., et al., *Interneurons of the neocortical inhibitory system.* Nat Rev Neurosci, 2004. **5**(10): p. 793-807.
28. Batista-Brito, R. and G. Fishell, *The developmental integration of cortical interneurons into a functional network.* Curr Top Dev Biol, 2009. **87**: p. 81-118.
29. Lau, D., et al., *Impaired fast-spiking, suppressed cortical inhibition, and increased susceptibility to seizures in mice lacking Kv3.2 K+ channel proteins.* J Neurosci, 2000. **20**(24): p. 9071-85.
30. Rudy, B., et al., *Contributions of Kv3 channels to neuronal excitability.* Ann N Y Acad Sci, 1999. **868**: p. 304-43.
31. Zaitsev, A.V., et al., *P/Q-type, but not N-type, calcium channels mediate GABA release from fast-spiking interneurons to pyramidal cells in rat prefrontal cortex.* J Neurophysiol, 2007. **97**(5): p. 3567-73.
32. Bucurenciu, I., et al., *Nanodomain coupling between Ca2+ channels and Ca2+ sensors promotes fast and efficient transmitter release at a cortical GABAergic synapse.* Neuron, 2008. **57**(4): p. 536-45.
33. Douglas, R.J., et al., *Recurrent excitation in neocortical circuits.* Science, 1995. **269**(5226): p. 981-5.
34. Hu, H., J. Gan, and P. Jonas, *Interneurons. Fast-spiking, parvalbumin(+) GABAergic interneurons: from cellular design to microcircuit function.* Science, 2014. **345**(6196): p. 1255263.
35. Pinto, D.J., J.C. Brumberg, and D.J. Simons, *Circuit dynamics and coding strategies in rodent somatosensory cortex.* J Neurophysiol, 2000. **83**(3): p. 1158-66.
36. Pouille, F., et al., *Input normalization by global feedforward inhibition expands cortical dynamic range.* Nat Neurosci, 2009. **12**(12): p. 1577-85.
37. Tamas, G., et al., *Proximally targeted GABAergic synapses and gap junctions synchronize cortical interneurons.* Nat Neurosci, 2000. **3**(4): p. 366-71.
38. Szabadics, J., A. Lorincz, and G. Tamas, *Beta and gamma frequency synchronization by dendritic gabaergic synapses and gap junctions in a network of cortical interneurons.* J Neurosci, 2001. **21**(15): p. 5824-31.
39. Cardin, J.A., et al., *Driving fast-spiking cells induces gamma rhythm and controls sensory responses.* Nature, 2009. **459**(7247): p. 663-7.
40. Sohal, V.S., et al., *Parvalbumin neurons and gamma rhythms enhance cortical circuit performance.* Nature, 2009. **459**(7247): p. 698-702.

41. Kuhlman, S.J., et al., *A disinhibitory microcircuit initiates critical-period plasticity in the visual cortex.* Nature, 2013. **501**(7468): p. 543-6.
42. Hennou, S., et al., *Early sequential formation of functional GABA(A) and glutamatergic synapses on CA1 interneurons of the rat foetal hippocampus.* Eur J Neurosci, 2002. **16**(2): p. 197-208.
43. Ben-Ari, Y., *Limbic seizure and brain damage produced by kainic acid: mechanisms and relevance to human temporal lobe epilepsy.* Neuroscience, 1985. **14**(2): p. 375-403.
44. Leinekugel, X., et al., *Synaptic GABAA activation induces Ca2+ rise in pyramidal cells and interneurons from rat neonatal hippocampal slices.* J Physiol, 1995. **487 (Pt 2)**: p. 319-29.
45. Delpire, E., *Cation-Chloride Cotransporters in Neuronal Communication.* News Physiol Sci, 2000. **15**: p. 309-312.
46. Rivera, C., et al., *The K+/Cl- co-transporter KCC2 renders GABA hyperpolarizing during neuronal maturation.* Nature, 1999. **397**(6716): p. 251-5.
47. Li, H., et al., *Patterns of cation-chloride cotransporter expression during embryonic rodent CNS development.* Eur J Neurosci, 2002. **16**(12): p. 2358-70.
48. Chattopadhyaya, B., et al., *Experience and activity-dependent maturation of perisomatic GABAergic innervation in primary visual cortex during a postnatal critical period.* J Neurosci, 2004. **24**(43): p. 9598-611.
49. Morales, B., S.Y. Choi, and A. Kirkwood, *Dark rearing alters the development of GABAergic transmission in visual cortex.* J Neurosci, 2002. **22**(18): p. 8084-90.
50. Lewis, D.A., D.W. Volk, and T. Hashimoto, *Selective alterations in prefrontal cortical GABA neurotransmission in schizophrenia: a novel target for the treatment of working memory dysfunction.* Psychopharmacology (Berl), 2004. **174**(1): p. 143-50.
51. Huang, Z.J., G. Di Cristo, and F. Ango, *Development of GABA innervation in the cerebral and cerebellar cortices.* Nat Rev Neurosci, 2007. **8**(9): p. 673-86.
52. Jiao, Y., et al., *Major effects of sensory experiences on the neocortical inhibitory circuits.* J Neurosci, 2006. **26**(34): p. 8691-701.
53. Bozzi, Y., et al., *Monocular deprivation decreases the expression of messenger RNA for brain-derived neurotrophic factor in the rat visual cortex.* Neuroscience, 1995. **69**(4): p. 1133-44.
54. Castren, E., et al., *Light regulates expression of brain-derived neurotrophic factor mRNA in rat visual cortex.* Proc Natl Acad Sci U S A, 1992. **89**(20): p. 9444-8.
55. Vicario-Abejon, C., et al., *Neurotrophins induce formation of functional excitatory and inhibitory synapses between cultured hippocampal neurons.* J Neurosci, 1998. **18**(18): p. 7256-71.
56. Rutherford, L.C., et al., *Brain-derived neurotrophic factor mediates the activity-dependent regulation of inhibition in neocortical cultures.* J Neurosci, 1997. **17**(12): p. 4527-35.
57. Pinal, C.S. and A.J. Tobin, *Uniqueness and redundancy in GABA production.* Perspect Dev Neurobiol, 1998. **5**(2-3): p. 109-18.
58. Chattopadhyaya, B., et al., *GAD67-mediated GABA synthesis and signaling regulate inhibitory synaptic innervation in the visual cortex.* Neuron, 2007. **54**(6): p. 889-903.
59. Patz, S., et al., *Neuronal activity and neurotrophic factors regulate GAD-65/67 mRNA and protein expression in organotypic cultures of rat visual cortex.* Eur J Neurosci, 2003. **18**(1): p. 1-12.

60. Benevento, L.A., B.W. Bakkum, and R.S. Cohen, *gamma-Aminobutyric acid and somatostatin immunoreactivity in the visual cortex of normal and dark-reared rats.* Brain Res, 1995. **689**(2): p. 172-82.
61. Baho, E. and G. Di Cristo, *Neural activity and neurotransmission regulate the maturation of the innervation field of cortical GABAergic interneurons in an age-dependent manner.* J Neurosci, 2012. **32**(3): p. 911-8.
62. Wu, X., et al., *GABA signaling promotes synapse elimination and axon pruning in developing cortical inhibitory interneurons.* J Neurosci, 2012. **32**(1): p. 331-43.
63. Rothbard, J.B., et al., *Differences in the carbohydrate structures of neural cell-adhesion molecules from adult and embryonic chicken brains.* J Biol Chem, 1982. **257**(18): p. 11064-9.
64. Di Cristo, G., et al., *Activity-dependent PSA expression regulates inhibitory maturation and onset of critical period plasticity.* Nat Neurosci, 2007. **10**(12): p. 1569-77.
65. Chattopadhyaya, B., et al., *Neural cell adhesion molecule-mediated Fyn activation promotes GABAergic synapse maturation in postnatal mouse cortex.* J Neurosci, 2013. **33**(14): p. 5957-68.
66. Ben-Ari, Y., et al., *gamma-Aminobutyric acid (GABA): a fast excitatory transmitter which may regulate the development of hippocampal neurones in early postnatal life.* Prog Brain Res, 1994. **102**: p. 261-73.
67. Kaneda, M., M. Farrant, and S.G. Cull-Candy, *Whole-cell and single-channel currents activated by GABA and glycine in granule cells of the rat cerebellum.* J Physiol, 1995. **485 (Pt 2)**: p. 419-35.
68. Uusi-Oukari, M. and E.R. Korpi, *Regulation of GABA(A) receptor subunit expression by pharmacological agents.* Pharmacol Rev, 2010. **62**(1): p. 97-135.
69. Olsen, R.W. and W. Sieghart, *GABA A receptors: subtypes provide diversity of function and pharmacology.* Neuropharmacology, 2009. **56**(1): p. 141-8.
70. Bailey, M.E., et al., *Genomic mapping and evolution of human GABA(A) receptor subunit gene clusters.* Mamm Genome, 1999. **10**(8): p. 839-43.
71. Russek, S.J., *Evolution of GABA(A) receptor diversity in the human genome.* Gene, 1999. **227**(2): p. 213-22.
72. Simon, J., et al., *Analysis of the set of GABA(A) receptor genes in the human genome.* J Biol Chem, 2004. **279**(40): p. 41422-35.
73. Patel, B., M. Mortensen, and T.G. Smart, *Stoichiometry of delta subunit containing GABA(A) receptors.* Br J Pharmacol, 2014. **171**(4): p. 985-94.
74. Jones, B.L. and L.P. Henderson, *Trafficking and potential assembly patterns of epsilon-containing GABAA receptors.* J Neurochem, 2007. **103**(3): p. 1258-71.
75. Fritschy, J.M. and P. Panzanelli, *GABAA receptors and plasticity of inhibitory neurotransmission in the central nervous system.* Eur J Neurosci, 2014. **39**(11): p. 1845-65.
76. LoTurco, J.J., et al., *GABA and glutamate depolarize cortical progenitor cells and inhibit DNA synthesis.* Neuron, 1995. **15**(6): p. 1287-98.
77. Owens, D.F., et al., *Excitatory GABA responses in embryonic and neonatal cortical slices demonstrated by gramicidin perforated-patch recordings and calcium imaging.* J Neurosci, 1996. **16**(20): p. 6414-23.
78. Manent, J.B., et al., *A noncanonical release of GABA and glutamate modulates neuronal migration.* J Neurosci, 2005. **25**(19): p. 4755-65.
79. Laurie, D.J., W. Wisden, and P.H. Seeburg, *The distribution of thirteen GABAA receptor subunit mRNAs in the rat brain. III. Embryonic and postnatal development.* J Neurosci, 1992. **12**(11): p. 4151-72.

80. Doischer, D., et al., *Postnatal differentiation of basket cells from slow to fast signaling devices.* J Neurosci, 2008. **28**(48): p. 12956-68.
81. Okaty, B.W., et al., *Transcriptional and electrophysiological maturation of neocortical fast-spiking GABAergic interneurons.* J Neurosci, 2009. **29**(21): p. 7040-52.
82. Le Magueresse, C., et al., *"Small axonless neurons": postnatally generated neocortical interneurons with delayed functional maturation.* J Neurosci, 2011. **31**(46): p. 16731-47.
83. Bosman, L.W., T.W. Rosahl, and A.B. Brussaard, *Neonatal development of the rat visual cortex: synaptic function of GABAA receptor alpha subunits.* J Physiol, 2002. **545**(Pt 1): p. 169-81.
84. Cohen, I., et al., *On the origin of interictal activity in human temporal lobe epilepsy in vitro.* Science, 2002. **298**(5597): p. 1418-21.
85. Dunning, D.D., et al., *GABA(A) receptor-mediated miniature postsynaptic currents and alpha-subunit expression in developing cortical neurons.* J Neurophysiol, 1999. **82**(6): p. 3286-97.
86. Hutcheon, B., P. Morley, and M.O. Poulter, *Developmental change in GABAA receptor desensitization kinetics and its role in synapse function in rat cortical neurons.* J Physiol, 2000. **522 Pt 1**: p. 3-17.
87. Hendrickson, A., et al., *Coincidental appearance of the alpha 1 subunit of the GABA-A receptor and the type I benzodiazepine receptor near birth in macaque monkey visual cortex.* Int J Dev Neurosci, 1994. **12**(4): p. 299-314.
88. Pinto, J.G., et al., *Developmental changes in GABAergic mechanisms in human visual cortex across the lifespan.* Front Cell Neurosci, 2010. **4**: p. 16.
89. Klausberger, T., J.D. Roberts, and P. Somogyi, *Cell type- and input-specific differences in the number and subtypes of synaptic GABA(A) receptors in the hippocampus.* J Neurosci, 2002. **22**(7): p. 2513-21.
90. Nusser, Z., et al., *The alpha 6 subunit of the GABAA receptor is concentrated in both inhibitory and excitatory synapses on cerebellar granule cells.* J Neurosci, 1996. **16**(1): p. 103-14.
91. Kralic, J.E., et al., *Compensatory alteration of inhibitory synaptic circuits in cerebellum and thalamus of gamma-aminobutyric acid type A receptor alpha1 subunit knockout mice.* J Comp Neurol, 2006. **495**(4): p. 408-21.
92. Zeller, A., et al., *Cortical glutamatergic neurons mediate the motor sedative action of diazepam.* Mol Pharmacol, 2008. **73**(2): p. 282-91.
93. Peng, Z., et al., *GABA(A) receptor changes in delta subunit-deficient mice: altered expression of alpha4 and gamma2 subunits in the forebrain.* J Comp Neurol, 2002. **446**(2): p. 179-97.
94. Peden, D.R., et al., *Developmental maturation of synaptic and extrasynaptic GABAA receptors in mouse thalamic ventrobasal neurones.* J Physiol, 2008. **586**(4): p. 965-87.
95. Rudolph, U., et al., *Benzodiazepine actions mediated by specific gamma-aminobutyric acid(A) receptor subtypes.* Nature, 1999. **401**(6755): p. 796-800.
96. Low, K., et al., *Molecular and neuronal substrate for the selective attenuation of anxiety.* Science, 2000. **290**(5489): p. 131-4.
97. Crestani, F., et al., *Contribution of the alpha1-GABA(A) receptor subtype to the pharmacological actions of benzodiazepine site inverse agonists.* Neuropharmacology, 2002. **43**(4): p. 679-84.

98. Yee, B.K., et al., *A schizophrenia-related sensorimotor deficit links alpha 3-containing GABAA receptors to a dopamine hyperfunction.* Proc Natl Acad Sci U S A, 2005. **102**(47): p. 17154-9.
99. Rudolph, U. and H. Mohler, *Analysis of GABAA receptor function and dissection of the pharmacology of benzodiazepines and general anesthetics through mouse genetics.* Annu Rev Pharmacol Toxicol, 2004. **44**: p. 475-98.
100. Engel, J., Jr., *Intractable epilepsy: definition and neurobiology.* Epilepsia, 2001. **42 Suppl 6**: p. 3.
101. Cossette, P., et al., *Mutation of GABRA1 in an autosomal dominant form of juvenile myoclonic epilepsy.* Nat Genet, 2002. **31**(2): p. 184-9.
102. Lachance-Touchette, P., et al., *Novel alpha1 and gamma2 GABAA receptor subunit mutations in families with idiopathic generalized epilepsy.* Eur J Neurosci, 2011. **34**(2): p. 237-49.
103. Macdonald, R.L., J.Q. Kang, and M.J. Gallagher, *Mutations in GABAA receptor subunits associated with genetic epilepsies.* J Physiol, 2010. **588**(Pt 11): p. 1861-9.
104. Gallagher, M.J., et al., *The GABAA receptor alpha1 subunit epilepsy mutation A322D inhibits transmembrane helix formation and causes proteasomal degradation.* Proc Natl Acad Sci U S A, 2007. **104**(32): p. 12999-3004.
105. Heitman, J., N.R. Movva, and M.N. Hall, *Targets for cell cycle arrest by the immunosuppressant rapamycin in yeast.* Science, 1991. **253**(5022): p. 905-9.
106. Brown, E.J., et al., *A mammalian protein targeted by G1-arresting rapamycin-receptor complex.* Nature, 1994. **369**(6483): p. 756-8.
107. Sabatini, D.M., et al., *RAFT1: a mammalian protein that binds to FKBP12 in a rapamycin-dependent fashion and is homologous to yeast TORs.* Cell, 1994. **78**(1): p. 35-43.
108. Sabers, C.J., et al., *Isolation of a protein target of the FKBP12-rapamycin complex in mammalian cells.* J Biol Chem, 1995. **270**(2): p. 815-22.
109. Sarbassov, D.D., et al., *Prolonged rapamycin treatment inhibits mTORC2 assembly and Akt/PKB.* Mol Cell, 2006. **22**(2): p. 159-68.
110. Meikle, L., et al., *Response of a neuronal model of tuberous sclerosis to mammalian target of rapamycin (mTOR) inhibitors: effects on mTORC1 and Akt signaling lead to improved survival and function.* J Neurosci, 2008. **28**(21): p. 5422-32.
111. Costa-Mattioli, M. and L.M. Monteggia, *mTOR complexes in neurodevelopmental and neuropsychiatric disorders.* Nat Neurosci, 2013. **16**(11): p. 1537-43.
112. Song, M.S., L. Salmena, and P.P. Pandolfi, *The functions and regulation of the PTEN tumour suppressor.* Nat Rev Mol Cell Biol, 2012. **13**(5): p. 283-96.
113. Huang, W., et al., *mTORC2 controls actin polymerization required for consolidation of long-term memory.* Nat Neurosci, 2013. **16**(4): p. 441-8.
114. Zinzalla, V., et al., *Activation of mTORC2 by association with the ribosome.* Cell, 2011. **144**(5): p. 757-68.
115. Laplante, M. and D.M. Sabatini, *mTOR signaling in growth control and disease.* Cell, 2012. **149**(2): p. 274-93.
116. Tang, H., et al., *Amino acid-induced translation of TOP mRNAs is fully dependent on phosphatidylinositol 3-kinase-mediated signaling, is partially inhibited by rapamycin, and is independent of S6K1 and rpS6 phosphorylation.* Mol Cell Biol, 2001. **21**(24): p. 8671-83.
117. Mayer, K., et al., *Characterisation of a novel TSC2 missense mutation in the GAP related domain associated with minimal clinical manifestations of tuberous sclerosis.* J Med Genet, 2004. **41**(5): p. e64.

118. Kantidakis, T., et al., *mTOR associates with TFIIIC, is found at tRNA and 5S rRNA genes, and targets their repressor Maf1.* Proc Natl Acad Sci U S A, 2010. **107**(26): p. 11823-8.
119. Shor, B., et al., *Requirement of the mTOR kinase for the regulation of Maf1 phosphorylation and control of RNA polymerase III-dependent transcription in cancer cells.* J Biol Chem, 2010. **285**(20): p. 15380-92.
120. Thoreen, C.C., et al., *An ATP-competitive mammalian target of rapamycin inhibitor reveals rapamycin-resistant functions of mTORC1.* J Biol Chem, 2009. **284**(12): p. 8023-32.
121. Yu, K., et al., *Biochemical, cellular, and in vivo activity of novel ATP-competitive and selective inhibitors of the mammalian target of rapamycin.* Cancer Res, 2009. **69**(15): p. 6232-40.
122. Duvel, K., et al., *Activation of a metabolic gene regulatory network downstream of mTOR complex 1.* Mol Cell, 2010. **39**(2): p. 171-83.
123. Zhang, H.H., et al., *Insulin stimulates adipogenesis through the Akt-TSC2-mTORC1 pathway.* PLoS One, 2009. **4**(7): p. e6189.
124. Jung, C.H., et al., *ULK-Atg13-FIP200 complexes mediate mTOR signaling to the autophagy machinery.* Mol Biol Cell, 2009. **20**(7): p. 1992-2003.
125. Hosokawa, N., et al., *Nutrient-dependent mTORC1 association with the ULK1-Atg13-FIP200 complex required for autophagy.* Mol Biol Cell, 2009. **20**(7): p. 1981-91.
126. Phung, T.L., et al., *Pathological angiogenesis is induced by sustained Akt signaling and inhibited by rapamycin.* Cancer Cell, 2006. **10**(2): p. 159-70.
127. Sarbassov, D.D., et al., *Phosphorylation and regulation of Akt/PKB by the rictor-mTOR complex.* Science, 2005. **307**(5712): p. 1098-101.
128. Guertin, D.A., et al., *Ablation in mice of the mTORC components raptor, rictor, or mLST8 reveals that mTORC2 is required for signaling to Akt-FOXO and PKCalpha, but not S6K1.* Dev Cell, 2006. **11**(6): p. 859-71.
129. Jacinto, E., et al., *SIN1/MIP1 maintains rictor-mTOR complex integrity and regulates Akt phosphorylation and substrate specificity.* Cell, 2006. **127**(1): p. 125-37.
130. Garcia-Martinez, J.M. and D.R. Alessi, *mTOR complex 2 (mTORC2) controls hydrophobic motif phosphorylation and activation of serum- and glucocorticoid-induced protein kinase 1 (SGK1).* Biochem J, 2008. **416**(3): p. 375-85.
131. Jacinto, E., et al., *Mammalian TOR complex 2 controls the actin cytoskeleton and is rapamycin insensitive.* Nat Cell Biol, 2004. **6**(11): p. 1122-8.
132. Sarbassov, D.D., et al., *Rictor, a novel binding partner of mTOR, defines a rapamycin-insensitive and raptor-independent pathway that regulates the cytoskeleton.* Curr Biol, 2004. **14**(14): p. 1296-302.
133. Shah, O.J., Z. Wang, and T. Hunter, *Inappropriate activation of the TSC/Rheb/mTOR/S6K cassette induces IRS1/2 depletion, insulin resistance, and cell survival deficiencies.* Curr Biol, 2004. **14**(18): p. 1650-6.
134. Masui, K., W.K. Cavenee, and P.S. Mischel, *mTORC2 in the center of cancer metabolic reprogramming.* Trends Endocrinol Metab, 2014. **25**(7): p. 364-73.
135. European Chromosome 16 Tuberous Sclerosis Consortium, 1993. *Identification andcharacterization of the tuberous sclerosis gene on chromosome 16*. Cell **75**,1305–1315.
136. Crino, P.B., K.L. Nathanson, and E.P. Henske, *The tuberous sclerosis complex.* N Engl J Med, 2006. **355**(13): p. 1345-56.
137. Asato, M.R. and A.Y. Hardan, *Neuropsychiatric problems in tuberous sclerosis complex.* J Child Neurol, 2004. **19**(4): p. 241-9.

138. Jansen, F.E., et al., *Overlapping neurologic and cognitive phenotypes in patients with TSC1 or TSC2 mutations.* Neurology, 2008. **70**(12): p. 908-15.
139. Green, A.J., M. Smith, and J.R. Yates, *Loss of heterozygosity on chromosome 16p13.3 in hamartomas from tuberous sclerosis patients.* Nat Genet, 1994. **6**(2): p. 193-6.
140. Sepp, T., J.R. Yates, and A.J. Green, *Loss of heterozygosity in tuberous sclerosis hamartomas.* J Med Genet, 1996. **33**(11): p. 962-4.
141. Kwiatkowski, D.J. and B.D. Manning, *Tuberous sclerosis: a GAP at the crossroads of multiple signaling pathways.* Hum Mol Genet, 2005. **14 Spec No. 2**: p. R251-8.
142. Tsai, V., et al., *Fetal brain mTOR signaling activation in tuberous sclerosis complex.* Cereb Cortex, 2014. **24**(2): p. 315-27.
143. Dibble, C.C., et al., *TBC1D7 is a third subunit of the TSC1-TSC2 complex upstream of mTORC1.* Mol Cell, 2012. **47**(4): p. 535-46.
144. Au, K.S., et al., *Molecular genetic basis of tuberous sclerosis complex: from bench to bedside.* J Child Neurol, 2004. **19**(9): p. 699-709.
145. Rose, V.M., Au, K.S., Pollom, G., Roach, E.S., Prashner, H.R., Northrup, H., 1999. Germ-line mosaicism in tuberous sclerosis: how common? American Journal of HumanGenetics 64, 986–992.
146. Verhoef, S., et al., *High rate of mosaicism in tuberous sclerosis complex.* Am J Hum Genet, 1999. **64**(6): p. 1632-7.
147. Sancak, O., et al., *Mutational analysis of the TSC1 and TSC2 genes in a diagnostic setting: genotype--phenotype correlations and comparison of diagnostic DNA techniques in Tuberous Sclerosis Complex.* Eur J Hum Genet, 2005. **13**(6): p. 731-41.
148. Knudson, A.G., *Two genetic hits (more or less) to cancer.* Nat Rev Cancer, 2001. **1**(2): p. 157-62.
149. Henske, E.P., et al., *Loss of tuberin in both subependymal giant cell astrocytomas and angiomyolipomas supports a two-hit model for the pathogenesis of tuberous sclerosis tumors.* Am J Pathol, 1997. **151**(6): p. 1639-47.
150. Roberts, P.S., et al., *Somatic mosaicism is rare in unaffected parents of patients with sporadic tuberous sclerosis.* J Med Genet, 2004. **41**(5): p. e69.
151. Jansen, F.E., et al., *Identification of the epileptogenic tuber in patients with tuberous sclerosis: a comparison of high-resolution EEG and MEG.* Epilepsia, 2006. **47**(1): p. 108-14.
152. Jansen, F.E., et al., *Epilepsy surgery in tuberous sclerosis: a systematic review.* Epilepsia, 2007. **48**(8): p. 1477-84.
153. Mizuguchi, M., *Abnormal giant cells in the cerebral lesions of tuberous sclerosis complex.* Congenit Anom (Kyoto), 2007. **47**(1): p. 2-8.
154. Mizuguchi, M. and S. Takashima, *Neuropathology of tuberous sclerosis.* Brain Dev, 2001. **23**(7): p. 508-15.
155. Jansen, F.E., et al., *Diffusion-weighted magnetic resonance imaging and identification of the epileptogenic tuber in patients with tuberous sclerosis.* Arch Neurol, 2003. **60**(11): p. 1580-4.
156. Jansen, F.E., van Huffelen, A.C., Bourez-Swart, M., van Nieuwenhuizen, O., 2005. Con-sistent localization of interictal epileptiform activity on EEGs of patients withtuberous sclerosis complex. Epilepsia 46, 415–419.
157. Bollo, R.J., et al., *Epilepsy surgery and tuberous sclerosis complex: special considerations.* Neurosurg Focus, 2008. **25**(3): p. E13.
158. van Eeghen, A.M., et al., *Understanding relationships between autism, intelligence, and epilepsy: a cross-disorder approach.* Dev Med Child Neurol, 2013. **55**(2): p. 146-53.

159. Major, P., et al., *Are cortical tubers epileptogenic? Evidence from electrocorticography.* Epilepsia, 2009. **50**(1): p. 147-54.
160. Boer, K., et al., *Clinicopathological and immunohistochemical findings in an autopsy case of tuberous sclerosis complex.* Neuropathology, 2008. **28**(6): p. 577-90.
161. Mori, K., et al., *Decreased benzodiazepine receptor and increased GABA level in cortical tubers in tuberous sclerosis complex.* Brain Dev, 2012. **34**(6): p. 478-86.
162. Talos, D.M., et al., *Cell-specific alterations of glutamate receptor expression in tuberous sclerosis complex cortical tubers.* Ann Neurol, 2008. **63**(4): p. 454-65.
163. Cepeda, C., et al., *Enhanced GABAergic network and receptor function in pediatric cortical dysplasia Type IIB compared with Tuberous Sclerosis Complex.* Neurobiol Dis, 2012. **45**(1): p. 310-21.
164. de Vries, P., et al., *Consensus clinical guidelines for the assessment of cognitive and behavioural problems in Tuberous Sclerosis.* Eur Child Adolesc Psychiatry, 2005. **14**(4): p. 183-90.
165. de Vries, P.J., *Genetics and neuropsychiatric disorders: genome-wide, yet narrow.* Nat Med, 2009. **15**(8): p. 850-1.
166. Ridler, K., et al., *Neuroanatomical correlates of memory deficits in tuberous sclerosis complex.* Cereb Cortex, 2007. **17**(2): p. 261-71.
167. Goorden, S.M., et al., *Cognitive deficits in Tsc1+/- mice in the absence of cerebral lesions and seizures.* Ann Neurol, 2007. **62**(6): p. 648-55.
168. Uhlmann, E.J., et al., *Astrocyte-specific TSC1 conditional knockout mice exhibit abnormal neuronal organization and seizures.* Ann Neurol, 2002. **52**(3): p. 285-96.
169. Meikle, L., et al., *A mouse model of tuberous sclerosis: neuronal loss of Tsc1 causes dysplastic and ectopic neurons, reduced myelination, seizure activity, and limited survival.* J Neurosci, 2007. **27**(21): p. 5546-58.
170. Anderl, S., et al., *Therapeutic value of prenatal rapamycin treatment in a mouse brain model of tuberous sclerosis complex.* Hum Mol Genet, 2011. **20**(23): p. 4597-604.
171. Goto, J., et al., *Regulable neural progenitor-specific Tsc1 loss yields giant cells with organellar dysfunction in a model of tuberous sclerosis complex.* Proc Natl Acad Sci U S A, 2011. **108**(45): p. E1070-9.
172. Carson, R.P., et al., *Neuronal and glia abnormalities in Tsc1-deficient forebrain and partial rescue by rapamycin.* Neurobiol Dis, 2012. **45**(1): p. 369-80.
173. Fu, C., et al., *GABAergic interneuron development and function is modulated by the Tsc1 gene.* Cereb Cortex, 2012. **22**(9): p. 2111-9.
174. Bauman, M.L. and T.L. Kemper, *Neuroanatomic observations of the brain in autism: a review and future directions.* Int J Dev Neurosci, 2005. **23**(2-3): p. 183-7.
175. Tsai, P.T., et al., *Autistic-like behaviour and cerebellar dysfunction in Purkinje cell Tsc1 mutant mice.* Nature, 2012. **488**(7413): p. 647-51.
176. Feliciano, D.M., et al., *Single-cell Tsc1 knockout during corticogenesis generates tuber-like lesions and reduces seizure threshold in mice.* J Clin Invest, 2011. **121**(4): p. 1596-607.
177. Jaworski, J., et al., *Control of dendritic arborization by the phosphoinositide-3'-kinase-Akt-mammalian target of rapamycin pathway.* J Neurosci, 2005. **25**(49): p. 11300-12.
178. Urbanska, M., et al., *Mammalian target of rapamycin complex 1 (mTORC1) and 2 (mTORC2) control the dendritic arbor morphology of hippocampal neurons.* J Biol Chem, 2012. **287**(36): p. 30240-56.
179. Bateup, H.S., et al., *Loss of Tsc1 in vivo impairs hippocampal mGluR-LTD and increases excitatory synaptic function.* J Neurosci, 2011. **31**(24): p. 8862-9.

180. Harris, K.M. and S.B. Kater, *Dendritic spines: cellular specializations imparting both stability and flexibility to synaptic function.* Annu Rev Neurosci, 1994. **17**: p. 341-71.
181. Kelleher, R.J., 3rd and M.F. Bear, *The autistic neuron: troubled translation?* Cell, 2008. **135**(3): p. 401-6.
182. Huttenlocher, P.R. and P.T. Heydemann, *Fine structure of cortical tubers in tuberous sclerosis: a Golgi study.* Ann Neurol, 1984. **16**(5): p. 595-602.
183. Machado-Salas, J.P., *Abnormal dendritic patterns and aberrant spine development in Bourneville's disease--a Golgi survey.* Clin Neuropathol, 1984. **3**(2): p. 52-8.
184. Tavazoie, S.F., et al., *Regulation of neuronal morphology and function by the tumor suppressors Tsc1 and Tsc2.* Nat Neurosci, 2005. **8**(12): p. 1727-34.
185. Krishnan, M.L., et al., *Diffusion features of white matter in tuberous sclerosis with tractography.* Pediatr Neurol, 2010. **42**(2): p. 101-6.
186. Widjaja, E., et al., *Diffusion tensor imaging identifies changes in normal-appearing white matter within the epileptogenic zone in tuberous sclerosis complex.* Epilepsy Res, 2010. **89**(2-3): p. 246-53.
187. Choi, Y.J., et al., *Tuberous sclerosis complex proteins control axon formation.* Genes Dev, 2008. **22**(18): p. 2485-95.
188. Kishi, M., et al., *Mammalian SAD kinases are required for neuronal polarization.* Science, 2005. **307**(5711): p. 929-32.
189. Morita, T. and K. Sobue, *Specification of neuronal polarity regulated by local translation of CRMP2 and Tau via the mTOR-p70S6K pathway.* J Biol Chem, 2009. **284**(40): p. 27734-45.
190. Magri, L., et al., *Sustained activation of mTOR pathway in embryonic neural stem cells leads to development of tuberous sclerosis complex-associated lesions.* Cell Stem Cell, 2011. **9**(5): p. 447-62.
191. Zhou, J. and L.F. Parada, *PTEN signaling in autism spectrum disorders.* Curr Opin Neurobiol, 2012. **22**(5): p. 873-9.
192. Endersby, R. and S.J. Baker, *PTEN signaling in brain: neuropathology and tumorigenesis.* Oncogene, 2008. **27**(41): p. 5416-30.
193. Pilarski, R., et al., *Cowden syndrome and the PTEN hamartoma tumor syndrome: systematic review and revised diagnostic criteria.* J Natl Cancer Inst, 2013. **105**(21): p. 1607-16.
194. Lynch, N.E., et al., *Bannayan-Riley-Ruvalcaba syndrome: a cause of extreme macrocephaly and neurodevelopmental delay.* Arch Dis Child, 2009. **94**(7): p. 553-4.
195. Rodriguez-Escudero, I., et al., *A comprehensive functional analysis of PTEN mutations: implications in tumor- and autism-related syndromes.* Hum Mol Genet, 2011. **20**(21): p. 4132-42.
196. O'Roak, B.J., et al., *Multiplex targeted sequencing identifies recurrently mutated genes in autism spectrum disorders.* Science, 2012. **338**(6114): p. 1619-22.
197. Kwon, C.H., et al., *Pten regulates neuronal arborization and social interaction in mice.* Neuron, 2006. **50**(3): p. 377-88.
198. Vogt, D., et al., *The parvalbumin/somatostatin ratio is increased in Pten mutant mice and by human PTEN ASD alleles.* Cell Rep, 2015. **11**(6): p. 944-56.
199. Lipton, J.O. and M. Sahin, *The neurology of mTOR.* Neuron, 2014. **84**(2): p. 275-91.
200. Dasgupta, B. and D.H. Gutmann, *Neurofibromin regulates neural stem cell proliferation, survival, and astroglial differentiation in vitro and in vivo.* J Neurosci, 2005. **25**(23): p. 5584-94.
201. Johannessen, C.M., et al., *TORC1 is essential for NF1-associated malignancies.* Curr Biol, 2008. **18**(1): p. 56-62.

202. Banerjee, S., et al., *Neurofibromatosis-1 regulates mTOR-mediated astrocyte growth and glioma formation in a TSC/Rheb-independent manner.* Proc Natl Acad Sci U S A, 2011. **108**(38): p. 15996-6001.
203. Colak, D., et al., *Promoter-bound trinucleotide repeat mRNA drives epigenetic silencing in fragile X syndrome.* Science, 2014. **343**(6174): p. 1002-5.
204. Auerbach, B.D., E.K. Osterweil, and M.F. Bear, *Mutations causing syndromic autism define an axis of synaptic pathophysiology.* Nature, 2011. **480**(7375): p. 63-8.
205. Sharma, A., et al., *Dysregulation of mTOR signaling in fragile X syndrome.* J Neurosci, 2010. **30**(2): p. 694-702.
206. Bhattacharya, A., et al., *Genetic removal of p70 S6 kinase 1 corrects molecular, synaptic, and behavioural phenotypes in fragile X syndrome mice.* Neuron, 2012. **76**(2): p. 325-37.
207. Homanics, G.E., et al., *Normal electrophysiological and behavioral responses to ethanol in mice lacking the long splice variant of the gamma2 subunit of the gamma-aminobutyrate type A receptor.* Neuropharmacology, 1999. **38**(2): p. 253-65.
208. Raab-Graham, K.F., et al., *Activity- and mTOR-dependent suppression of Kv1.1 channel mRNA translation in dendrites.* Science, 2006. **314**(5796): p. 144-8.
209. Hsu, C.I., et al., *Quantitative study of the developmental changes in calcium-permeable AMPA receptor-expressing neurons in the rat somatosensory cortex.* J Comp Neurol, 2010. **518**(1): p. 75-91.
210. Fazzari, P., et al., *Control of cortical GABA circuitry development by Nrg1 and ErbB4 signalling.* Nature, 2010. **464**(7293): p. 1376-80.
211. Xu, Q., M. Tam, and S.A. Anderson, *Fate mapping Nkx2.1-lineage cells in the mouse telencephalon.* J Comp Neurol, 2008. **506**(1): p. 16-29.
212. Taniguchi, H., et al., *A resource of Cre driver lines for genetic targeting of GABAergic neurons in cerebral cortex.* Neuron, 2011. **71**(6): p. 995-1013.
213. Curatolo, P., M. Verdecchia, and R. Bombardieri, *Vigabatrin for tuberous sclerosis complex.* Brain Dev, 2001. **23**(7): p. 649-53.
214. Swann, J.W., et al., *Spine loss and other dendritic abnormalities in epilepsy.* Hippocampus, 2000. **10**(5): p. 617-25.
215. Bourgeron, T., *A synaptic trek to autism.* Curr Opin Neurobiol, 2009. **19**(2): p. 231-4.
216. Marin O (2012) Interneuron dysfunction in psychiatric disorders. Nat Rev Neurosci **13**: p. 107-120.